

ADVANCES IN IMPLICIT AND OUTPUT SPACE MAPPING
TECHNOLOGY

To my parents and my wife Lei Tang

ADVANCES IN SPACE MAPPING TECHNOLOGY
EXPLOITING IMPLICIT SPACE MAPPING AND
OUTPUT SPACE MAPPING

By

QINGSHA CHENG, M.ENG.

A Thesis

Submitted to the School of Graduate Studies

in Partial Fulfilment of the Requirements

for the Degree

Doctor of Philosophy

McMaster University

© Copyright by Qingsha Cheng, February 2004

DOCTOR OF PHILOSOPHY (2004)
(Electrical and Computer Engineering)

McMASTER UNIVERSITY
Hamilton, Ontario

TITLE: **Advances in Space Mapping Technology Exploiting
Implicit Space Mapping and Output Space Mapping**

AUTHOR: Qingsha S. Cheng
M.Eng.
(Department of Automation, Chongqing University)
B.Eng.
(Department of Automation, Chongqing University)

SUPERVISOR: J.W. Bandler, Professor Emeritus, Department of
Electrical and Computer Engineering
B.Sc. (Eng.), Ph.D., D.Sc. (Eng.) (University of
London)
D.I.C. (Imperial College)
P.Eng. (Province of Ontario)
C.Eng. F.I.E.E. (United Kingdom)
Fellow, IEEE
Fellow, Royal Society of Canada
Fellow, Engineering Institute of Canada
Fellow, Canadian Academy of Engineering

NUMBER OF PAGES: xx, 159

ABSTRACT

This thesis contributes to advances in Space Mapping (SM) technology in computer-aided modeling, design and optimization of engineering components and devices. Our developments in modeling and optimization of microwave circuits include the SM framework and SM-based surrogate modeling; implicit SM optimization exploiting preassigned parameters; implicit, frequency and output SM surrogate modeling and design; an SM design framework and implementation techniques.

We review the state of the art in space mapping and the SM-based surrogate (modeling) concept and applications. In the review, we recall proposed SM-based optimization approaches including the original algorithm, the Broyden-based aggressive SM algorithm, various trust region approaches, neural space mapping and implicit space mapping. Parameter extraction (PE) is developed as an essential SM subproblem. Different approaches to enhance uniqueness of PE are reviewed. Novel physical illustrations are presented, including the cheese-cutting problem. A framework of space mapping steps is extracted.

Implicit Space Mapping (ISM) optimization exploits preassigned parameters. We introduce ISM and show how it relates to the now well-

ABSTRACT

established (explicit) space mapping between coarse and fine device models. Through comparison a general space-mapping concept is proposed. A simple ISM algorithm is implemented. It is illustrated on the contrived “cheese-cutting problem” and applied to EM-based microwave modeling and design. An auxiliary set of parameters (selected preassigned parameters) is extracted to match the coarse model with the fine model. The calibrated coarse model (the surrogate) is then (re)optimized to predict an improved fine model solution. This is an easy SM technique to implement since the mapping itself is embedded in the calibrated coarse model and updated automatically in the procedure of parameter extraction.

We discuss the enhancement of the ISM by “output space” mapping (OSM) specifically, response residual space mapping (RRSM), when the model cannot be aligned. ISM calibrates a suitable coarse (surrogate) model against a fine model (full-wave EM simulation) by relaxing certain coarse model preassigned parameters. Based on an explanation of residual response misalignment, our new approach further fine-tunes the surrogate by the RRSM. We present an RRSM approach. A novel, simple “multiple cheese-cutting” problem illustrates the technique. The approach is implemented entirely in the Agilent ADS design environment.

A new design framework which implements various SM techniques is presented. We demonstrate the steps, for microwave devices, within the ADS (2003) schematic design framework. The design steps are friendly. The framework runs with Agilent Momentum, HFSS and Sonnet *em*. Finally, we review various engineering

ABSTRACT

applications and implementations of the SM technique.

ABSTRACT

ACKNOWLEDGEMENTS

The author wishes to express his sincere appreciation to Dr. John W. Bandler, director of research in the Simulation Optimization Systems Research Laboratory at McMaster University and President of Bandler Corporation, for his expert guidance, continued support, encouragement and supervision throughout the course of this work.

The author would like also to express his appreciation to Dr. Mohamed H. Bakr for his continuous encouragement and useful discussions as a colleague in the Simulation Optimization Systems Research Laboratory and later as a Supervisory Committee member from the Department of Electrical and Computer Engineering at McMaster University. Thanks are extended to Dr. Tamás Terlaky in the Department of Computing and Software at McMaster University, Supervisory Committee member, for his continuous support and interest.

The author thanks Dr. Mostafa A. Ismail, now with Com Dev Ltd., for useful discussions during earlier parts of this work. The author also thanks Dr. N.K. Nikolova, Mr. A.S. Mohamed, Mr. S.A. Dakroury, Mr. D. Hailu, Dr. S. Koziel of the Department of Electrical and Computer Engineering at McMaster

ACKNOWLEDGEMENTS

University and Dr. J.E. Rayas-Sánchez, now with Dept. de Electrónica, Sistemas e Informática, ITESO, Mexico, for their good company and useful discussions.

The author thanks Dr. K. Madsen and Dr. J. Søndergaard of the Institute of Mathematical Modeling and Mr. F. Pedersen of the Department of Civil Engineering, Technical University of Denmark, for productive collaboration and stimulating discussions.

The author has benefited from working with the OSA90/hope™ and Empipe™ microwave computer-aided design systems developed by Optimization Systems Associates Inc., now part of Agilent EEsof EDA. The author is also grateful to Dr. J.C. Rautio, President, Sonnet Software, Inc., North Syracuse, NY, for making *em*™ available and to Agilent Technologies, Santa Rosa, CA, for making ADS Momentum™ and HFSS available.

The author was motivated to explore the idea of implicit SM after relevant remarks by Dr. Wolfgang J.R. Hoefer, University of Victoria, Canada, and comments by Dr. Donald R. Jones, General Motors, USA.

Financial assistance was awarded to the author from several sources: from the Natural Sciences and Engineering Research Council of Canada through grants OGP0007239 and STR234854, through the Micronet Network of Centres of Excellence, from the Department of Electrical and Computer Engineering through a Teaching Assistantship, Research Assistantship and Scholarship, and through a Nortel Networks Ontario Graduate Scholarship in Science and Technology (OGSST).

ACKNOWLEDGEMENTS

Finally, thanks are due to my family for encouragement, understanding, patience and continuous loving support.

ACKNOWLEDGEMENTS

CONTENTS

ABSTRACT	iii
ACKNOWLEDGEMENTS	vii
LIST OF FIGURES	xv
LIST OF TABLES	xix
Chapter 1 INTRODUCTION	1
Chapter 2 SPACE MAPPING: THE STATE OF THE ART	7
2.1 Introduction.....	7
2.2 The Space Mapping Approach.....	13
2.2.1 The Optimization Problem.....	13
2.2.2 The Space Mapping Concept.....	13
2.2.3 Jacobian Relationships.....	15
2.2.4 Interpretation of Space Mapping Optimization	15
2.3 Original Space Mapping Approach	16
2.4 Aggressive Space Mapping Approach.....	17
2.4.1 Theory	18
2.4.2 Unit Mapping.....	18
2.4.3 Broyden-like Updates	19
2.4.4 Jacobian Based Updates.....	19
2.4.5 Constrained Update.....	20
2.4.6 Cheese-cutting Problem	20
2.5 Parameter Extraction.....	21
2.5.1 Single Point Parameter Extraction (SPE)	22
2.5.2 Multipoint Parameter Extraction (MPE).....	23
2.5.3 Statistical Parameter Extraction.....	23

CONTENTS

2.5.4	Penalized Parameter Extraction	23
2.5.5	PE Involving Frequency Mapping	23
2.5.6	Gradient Parameter Extraction (GPE)	25
2.5.7	Other Considerations	25
2.6	Expanded Space Mapping Exploiting Preassigned Parameters	26
2.7	Output Space Mapping	28
2.8	Discussion of Surrogate Modeling and Space Mapping	28
2.8.1	Building and Using Surrogates (Dennis)	28
2.8.2	Building and Using Surrogates	29
2.8.3	The Space Mapping Concept	30
2.8.4	Space Mapping Framework Optimization Steps	30
2.8.5	Space Mapping Classification	32
2.9	Conclusions	34
Chapter 3	IMPLICIT SPACE MAPPING OPTIMIZATION	37
3.1	Introduction	37
3.2	Space Mapping Technology	39
3.2.1	Explicit Space Mapping	39
3.2.2	Implicit Space Mapping	40
3.3	Implicit Space Mapping (ISM): The Concept	42
3.3.1	Implicit Space Mapping	42
3.3.2	Interpretation and Insight	44
3.3.3	Relationship with Explicit Space Mapping	46
3.3.4	Cheese-Cutting Illustration	48
3.3.5	Three-section 3:1 Microstrip Transformer Illustration	50
3.4	Implicit Space Mapping (ISM): An Algorithm	52
3.5	Frequency Implicit Space Mapping	54
3.6	HTS Filter Example	55
3.7	Conclusions	60
Chapter 4	RESPONSE RESIDUAL SPACE MAPPING TECHNIQUES	63
4.1	Introduction	63
4.2	Response Residual Space Mapping	64

CONTENTS

4.3	Implicit and Response Residual Space Mapping Surrogate	66
4.4	HTS Filter Example	67
4.5	Response Residual Space Mapping Approach	71
4.5.1	Surrogate	71
4.5.2	Multiple Cheese-cutting Problem	72
4.6	H-plane Waveguide Filter Design	76
4.6.1	Optimization Steps	76
4.6.2	Six-Section H-plane Waveguide Filter	76
4.7	Conclusions	78
Chapter 5	IMPLEMENTABLE SPACE MAPPING DESIGN FRAMEWORK	81
5.1	Introduction	81
5.2	ADS Schematic Design Framework for SM	82
5.2.1	ADS Schematic Design Framework	82
5.2.2	ADS Schematic Design Framework for SM	83
5.2.3	Three-Section Microstrip Transformer	85
5.2.4	Response Residual SM Implementation of HTS Filter	91
5.3	Review of Other SM Implementations and Applications	92
5.3.1	RF and Microwave Implementation	92
5.3.2	Electrical Engineering Implementation	97
5.3.3	Other Engineering Implementation	98
5.4	Conclusions	98
Chapter 6	CONCLUSIONS	101
Appendix A	SMX OBJECT-ORIENTED OPTIMIZATION SYSTEM	107
A.1	SMX Architecture	108
A.2	Algorithm Core: SMX Engine	110
A.3	HTS Filter Example	111
Appendix B	CHEESE-CUTTING PROBLEMS	115
B.1	Cheese-cutting problem	115

CONTENTS

B.2	Multiple Cheese-cutting Problem	118
B.2.1	Aggressive Space Mapping.....	119
B.2.2	Response Residual ASM.....	122
B.2.3	Implicit SM	124
B.2.4	Response Residual SM Surrogate.....	127
B.2.5	Implicit SM and RRSM	128
BIBLIOGRAPHY		131
AUTHOR INDEX		141
SUBJECT INDEX		151

LIST OF FIGURES

Fig. 2.1	Linking companion coarse (empirical) and fine (EM) models through a mapping.	8
Fig. 2.2	Illustration of the fundamental notation of space mapping (Steer, Bandler and Snowden, 2002).	14
Fig. 2.3	Cheese-cutting problem solved by aggressive space mapping of model lengths.	22
Fig. 2.4	Space mapping framework.	32
Fig. 3.1	Illustration of explicit SM.	39
Fig. 3.2	Illustration of ISM, (a) implicit mapping within the surrogate, (b) with extra mapping and output mapping.	41
Fig. 3.3	Illustration of ISM modeling. Here, $\mathbf{Q} = \mathbf{0}$ is solved for \mathbf{x}	43
Fig. 3.4	Illustration of ISM prediction. Here, $\mathbf{Q} = \mathbf{0}$ is solved for \mathbf{x}_c^*	43
Fig. 3.5	Synthetic illustration of ISM optimization with intermediate parameters.	45
Fig. 3.6	When we set the preassigned parameters $\mathbf{x} = \Delta\mathbf{x}_c$, ISM is consistent with the explicit SM process. (a) The original SM. (b) The ISM process interpreted in the same spaces.	47
Fig. 3.7	Cheese-cutting problem—a demonstration of the ISM algorithm.	49
Fig. 3.8	Cheese-cutting problem—illustration of an intermediate parameter, $x_i = w \times l$	51
Fig. 3.9	Implicit space mapping diagram for cheese problem.	51

LIST OF FIGURES

Fig. 3.10	Three-section 3:1 microstrip transformer illustration.	51
Fig. 3.11	Calibrating (optimizing) the preassigned parameters \mathbf{x} in Set A results in aligning the coarse model (b) or (c) with the fine model (a). In (c) we illustrate the ES MDF approach (Bandler, Ismail and Rayas-Sánchez, 2002), where $\mathbf{P}(\cdot)$ is a mapping from optimizable design parameters to preassigned parameters.	53
Fig. 3.12	The HTS filter (Bandler, Biernacki, Chen, Getsinger, Grobelny, Moskowitz and Talisa, 1995), (a) the physical structure, (b) the coarse model as implemented in Agilent ADS (2000).	57
Fig. 3.13	The Momentum fine (\circ) and optimal coarse ADS model (—) responses of the HTS filter at the initial solution (a) and at the final iteration (b) after 2 iterations (3 fine model evaluations).	58
Fig. 3.14	The Sonnet <i>em</i> fine (\circ) and optimal coarse ADS model (—) responses of the HTS filter at the initial solution (a) and at the final iteration (b) after one iteration (2 fine model evaluations).	59
Fig. 4.1	Error plots for a two-section capacitively loaded impedance transformer (Søndergaard, 2003) exhibiting the quasi-global effectiveness of space mapping (light grid) versus a classical Taylor approximation (dark grid). See text.	66
Fig. 4.2	The fine (\circ) and optimal coarse model (—) magnitude responses of the HTS filter, at the final iteration using ISM (a), followed by one iteration of RRSM (b).	68
Fig. 4.3	The fine (\circ) and optimal coarse model (—) responses of the HTS filter in dB at the initial solution (a), at the final iteration using ISM (b), and at the final iteration using ISM and RRSM (c).	70
Fig. 4.4	Illustration of the RRSM surrogate.	72
Fig. 4.5	Multiple cheese-cutting problem: (a) the coarse model (b) and fine model.	73
Fig. 4.6	“Multiple cheese-cutting” problem: implicit SM and RRSM optimization: step by step.	74

LIST OF FIGURES

Fig. 4.7	Parameter difference between the RRSM design and minimax direct optimization. Finally, $x_f = x_f^* = 12$	75
Fig. 4.8	(a) Six-section H-plane waveguide filter (b) ADS coarse model.	77
Fig. 4.9	H-plane filter optimal coarse model response (—), and the fine model response at: (a) initial solution (○); (b) solution reached via RRSM after 4 iterations (○).....	79
Fig. 5.1	S2P (2-Port S-Parameter File) symbol with terminals.....	82
Fig. 5.2	The three-section 3:1 microstrip impedance transformer.....	85
Fig. 5.3	Coarse model optimization. Coarse model optimization of the three-section impedance transformer. The coarse model is optimized using the minimax algorithm.	86
Fig. 5.4	Fine model simulated in ADS Momentum.....	86
Fig. 5.5	Coarse (—) and fine (○) model responses $ S_{11} $ at the initial solution of the three-section transformer.....	87
Fig. 5.6	The calibration of the coarse model of the three-section impedance transformer. This schematic extracts preassigned parameters x . The coarse and fine models are within the broken line. The goal is to match the coarse and fine model real and imaginary S_{11} from 5 to 15 GHz. The optimization algorithm uses the Quasi-Newton method.....	88
Fig. 5.7	Reoptimization of the coarse model of the three-section impedance transformer using the fixed preassigned parameter values obtained from the previous calibration (parameter extraction). This schematic uses the minimax optimization algorithm. The goal is to minimize $ S_{11} $ of the calibrated coarse model.	89
Fig. 5.8	Optimal coarse (—) and fine model (○) responses $ S_{11} $ for the three-section transformer using Momentum after 1 iteration (2 fine model simulations). The process satisfies the stopping criteria.	90
Fig. 5.9	Implementation of response residual space mapping in Agilent ADS.	91

LIST OF FIGURES

Fig. A.1	The modules of SMX.....	109
Fig. A.2	Illustration of the derivation of basic optimizer class.....	111
Fig. A.3	Case 1: The initial response of the HTS filter for the “fine” model (OSA90).....	112
Fig. A.4	Case 1: The optimal “fine” model (OSA90) response of the HTS filter.....	112
Fig. A.5	Case 2: The SMX optimized fine model (Agilent Momentum) response of the HTS filter.....	113
Fig. A.6	Case 2: The final Momentum optimized fine model response of the HTS filter with a fine interpolation step of 0.1mil.....	113
Fig. B.1	The aggressive SM may not converge to the optimal fine model solution in this case.....	116
Fig. B.2	The RRSM solves the problem in one iteration (two fine model evaluations).....	117
Fig. B.3	The multiple cheese-cutting problem: (a) the coarse model (b) and fine model.....	118
Fig. B.4	The ASM algorithm may not converge in this case.....	121
Fig. B.5	The response residual ASM algorithm converges in two iterations.....	123
Fig. B.6	Parameter errors between the ISM algorithm and minimax direct optimization. Here $x_f = 12.2808$ and $x_f^* = 12$	125
Fig. B.7	Case 1: $c_0 = 2, f_0 = 4$, the ISM solution is $\bar{x}_f = 12.2808$ vs. minimax solution $x_f = 12$; case 2: $c_0 = 4, f_0 = 4$, the ISM solution is $\bar{x}_f = 12$ vs. minimax solution $x_f = 12$	127
Fig. B.8	RRSM step-by-step iteration demonstration—different heights for the fine model.....	129
Fig. B.9	Parameter errors between the RRSM algorithm and minimax direct optimization. Here $x_f = 12.5$ and $x_f^* = 12.5$ in the final iteration (different heights for the fine model).....	130

LIST OF TABLES

TABLE 2.1 SPACE MAPPING CLASSIFICATION.....	33
TABLE 2.2 SPACE MAPPING CATEGORY EXPLANATION	34
TABLE 3.1 AGILENT MOMENTUM/SONNET <i>em</i> OPTIMIZABLE PARAMETER VALUES OF THE HTS FILTER	61
TABLE 3.2 THE INITIAL AND FINAL PREASSIGNED PARAMETERS OF THE CALIBRATED COARSE MODEL OF THE HTS FILTER	61
TABLE 4.1 OPTIMIZABLE PARAMETER VALUES OF THE HTS FILTER.....	69
TABLE 4.2 OPTIMIZABLE PARAMETER VALUES OF THE SIX- SECTION H-PLANE WAVEGUIDE FILTER	80
TABLE 5.1 OPTIMIZABLE PARAMETER VALUES OF THE THREE- SECTION IMPEDANCE TRANSFORMER.....	90
TABLE A.1 THE INITIAL AND FINAL DESIGNS OF THE FINE MODEL (OSA90) FOR THE HTS FILTER.....	114

LIST OF TABLES

Chapter 1

INTRODUCTION

The manufacturability-driven design and time-to-market products in the electronics industry demand powerful computer-aided design (CAD) techniques. As signal speed and frequency increase, conventional electrical models for components are no longer adequate. Design and modeling with physical/geometrical information, including electromagnetic (EM)/physics effects, become necessary.

The first CAD techniques in circuit design appeared in the sixties of the last century. Temes and Calahan (1967) advocated CAD technology for filter design. Since then design and modeling of microwave circuits applying optimization techniques have been extensively researched.

With the dramatic increase in computer hardware performance, EM simulators could be built to solve Maxwell's equations for circuits of arbitrary geometrical shapes. Analysis technologies such as the finite element method (FEM), the method of moments (MoM), etc., are used. Rautio and Harrington (1987a, 1987b) presented excellent agreement between EM field solvers and measurements. We can single out the High Frequency Structure Simulator

(HFSS) from Ansoft and HP (Agilent) as the flagship FEM solver(s) and the MoM product *em* from Sonnet Software as the benchmark planar solver.

Due to the computational expense of EM/physics models, simply substituting conventional equivalent electrical models by EM/physics models into the design optimization process will not work, because of extremely long or prohibitive computation. CAD procedures such as statistical analysis and yield optimization taking into account process variations and manufacturing tolerances in the components demands that the component models are accurate and fast so that design solutions can be achieved feasibly and reliably (Bandler, Cheng, Dakroury, Mohamed, Bakr, Madsen and Søndergaard, 2004, Steer, Bandler and Snowden, 2002). To achieve success in modern, high-frequency, circuit and systems design optimization, we need EM/physics-based component solutions on a much larger scale, a task beyond the reach of available design tools.

Space Mapping (SM) is an optimization concept, allowing expensive EM optimization to be performed efficiently with the help of fast and approximate “coarse” or surrogate models (Bandler, Cheng, Dakroury, Mohamed, Bakr, Madsen and Søndergaard, 2004, Steer, Bandler and Snowden, 2002, Bandler, Biernacki, Chen, Grobelny and Hemmers, 1994, Bandler, Biernacki, Chen, Hemmers and Madsen, 1995, Bakr, Bandler, Biernacki, Chen and Madsen, 1998, Bakr, Bandler, Madsen and Søndergaard, 2001, Bandler, Georgieva, Ismail, Rayas-Sánchez and Zhang, 2001, Bandler, Ismail and Rayas-Sánchez, 2002, Bakr, Bandler, Ismail, Rayas-Sánchez and Zhang, 2000, Bandler, Cheng,

Nikolova and Ismail, 2004). It has been applied with great success to otherwise expensive direct EM optimizations of microwave components and circuits with substantial computation speedup. Research is being carried out on mathematical motivation, to place SM into the context of classical optimization. The aim of SM is to achieve a satisfactory design solution with a minimal number of computationally expensive “fine” model evaluations. Procedures iteratively update and optimize surrogates based on fast physically-based “coarse” models.

Space mapping was first introduced by Bandler, Biernacki, Chen, Grobelny and Hemmers (1994). In its ten-year history, researchers explored a number of variations and enormously successful applications. The theory is still in its infancy, but SM is accepted by the mathematical and engineering communities as a significant contribution.

This thesis addresses advances in SM technology in the computer-aided modeling, design and optimization. An objective is to present our developments in modeling and optimization of microwave circuits. These developments include the SM framework and surrogate modeling for SM technology (Bandler, Cheng, Dakrouy, Mohamed, Bakr, Madsen and Søndergaard, 2004), implicit SM optimization exploiting preassigned parameters (Bandler, Cheng, Nikolova and Ismail, 2004), implicit, frequency and output SM surrogate modeling and design (Bandler, Cheng, Gebre-Mariam, Madsen, Pedersen and Søndergaard, 2003), an implementable SM design framework (Bandler, Cheng, Hailu and Nikolova, 2004) and various other implementations and applications.

Chapter 2 addresses basic concepts and notation of Space Mapping. We review the state of the art of SM technology and the SM-based surrogate (modeling) concept and applications in engineering optimization. We recall proposed approaches to SM-based optimization, including the original algorithm, the Broyden-based aggressive SM algorithm, various trust region approaches, neural space mapping and implicit space mapping. Different approaches to enhance uniqueness of parameter extraction are reviewed. Novel physical illustrations are presented, including the cheese-cutting problem. SM framework steps are extracted.

In Chapter 3, we discuss implicit SM (ISM) optimization exploiting preassigned parameters. We show how it relates to the well-established (explicit) SM between coarse and fine device models. Through comparison a general SM concept is proposed. A simple ISM algorithm is implemented. It is illustrated on a contrived “cheese-cutting problem” and applied to EM-based microwave modeling and design. An auxiliary set of parameters (selected preassigned parameters) is extracted to match the coarse model with the fine model. The calibrated coarse model (the surrogate) is then (re)optimized to predict a better fine model solution. The mapping itself is embedded in the calibrated coarse model and updated automatically in the procedure of parameter extraction. We illustrate our approach through optimization of an HTS filter using Agilent ADS (2000) with Momentum (2000) and Agilent ADS with Sonnet’s *em* (2001).

In Chapter 4, we discuss the enhancement of ISM by an “output space”

mapping (OSM) or specifically, “response residual space” mapping (RRSM) when the coarse and fine model cannot be aligned. We present a significant improvement to ISM for EM-based microwave modeling and design. ISM calibrates a suitable coarse (surrogate) model against a fine model (full-wave EM simulation) by relaxing certain coarse model preassigned parameters. Based on an explanation of residual response misalignment, our approach further fine-tunes the surrogate by exploiting RRSM. An accurate design of an HTS filter, easily implemented in Agilent ADS, emerges after only four EM simulations using ISM and RRSM with sparse frequency sweeps. We also present an RRSM approach. A new “multiple cheese-cutting” design problem illustrates the concept. Our approach is implemented entirely in the ADS framework. An H-plane filter design demonstrates the method.

In Chapter 5, we discuss a number of SM implementation frameworks and examples. We present and demonstrate an Agilent ADS schematic framework for SM. Using this framework, a number of SM techniques are implemented in ADS with Momentum, Sonnet *em*, and Agilent HFSS in an interactive way. We review significant practical applications done by various groups and researchers from different engineering and mathematical communities.

We conclude in Chapter 6 with some suggestions for future research.

The author contributed substantially to the following original developments presented in this thesis:

- (1) Development of a space-mapping framework for space mapping

algorithms.

- (2) Development of an implicit space-mapping algorithm to simplify microwave device design.
- (3) Development of an implicit and output space-mapping (RRSM) algorithm to fine-tune microwave designs.
- (4) Contribution to the review paper: “Space mapping: the state of the art.”
- (5) Implementation of the implicit and output space-mapping (RRSM) algorithm.
- (6) Development of the software package SMX to automate the SM optimization exploiting surrogates algorithm (Bakr, Bandler, Madsen, Rayas-Sánchez and Søndergaard, 2000).
- (7) Development of the demonstration “cheese-cutting” problem and “multiple cheese-cutting” problem.
- (8) Design of an ADS schematic framework for SM. Entirely within this framework, implicit SM and output space mappings (RRSM) are implemented.

Chapter 2

SPACE MAPPING: THE STATE OF THE ART

2.1 INTRODUCTION

Engineers have been using optimization techniques for device, component and system modeling and CAD for decades (Steer, Bandler and Snowden, 2002). The target of component design is to determine a set of physical parameters to satisfy certain design specifications. Traditional optimization techniques (Bandler, Kellermann and Madsen, 1985, Bandler and Chen, 1988) directly utilize the simulated responses and possibly available derivatives to force the responses to satisfy the design specifications. Circuit-theory based simulation and CAD tools using empirical device models are fast: analytical solutions or available exact derivatives may promote optimization convergence. Electromagnetic (EM) simulators, long used for design verification, need to be exploited in the optimization process. But the higher the fidelity (accuracy) of the simulation the more expensive direct optimization is expected to be. For complex problems this cost may be prohibitive.

Alternative design schemes combining the speed and maturity of circuit simulators with the accuracy of EM solvers are desirable. The recent exploitation

of iteratively refined surrogates of fine, accurate or high-fidelity models, and the implementation of Space Mapping (SM) methodologies (Bandler, Cheng, Dakroury, Mohamed, Bakr, Madsen and Søndergaard, 2004) address this issue. Through the construction of a space mapping, a suitable surrogate is obtained. This surrogate is faster than the “fine” model and at least as accurate as the underlying “coarse” model. The SM approach updates the surrogate to better approximate the corresponding fine model.

Bandler conceived the SM approach in 1993 for modeling and design of engineering devices and systems, e.g., RF and microwave components using EM simulators. Bandler *et al.* (1994, 1995) demonstrated how SM intelligently links companion “coarse” (ideal, fast or low-fidelity) and “fine” (accurate, practical or

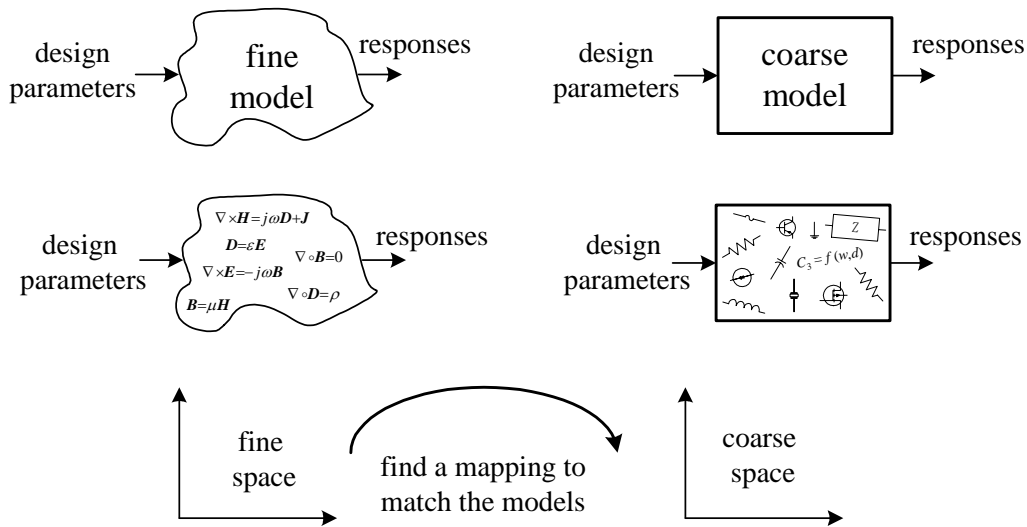


Fig. 2.1 Linking companion coarse (empirical) and fine (EM) models through a mapping.

high-fidelity) models of different complexities. An EM simulator could serve as a fine model. A low fidelity EM simulation or empirical circuit model could be a coarse model (see Fig. 2.1).

Generally, SM-based optimization algorithms comprise four steps.

- (1) fine model simulation (verification)
- (2) extraction of the parameters of a coarse or surrogate model
- (3) updating the surrogate
- (4) (re)optimization of the surrogate.

The original SM-based optimization algorithm was introduced by Bandler, Biernacki, Chen, Grobelny and Hemmers (1994), where a linear mapping is assumed between the parameter spaces of the coarse and fine models. It is evaluated by a least squares solution of the linear equations resulting from associating corresponding data points in the two spaces. Hence, the surrogate is a linearly mapped coarse model.

The aggressive space mapping (ASM) approach (Bandler, Biernacki, Chen, Hemmers and Madsen, 1995) eliminates the simulation overhead required in (Bandler, Biernacki, Chen, Grobelny and Hemmers, 1994) by exploiting each fine model iterate as soon as it is available. This iterate, determined by a quasi-Newton step, optimizes the (current) surrogate model.

Parameter Extraction (PE) is the key to establishing the mapping and updating the surrogate. In this step, the surrogate is locally aligned with a given fine model through various techniques. However, nonuniqueness of the PE step

may cause breakdown of the algorithm (Bandler, Biernacki and Chen, 1996).

Many approaches are suggested to improve the uniqueness of the PE step. Multi-point PE (Bandler, Biernacki and Chen, 1996, Bandler, Biernacki, Chen and Omeragic, 1999), a statistical PE (Bandler, Biernacki, Chen and Omeragic, 1999), a penalty PE (Bandler, Biernacki, Chen and Huang, 1997) and an aggressive PE (Bakr, Bandler and Georgieva, 1999) are such approaches. A recent gradient PE approach (Bandler, Mohamed, Bakr, Madsen and Søndergaard, 2002) takes into account not only the responses of the fine model and the surrogate, but the corresponding gradients w.r.t. design parameters as well.

A mathematical motivation (Bandler, Cheng, Dakroury, Mohamed, Bakr, Madsen and Søndergaard, 2004) places SM into the context of classical optimization based on local Taylor approximations. If the coarse model reflects the nonlinearity of the fine model then the space mapping is expected to involve less curvature (less nonlinearity) than the two physical models. The SM model is then expected to yield a good approximation over a large region, i.e., it generates large descent iteration steps. Close to the solution, however, only small steps are needed, in which case the classical optimization strategy based on local Taylor models is better. A combination of the two strategies gives the highest solution accuracy and fast convergence.

SM techniques require sufficiently faithful coarse models to assure good results. Sometimes the coarse model and fine models are severely misaligned, i.e., it is hard to make the PE process work. The hybrid aggressive SM algorithm

(Bakr, Bandler, Georgieva and Madsen, 1999) overcomes this by alternating between (re)optimization of a surrogate and direct response matching. More recently, the surrogate model based SM (Bakr, Bandler, Madsen, Rayas-Sánchez and Søndergaard, 2000) optimization algorithm combines a mapped coarse model with a linearized fine model and defaults to direct optimization of the fine model.

Neural space mapping approaches (Bandler, Ismail, Rayas-Sánchez and Zhang, 1999, Bakr, Bandler, Ismail, Rayas-Sánchez and Zhang, 2000, Bandler, Ismail, Rayas-Sánchez and Zhang, 2003) utilize Artificial Neural Networks (ANN) in EM-based modeling and design of microwave devices. This is consistent with the knowledge-based modeling techniques of Zhang and Gupta (2000). After updating an ANN-based surrogate (Bandler, Ismail, Rayas-Sánchez and Zhang, 1999), a fine model optimal design is predicted in NSM (Bakr, Bandler, Ismail, Rayas-Sánchez and Zhang, 2000) by (re)optimizing the surrogate. Neural inverse SM simplifies (re)optimization by inversely connecting the ANN (Bandler, Ismail, Rayas-Sánchez and Zhang, 2003). The next fine model iterate is then only an ANN evaluation.

The latest development of SM is implicit space mapping (ISM) (Bandler, Cheng, Nikolova and Ismail, 2004). An auxiliary set of parameters (selected preassigned parameters such as dielectric constant or substrate height) is extracted to match the coarse and fine model responses. The resulting (calibrated) coarse model, the surrogate, is then (re)optimized to evaluate the next iterate (fine model point).

The SMX (Bakr, Bandler, Cheng, Ismail and Rayas-Sánchez, 2001) system is a first attempt to automate SM optimization by linking different simulators.

The SM technology has been recognized as a contribution to engineering design (Zhang and Gupta, 2000, Hong and Lancaster, 2001, Conn, Gould and Toint, 2000, Bakr, 2000, Rayas-Sánchez, 2001, Ismail, 2001), especially in the microwave and RF arena. Zhang and Gupta (2000) have considered the integration of the SM concept into neural network modeling for RF and microwave design. Hong and Lancaster (2001) describe the aggressive SM algorithm as an elegant approach to microstrip filter design. Conn, Gould and Toint (2000) have stated that trust region methods have been effective in the SM framework, especially in circuit design. Bakr (2000) introduces advances in SM algorithms, Rayas-Sánchez (2001) employs artificial neural networks and Ismail (Ismail, 2001) studies SM-based model enhancement.

Mathematicians are addressing mathematical interpretations of the formulation and convergence issues of SM algorithms (Bakr, Bandler, Madsen and Søndergaard, 2001, Søndergaard, 1999, 2003a, Pedersen, 2001, Søndergaard, 2003b, Vicente, 2002, 2003a, 2003b). For example, Madsen's group (Bakr, Bandler, Madsen and Søndergaard, 2001, Søndergaard, 1999, 2003a, Pedersen, 2001) considers the SM as an effective preprocessor for engineering optimizations. Madsen and Søndergaard investigate convergence properties of SM algorithms (Madsen and Søndergaard, 2004). Vicente studies convergence

properties of SM for design using the least squares formulation (Vicente, 2002, 2003b), and introduces SM to solve optimal control problems (Vicente, 2003a).

2.2 THE SPACE MAPPING APPROACH

The SM approach introduced by Bandler, Biernacki, Chen, Grobelny and Hemmers (1994) involves a calibration of a physically-based “coarse” surrogate by a “fine” model to accelerate design optimization. This simple CAD methodology embodies the learning process of a designer. It makes effective use of the surrogate’s fast evaluation to sparingly manipulate the iterations of the fine model.

2.2.1 The Optimization Problem

The design optimization problem to be solved is given by

$$\mathbf{x}_f^* \triangleq \arg \min_{\mathbf{x}_f} U(\mathbf{R}_f(\mathbf{x}_f)) \quad (2-1)$$

where $\mathbf{R}_f \in \Re^{m \times 1}$ is a vector of m responses of the model, e.g., $|S_{11}|$ at m selected frequency points ω or sample points. $\mathbf{x}_f \in \Re^{n \times 1}$ is the vector of n design parameters and U is a suitable objective function. For example, U could be the minimax objective function with upper and lower specifications. \mathbf{x}_f^* is the optimal solution to be determined. It is assumed to be unique.

2.2.2 The Space Mapping Concept

As depicted in Fig. 2.2, the coarse and fine model design parameters are

denoted by \mathbf{x}_c and $\mathbf{x}_f \in \mathfrak{R}^{n \times 1}$, respectively. The corresponding response vectors are denoted by \mathbf{R}_c and $\mathbf{R}_f \in \mathfrak{R}^{m \times 1}$, respectively.

We propose to find a mapping \mathbf{P} relating the fine and coarse model parameters as

$$\mathbf{x}_c = \mathbf{P}(\mathbf{x}_f) \quad (2-2)$$

such that

$$\mathbf{R}_c(\mathbf{P}(\mathbf{x}_f)) \approx \mathbf{R}_f(\mathbf{x}_f) \quad (2-3)$$

in a region of interest.

Then we can avoid using direct optimization, i.e., solving (2-1) to find \mathbf{x}_f^* .

Instead, we declare $\bar{\mathbf{x}}_f$, given by

$$\bar{\mathbf{x}}_f \triangleq \mathbf{P}^{-1}(\mathbf{x}_c^*) \quad (2-4)$$

as a good estimate of \mathbf{x}_f^* , where \mathbf{x}_c^* is the result of coarse model optimization.

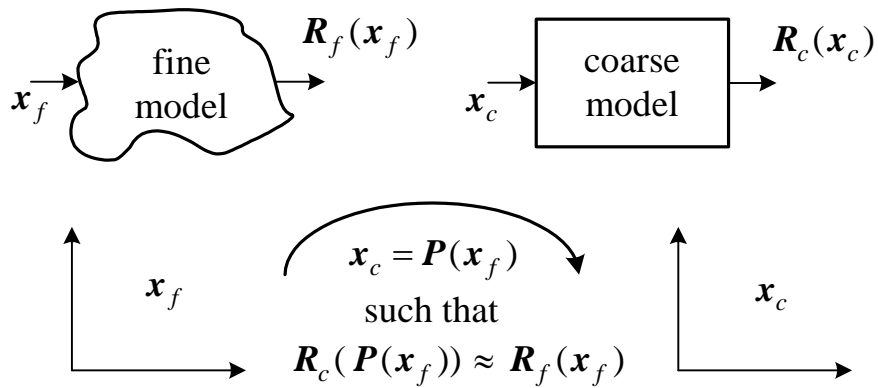


Fig. 2.2 Illustration of the fundamental notation of space mapping (Steer, Bandler and Snowden, 2002).

2.2.3 Jacobian Relationships

Using (2-2), the Jacobian of \mathbf{P} is given by

$$\mathbf{J}_P \triangleq \mathbf{J}_P(\mathbf{x}_f) = \left(\frac{\partial \mathbf{P}^T}{\partial \mathbf{x}_f} \right)^T = \left(\frac{\partial (\mathbf{x}_c^T)}{\partial \mathbf{x}_f} \right)^T \quad (2-5)$$

An approximation to the mapping Jacobian is designated by the matrix $\mathbf{B} \in \mathfrak{R}^{n \times n}$, i.e., $\mathbf{B} \approx \mathbf{J}_P(\mathbf{x}_f)$. Using (2-3) we obtain (Bakr, Bandler, Georgieva and Madsen, 1999)

$$\mathbf{J}_f \approx \mathbf{J}_c \mathbf{B} \quad (2-6)$$

where \mathbf{J}_f and \mathbf{J}_c are the Jacobians of the fine and coarse models, respectively. This relation can be used to estimate the fine model Jacobian if the mapping is already established.

An expression for \mathbf{B} which satisfies (2-6) can be derived as (Bakr, Bandler, Georgieva and Madsen, 1999)

$$\mathbf{B} = (\mathbf{J}_c^T \mathbf{J}_c)^{-1} \mathbf{J}_c^T \mathbf{J}_f \quad (2-7)$$

If the coarse and fine model Jacobians are available, the mapping can be established through (2-7), provided that \mathbf{J}_c has full rank and $m \geq n$.

2.2.4 Interpretation of Space Mapping Optimization

SM algorithms initially optimize the coarse model to obtain the optimal design \mathbf{x}_c^* , for instance in the minimax sense. Subsequently, a mapped solution is found by minimizing the objective function $\|\mathbf{g}\|_2^2$, where \mathbf{g} is defined by

$$\mathbf{g} = \mathbf{g}(\mathbf{x}_f) \triangleq \mathbf{R}_f(\mathbf{x}_f) - \mathbf{R}_c(\mathbf{x}_c^*) \quad (2-8)$$

Correspondingly, according to Bakr, Bandler, Madsen and Søndergaard (2001), $\mathbf{R}_c(\mathbf{P}(\mathbf{x}_f))$ is optimized in the effort of finding a solution to (2-1). Here, $\mathbf{R}_c(\mathbf{P}(\mathbf{x}_f))$ is an expression of an “enhanced” coarse model or “surrogate.” Thus, the problem formulation can be rewritten as

$$\bar{\mathbf{x}}_f = \arg \min_{\mathbf{x}_f} U(\mathbf{R}_c(\mathbf{P}(\mathbf{x}_f))) \quad (2-9)$$

where $\bar{\mathbf{x}}_f$ may be close to \mathbf{x}_f^* if \mathbf{R}_c is close enough to \mathbf{R}_f . If \mathbf{x}_c^* is unique then the solution of (2-9) is equivalent to driving the following residual vector \mathbf{f} to zero

$$\mathbf{f} = \mathbf{f}(\mathbf{x}_f) \triangleq \mathbf{P}(\mathbf{x}_f) - \mathbf{x}_c^* \quad (2-10)$$

2.3 ORIGINAL SPACE MAPPING APPROACH

In this approach (Bandler, Biernacki, Chen, Grobelny and Hemmers, 1994), an initial approximation of the mapping, $\mathbf{P}^{(0)}$ is obtained by performing fine model analyses at a pre-selected set of at least m_0 base points, $m_0 \geq n+1$. A corresponding set of coarse model points is then constructed through the parameter extraction (PE) process

$$\mathbf{x}_c^{(j)} \triangleq \arg \min_{\mathbf{x}_c} \left\| \mathbf{R}_f(\mathbf{x}_f^{(j)}) - \mathbf{R}_c(\mathbf{x}_c) \right\| \quad (2-11)$$

The additional $m_0 - 1$ points apart from $\mathbf{x}_f^{(1)}$ are required to establish full-rank conditions leading to the first mapping approximation $\mathbf{P}^{(0)}$. Bandler, Biernacki, Chen, Grobelny and Hemmers (1994) assumed a linear mapping between the two spaces, i.e.,

$$\mathbf{x}_c = \mathbf{P}^{(j)}(\mathbf{x}_f) = \mathbf{B}^{(j)}\mathbf{x}_f + \mathbf{c}^{(j)} \quad (2-12)$$

where $\mathbf{B}^{(j)} \in \Re^{n \times n}$ and $\mathbf{c}^{(j)} \in \Re^{n \times 1}$.

At the j th iteration, the sets of points in the two spaces may be expanded to contain, in general, m_j points which are used to establish the updated mapping $\mathbf{P}^{(j)}$. Since the analytical form of \mathbf{P} is not available, SM uses the current approximation $\mathbf{P}^{(j)}$, to estimate \mathbf{x}_f^* at the j th iteration as

$$\bar{\mathbf{x}}_f \approx \mathbf{x}_f^{(m_j+1)} = (\mathbf{P}^{(j)})^{-1}(\mathbf{x}_c^*) \quad (2-13)$$

The process continues iteratively until $\mathbf{R}_f(\mathbf{x}_f^{(m_j+1)})$ is close enough to $\mathbf{R}_c(\mathbf{x}_c^*)$. If so, $\mathbf{P}^{(j)}$ is assumed close enough to our desired \mathbf{P} . If not, the set of base points in the fine space is augmented by $\mathbf{x}_f^{(m_j+1)}$, and $\mathbf{x}_c^{(m_j+1)}$, as determined by (2-11), augments the set of base points in the coarse space. Upon termination, we set the SM design as in (2-13).

This algorithm is simple but has pitfalls. First, m_0 upfront high-cost fine model analyses are needed. Second, a linear mapping may not be valid for significantly misaligned models. Third, nonuniqueness in the PE process may lead to an erroneous mapping estimation and algorithm breakdown.

2.4 AGGRESSIVE SPACE MAPPING APPROACH

The aggressive SM algorithm (Bandler, Biernacki, Chen, Hemmers and Madsen, 1995) incorporates a quasi-Newton iteration using the classical Broyden formula (1965). A rapidly improved design is anticipated following each fine

model simulation, while the bulk of the computational effort (optimization, parameter extraction) is carried out in the coarse model space.

2.4.1 Theory

The aggressive SM technique iteratively solves the nonlinear system

$$\mathbf{f}(\mathbf{x}_f) = \mathbf{0} \quad (2-14)$$

for \mathbf{x}_f . Note, from (2-10), that at the j th iteration, the error vector $\mathbf{f}^{(j)}$ requires an evaluation of $\mathbf{P}^{(j)}(\mathbf{x}_f^{(j)})$. This is executed indirectly through the PE (evaluation of $\mathbf{x}_c^{(j)}$). Coarse model optimization produces \mathbf{x}_c^* .

The quasi-Newton step in the fine space is given by

$$\mathbf{B}^{(j)}\mathbf{h}^{(j)} = -\mathbf{f}^{(j)} \quad (2-15)$$

where $\mathbf{B}^{(j)}$, the approximation of the mapping Jacobian \mathbf{J}_p defined in (2-5), is updated using Broyden's rank one update. Solving (2-15) for $\mathbf{h}^{(j)}$ provides the next iterate $\mathbf{x}_f^{(j+1)}$

$$\mathbf{x}_f^{(j+1)} = \mathbf{x}_f^{(j)} + \mathbf{h}^{(j)} \quad (2-16)$$

The algorithm terminates if $\|\mathbf{f}^{(j)}\|$ becomes sufficiently small. The output of the algorithm is an approximation to $\bar{\mathbf{x}}_f = \mathbf{P}^{-1}(\mathbf{x}_c^*)$ and the mapping matrix \mathbf{B} .

The matrix \mathbf{B} can be obtained in several ways.

2.4.2 Unit Mapping

A “steepest-descent” approach may succeed if the mapping between the two spaces is essentially represented by a shift. In this case Broyden's updating

formula is not utilized. We can solve (2-15) keeping the matrix $\mathbf{B}^{(j)}$ fixed at $\mathbf{B}^{(j)} = \mathbf{I}$. Bila, Baillargeat, Verdeyme, Guillon (1998) and Pavio (1999) utilized this special case.

2.4.3 Broyden-like Updates

An initial approximation to \mathbf{B} can be taken as $\mathbf{B}^{(0)} = \mathbf{I}$, the identity matrix. $\mathbf{B}^{(j)}$ can be updated using Broyden’s rank one formula (1965)

$$\mathbf{B}^{(j+1)} = \mathbf{B}^{(j)} + \frac{\mathbf{f}^{(j+1)} - \mathbf{f}^{(j)} - \mathbf{B}^{(j)}\mathbf{h}^{(j)}}{\mathbf{h}^{(j)T}\mathbf{h}^{(j)}}\mathbf{h}^{(j)T} \quad (2-17)$$

When $\mathbf{h}^{(j)}$ is the quasi-Newton step, (2-17) can be simplified using (2-15) to

$$\mathbf{B}^{(j+1)} = \mathbf{B}^{(j)} + \frac{\mathbf{f}^{(j+1)}}{\mathbf{h}^{(j)T}\mathbf{h}^{(j)}}\mathbf{h}^{(j)T} \quad (2-18)$$

2.4.4 Jacobian Based Updates

If we have exact Jacobians w.r.t. \mathbf{x}_f and \mathbf{x}_c at corresponding points we can use them to obtain \mathbf{B} at each iteration through a least squares solution (Bandler, Mohamed, Bakr, Madsen and Søndergaard, 2002, Bakr, Bandler, Georgieva and Madsen, 1999) as given in (2-7).

Note that \mathbf{B} can be fed back into the PE process and iteratively refined before making a step in the fine model space.

Hybrid schemes can be developed following the integrated gradient approximation approach to optimization (Bandler, Chen, Daijavad and Madsen, 1988). One approach incorporates finite difference approximations and the

Broyden formula (Bandler, Mohamed, Bakr, Madsen and Søndergaard, 2002). Finite difference approximations could provide initial estimates of \mathbf{J}_f and \mathbf{J}_c . These are then used to obtain a good approximation to $\mathbf{B}^{(0)}$. The Broyden formula is subsequently used to update \mathbf{B} .

2.4.5 Constrained Update

On the assumption that the fine and coarse models share the same physical background, Bakr, Bandler, Madsen and Søndergaard (2000) suggested that \mathbf{B} could be better conditioned in the PE process if it is constrained to be close to the identity matrix \mathbf{I} by letting

$$\mathbf{B} = \arg \min_{\mathbf{B}} \left\| \begin{bmatrix} \mathbf{e}_1^T & \cdots & \mathbf{e}_n^T & \eta \Delta \mathbf{b}_1^T & \cdots & \eta \Delta \mathbf{b}_n^T \end{bmatrix}^T \right\|_2^2 \quad (2-19)$$

where η is a user-assigned weighting factor, \mathbf{e}_i and $\Delta \mathbf{b}_i$ are the i th columns of \mathbf{E} and $\Delta \mathbf{B}$, respectively, defined as

$$\begin{aligned} \mathbf{E} &= \mathbf{J}_f - \mathbf{J}_c \mathbf{B} \\ \Delta \mathbf{B} &= \mathbf{B} - \mathbf{I} \end{aligned} \quad (2-20)$$

The analytical solution of (2-19) is given by

$$\mathbf{B} = (\mathbf{J}_c^T \mathbf{J}_c + \eta^2 \mathbf{I})^{-1} (\mathbf{J}_c^T \mathbf{J}_f + \eta^2 \mathbf{I}) \quad (2-21)$$

2.4.6 Cheese-cutting Problem

This simple physical example, depicted in Fig. 2.3, demonstrates the aggressive SM approach. Our “response” is *weight*. The designable parameter is *length*. A density of one is assumed. The goal is a desired *weight*.

Our idealized “coarse” model is a uniform cuboidal block (top block of Fig. 2.3). The optimal *length* x_c^* is easily calculated.

Let the actual block (“fine” model) be similar but imperfect (second block of Fig. 2.3). We take the optimal coarse model *length* as the initial guess for the fine model solution, i.e., cutting the cheese so that $x_f^{(1)} = x_c^*$. This does not satisfy our goal. We realign our coarse model to match the outcome of the cut. This is a PE step in which we obtain a solution $x_c^{(1)}$ (third block of Fig. 2.3). Thus, we have corresponding values $x_f^{(1)}$ and $x_c^{(1)}$. Assuming a unit mapping, we can write for $j = 1$

$$x_f^{(j+1)} = x_f^{(j)} + x_c^* - x_c^{(j)} \quad (2-22)$$

to predict the next fine model *length* (last block of Fig. 2.3).

Note that we assume that the actual block (fine model) perfectly matches its coarse model, except for the missing piece; also that the first and second attempts (cuts) to achieve our goal are confined to a uniform section. Our goal is achieved in one SM step, a result consistent with expectations.

Observe that the *length* of the coarse model is shrunk during PE to match our first outcome. The difference between the proposed initial *length* of the block and the shrunk *length* is applied through the (unit) mapping to predict a new cut. This procedure can be repeated until the goal is satisfied.

2.5 PARAMETER EXTRACTION

Parameter Extraction (PE) is crucial to successful SM. Typically, an

optimization process extracts the parameters of a coarse model or surrogate to match the fine model. Inadequate response data in the PE process may lead to nonunique solutions. Sufficient data to overdetermine a solution should be sought. For example, we may use responses such as real and imaginary parts of the S -parameters in the PE even though the design criteria may include the magnitude of S_{11} only.

2.5.1 Single Point Parameter Extraction (SPE)

The traditional SPE (Bandler, Biernacki, Chen, Grobelny and Hemmers, 1994) is described by the optimization problem given in (2-11). It is simple and works in many cases.

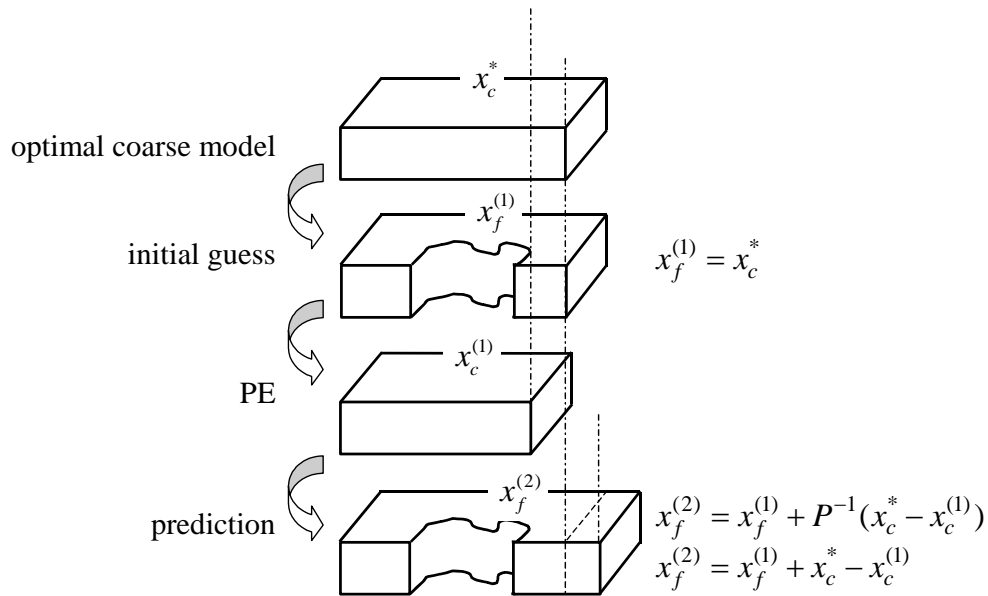


Fig. 2.3 Cheese-cutting problem solved by aggressive space mapping of model lengths.

2.5.2 Multipoint Parameter Extraction (MPE)

The MPE approach (Bandler, Biernacki and Chen, 1996, Bandler, Biernacki, Chen and Omeragic, 1999) simultaneously matches the responses at a number of corresponding points in the coarse and fine model spaces. A more reliable algorithm is presented by Bakr, Bandler, Biernacki, Chen and Madsen (1998) and improved by Bakr, Bandler and Georgieva (1999).

2.5.3 Statistical Parameter Extraction

Bandler, Biernacki, Chen and Omeragic suggest a statistical approach to PE. The SPE process is initiated from several starting points and is declared unique if consistent extracted parameters are obtained. Otherwise, the best solution is selected.

2.5.4 Penalized Parameter Extraction

Another approach is suggested in (Bandler, Biernacki, Chen and Huang, 1997). Here, the point $\mathbf{x}_c^{(j+1)}$ is obtained by solving the penalized SPE process

$$\mathbf{x}_c^{(j+1)} = \arg \min_{\mathbf{x}_c} \left\| \mathbf{R}_c(\mathbf{x}_c) - \mathbf{R}_f(\mathbf{x}_f^{(j+1)}) \right\| + w \left\| \mathbf{x}_c - \mathbf{x}_c^* \right\| \quad (2-23)$$

where w is a user-assigned weighting factor.

2.5.5 PE Involving Frequency Mapping

Alignment of the models might be achieved by simulating the coarse model at a transformed set of frequencies (Bandler, Ismail, Rayas-Sánchez and

Zhang, 1999). For example, an EM model of a microwave structure usually exhibits a frequency shift w.r.t. an idealized representation. Also, available quasi-static empirical models exhibit good accuracy over a limited range of frequencies, which can be alleviated by frequency transformation. Frequency mapping introduces new degrees of freedom (Bakr, Bandler, Madsen, Rayas-Sánchez and Søndergaard, 2000).

A suitable mapping can be as simple as frequency shift and scaling given by Bandler, Biernacki, Chen, Hemmers and Madsen (1995)

$$\omega_c = P_\omega(\omega) \triangleq \sigma\omega + \delta \tag{2-24}$$

where σ represents a scaling factor and δ is an offset (shift).

The approach can be divided into two phases (Bandler, Biernacki, Chen, Hemmers and Madsen, 1995). In *Phase 1*, we determine σ_0 and δ_0 that align \mathbf{R}_f and \mathbf{R}_c in the frequency domain. This is done by finding

$$\arg \min_{\sigma_0, \delta_0} \left\| \mathbf{R}_c(\mathbf{x}_c, \sigma_0\omega_i + \delta_0) - \mathbf{R}_f(\mathbf{x}_f) \right\|, \quad i = 1, 2, \dots, k \tag{2-25}$$

In *Phase 2*, the coarse model point \mathbf{x}_c is extracted to match \mathbf{R}_c with \mathbf{R}_f , starting with $\sigma = \sigma_0$ and $\delta = \delta_0$. Three algorithms (Bandler, Biernacki, Chen, Hemmers and Madsen, 1995) can implement this phase: a sequential algorithm and two exact-penalty function algorithms, one using the l_1 norm and the other is suitable for minimax optimization (Bandler, Biernacki, Chen, Hemmers and Madsen, 1995).

2.5.6 Gradient Parameter Extraction (GPE)

GPE (Bandler, Mohamed, Bakr, Madsen and Søndergaard, 2002) exploits the availability of exact Jacobians \mathbf{J}_f and \mathbf{J}_c . At the j th iteration $\mathbf{x}_c^{(j)}$ is obtained through a GPE process. GPE matches not only the responses but also the derivatives of both models through the optimization problem.

This approach reflects the idea of the MPE (Bandler, Biernacki and Chen, 1996) process, but permits the use of exact or implementable sensitivity techniques (Bandler, Zhang and Biernacki, 1988, Bandler, Zhang, Song and Biernacki, 1990, Alessandri, Mongiardo and Sorrentino, 1993, Georgieva, Glavic, Bakr and Bandler, 2002a, 2002b, Nikolova, Bandler and Bakr, 2004). Finite differences can be employed to estimate derivatives if exact ones are unavailable.

2.5.7 Other Considerations

We can broaden the scope of parameters that are varied in an effort to match the coarse (surrogate) and fine models. We already discussed the scaling factor and shift parameters in the frequency mapping. We can also consider neural weights in neural SM, preassigned parameters in implicit SM, mapping coefficients \mathbf{B} , etc., as in the generalized SM tableau approach (Bandler, Georgieva, Ismail, Rayas-Sánchez and Zhang, 2001) and surrogate model-based SM (Bakr, Bandler, Madsen, Rayas-Sánchez and Søndergaard, 2000).

2.6 EXPANDED SPACE MAPPING EXPLOITING PREASSIGNED PARAMETERS

A design framework for microwave circuits is proposed by Bandler, Ismail and Rayas-Sánchez (2002). The original SM technique is expanded by allowing some preassigned parameters (which are not used in optimization) to change in some components of the coarse model (Bandler, Ismail and Rayas-Sánchez, 2002). Those components are referred to as “relevant” components and a method based on sensitivity analysis is used to identify them. As a result, the coarse model can be calibrated to align with the fine model.

The concept of calibrating coarse models (circuit based models) to align with fine models (typically an EM simulator) in microwave circuit design has been exploited by several authors (Bandler, Biernacki, Chen, Grobelny and Hemmers, 1994, Bandler, Georgieva, Ismail, Rayas-Sánchez and Zhang, 2001, Ye and Mansour, 1997). In Bandler, Biernacki, Chen, Grobelny and Hemmers (1994) and Bandler, Georgieva, Ismail, Rayas-Sánchez and Zhang (2001), this calibration is performed by means of optimizable parameter space transformation known as space mapping. In Ye and Mansour (1997), this is done by adding circuit components to nonadjacent individual coarse model elements. Here, the SM technique is expanded to calibrating the coarse model by allowing some preassigned parameters (we call them key preassigned parameters (KPP)) to change in certain coarse model components.

Examples of KPP are dielectric constant and substrate height in microstrip structures. It is assumed that the coarse model consists of several components such as transmission lines, junctions, etc. The coarse model is decomposed into two sets of components. The KPPs are allowed to change in the first set and are kept intact in the second set. Ismail (2001) presents a method based on sensitivity analysis to perform this decomposition.

At each iteration, the Expanded Space Mapping Design Framework (ESMDF) algorithm calibrates the coarse model by extracting the KPP such that the coarse model matches the fine model. Then it establishes a mapping from some of the optimizable parameters to the KPP. The mapped coarse model (the coarse model with the mapped KPP) is then optimized subject to a trust region size. The optimization step is accepted only if it results in an improvement in the fine model objective function. The trust region size is updated (Bakr, Bandler, Biernacki, Chen and Madsen, 1998, Alexandrov, Dennis, Lewis and Torczon, 1998, Søndergaard, 1999) according to the agreement between the fine and mapped coarse model. Therefore, the algorithm enhances the coarse model at each iteration either by extracting the KPP and updating the mapping or by reducing the region in which the mapped coarse model is to be optimized. The algorithm terminates if one of certain relevant stopping criteria is satisfied. Possible practical stopping criteria are elaborated in (Ismail, 2001). Some solutions to overcome the problems associated with the KPP extraction process is also presented.

2.7 OUTPUT SPACE MAPPING

The “output” or response SM concept could address a residual misalignment in the optimal responses of the coarse and fine models. For example, a coarse model such as $R_c = x^2$ will never match the fine model $R_f = x^2 - 2$ around its minimum with any mapping $x_c = P(x_f)$, $x_c, x_f \in \mathfrak{R}$. An “output” or response mapping can overcome this deficiency by introducing a transformation of the coarse model response based on a Taylor approximation (Dennis, 2001, 2002). Current research is directed to this topic (Bandler, Cheng, Gebre-Mariam, Madsen, Pedersen and Søndergaard, 2003).

2.8 DISCUSSION OF SURROGATE MODELING AND SPACE MAPPING

2.8.1 Building and Using Surrogates (Dennis)

In his summarizing comments (Dennis, 2000) on the Workshop on Surrogate Modelling and Space Mapping (2000) Dennis integrates the terminology “coarse” and “fine” from the SM community with his own. Dennis uses the term “surrogate” to denote the function s to which an optimization routine is applied in lieu of applying optimization to the fine model f . Another piece of terminology he uses is “surface” to denote a function (it may be vector valued) trained to fit or to smooth fine model data.

Dennis mentions several ways to choose fine model data sites, also known as experimental designs. The surfaces are generated from the data sites. He notes

that “surfaces (are) designed to correct a coarse model and to be combined with the coarse model to act as a surrogate in optimization.” Then he used the surface concept to interpret SM. Here, “The surrogate is the coarse model applied to the image of the fine model parameters under the space mapping surface.”

Dennis discusses “heuristics” that optimize the surrogate and (perhaps) correct the surface part of the surrogate. He classifies SM in terms of “local space mappings and methods that use poised designs implicitly or explicitly approximate derivatives. The former do this by Broyden updates and the latter by the derivatives of the surface.”

Dennis’s definition of surrogate agrees with our definition in the sense that the surrogate is an enhanced coarse model. Dennis regards the mapping as a surface.

We think of the mapping as that part of the surrogate, an approximation to which needs to be updated in each iteration. The mapping (surface) is the same during all iterations.

2.8.2 Building and Using Surrogates

In an editorial, Bandler and Madsen (2001) emphasize that “surrogate optimization” refers to the process of applying an optimization routine directly to a coarse model, a surrogate, which is a function (or a model) that replaces the original fine model. Some surrogates attempt to fit the fine model directly (e.g., by polynomials), in other cases the information gained during the optimization

process is used to train the surrogate to fit the data derived from evaluation of the fine model (e.g., by artificial neural networks). In the SM approach, coarse models may be enhanced by mapping (transforming, correcting) the optimization variables. In this case, surrogates of increasing fidelity are developed during the optimization process.

2.8.3 The Space Mapping Concept

The SM-based optimization algorithms we review have four major steps. The first is fine model simulation (verification). The fine model is verified and checked to see if it satisfies the design specifications. The second is PE, in which the coarse model is (re)aligned with the fine model to permit (re)calibration. The third is updating or (re)mapping the surrogate using the information obtained from the first two steps. At last the aligned, calibrated, mapped or enhanced coarse model (the surrogate) is (re)optimized. This suggests a new fine model design iterate.

2.8.4 Space Mapping Framework Optimization Steps

A flowchart of general SM is shown in Fig. 2.4.

Step 1 Select a coarse model suitable for the fine model.

Step 2 Select a mapping process (original, aggressive SM, neural or ISM, etc.)

Step 3 Optimize the coarse model (initial surrogate) w.r.t. design parameters.

Step 4 Simulate the fine model at this solution.

Step 5 Terminate if a stopping criterion is satisfied, e.g., response meets specifications.

Step 6 Apply parameter extraction using preassigned parameters (Bandler, Ismail and Rayas-Sánchez, 2002), neuron weights (Bandler, Ismail, Rayas-Sánchez and Zhang, 1999), coarse space parameters, etc.

Step 7 Rebuild surrogate (may be implied within Step 6 or Step 8).

Step 8 Reoptimize the “mapped coarse model” (surrogate) w.r.t. design parameters (or evaluate the inverse mapping if it is available).

Step 9 Go to Step 4.

Comments

As shown in Fig. 2.4, we use symbol Δ , \times and \circ to represent Step 6, 7 and 8, respectively. We let operator (\cdot) represent implied. We can see that rebuilding the surrogate (Step 7) may be implied in either the PE process (Step 6) or in the reoptimization (Step 8). Steps 6, 7 and 8 are separate steps in neural space mapping (training data is obtained by parameter extraction, the surrogate is rebuilt by the neural network training process and prediction is obtained by evaluating the neural network). However, Step 7 may be implied in either the parameter extraction process (Step 6), e.g., ISM, where the surrogate is rebuilt by extracting preassigned parameters, or in the prediction (Step 8), e.g., aggressive SM, where the surrogate is not explicitly rebuilt. Step 6 can be termed modeling

for some cases.

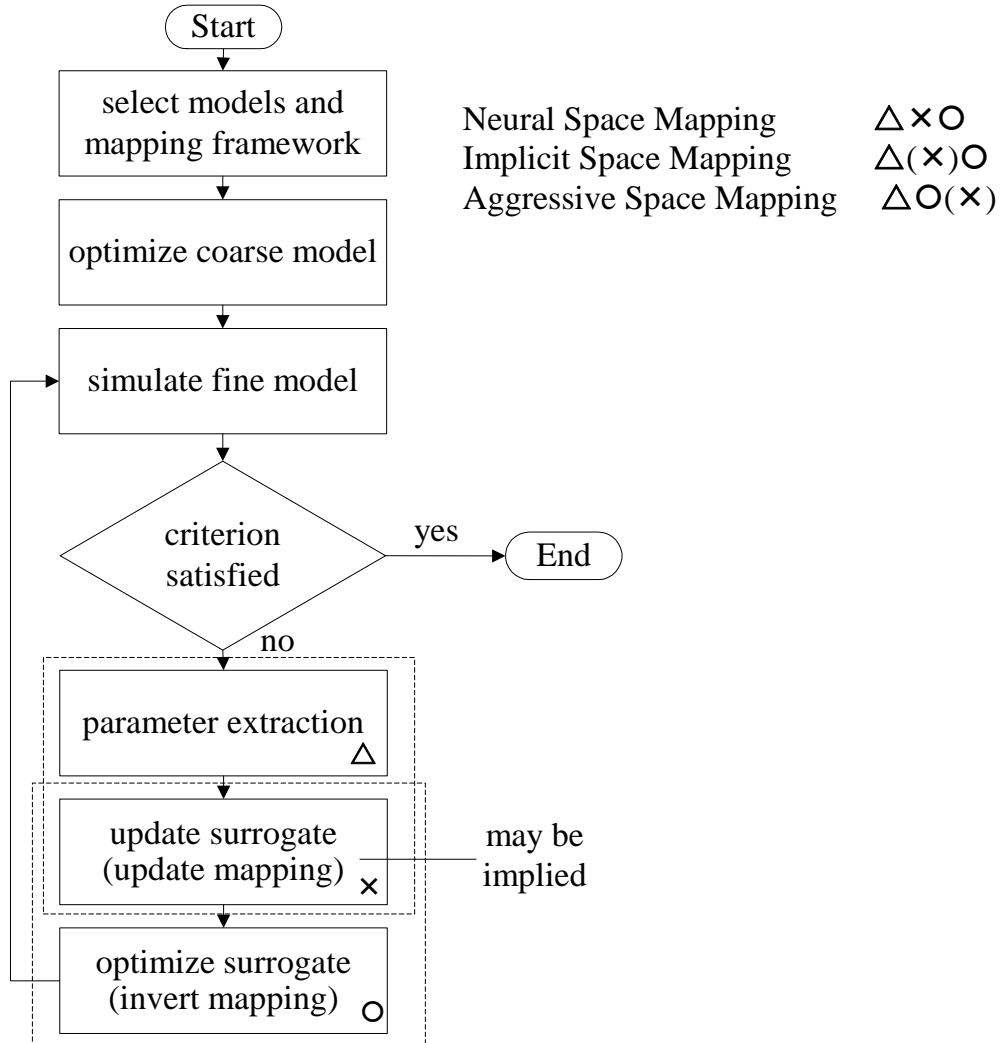


Fig. 2.4 Space mapping framework.

2.8.5 Space Mapping Classification

TABLE 2.1 classifies SM. In this table, a number of SM technologies are categorized in 3 types: explicit/input, implicit and output SM. Their properties are in two categories: model alignment and fine model prediction. Each category has a few sub-categories to specify the details of the SM techniques. TABLE 2.2

shows the explanations of these categories.

TABLE 2.1
SPACE MAPPING CLASSIFICATION

		<i>explicit SM/input SM</i>						<i>ISM</i>	<i>OSM</i>		
		<i>original SM</i>	<i>ASM</i>	<i>NISM</i>	<i>SMN</i>	<i>neural SM</i>	<i>tableau approach</i>		<i>partial SM</i>	<i>IOSM</i>	<i>SMIS</i>
<i>aligning surrogate/ realign (updating) surrogate</i>	<i>using upfront fine model points</i>	•			•	•	•				
	<i>fine model gradient required</i>		• ¹					•		•	
	<i>multi-point PE</i>	•	•				•	•	• ¹	•	
	<i>by design parameters</i>	•	•	•				•			
	<i>by non-designable parameters</i>			• ²	•	•	•		• ³	•	•
	<i>model generation</i>	•			•	•	•		•	•	•
	<i>linear mapping</i>	•	•	• ⁴	• ⁴	• ⁴	•	•		• ⁵	•
	<i>nonlinear mapping</i>			•	•	•			•	• ⁶	
<i>predicting fine model</i>	<i>by optimizing surrogate</i>				• ⁷	•	• ⁷		•	•	•
	<i>by inverting mapping⁸</i>	•	•					•			
	<i>by evaluating inverse mapping</i>			•							

¹ applicable but not implemented

² extract neural weights

³ extract preassigned parameters

⁴ for single-layer perceptron case

⁵ output SM only

⁶ implicit SM only

⁷ modeling approach, can be used in optimization

⁸ by solving system of equations

TABLE 2.2
SPACE MAPPING CATEGORY EXPLANATION

category	explanation
using upfront fine model points	using more than one fine model point to start the design
fine model gradient required	using fine model Jacobian in the loop
multi-point PE	using several points to extract parameters
by design parameters	extracting designable parameters in PE
by non-designable parameters	extracting non-designable parameters in PE
model generation	a calibrated model (surrogate) is available for modeling purposes
linear mapping	the mapping is linear
nonlinear mapping	the mapping is nonlinear
by optimization surrogate	obtain the prediction by optimizing the surrogate
by inverting mapping	obtain the prediction by inverting the mapping i.e. solving a system of equations
by evaluating inverse mapping	obtain the prediction by evaluating the inverse mapping

2.9 CONCLUSIONS

In this chapter we reviewed the SM techniques and the SM-oriented surrogate (modeling) concept and their applications in engineering design optimization. The simple CAD methodology follows the traditional experience

and intuition of engineers, yet appears to be amenable to rigorous mathematical treatment. The aim and advantages of SM are described. The general steps for building surrogates and SM are indicated. Proposed approaches to SM-based optimization include the original SM algorithm, the Broyden-based aggressive space mapping, trust region aggressive space mapping, hybrid aggressive space mapping, neural space mapping and implicit space mapping. Parameter extraction is an essential subproblem of any SM optimization algorithm. It is used to align the surrogate with the fine model at each iteration. Different approaches to enhance the uniqueness of parameter extraction are reviewed, including the gradient parameter extraction process.

A design framework we call expanded space mapping exploiting preassigned parameters is reviewed. This technique expands original space mapping allowing some preassigned parameters (which are not used in optimization) to change in some components of the coarse model. The mapped coarse model is then optimized subject to a trust region size.

SM concepts and an SM framework are discussed. SM techniques are categorized through their properties.

Chapter 3

IMPLICIT SPACE MAPPING OPTIMIZATION

3.1 INTRODUCTION

In this chapter, we introduce the idea of implicit space mapping (ISM) (Bandler, Cheng, Nikolova and Ismail, 2004) and show how it relates to the well-established (explicit) SM between coarse and fine device models. Through comparison a general SM concept is proposed. A simple ISM algorithm is implemented. It is illustrated on a contrived “cheese-cutting problem” and is applied to EM-based microwave modeling and design. An auxiliary set of parameters (selected preassigned parameters) is extracted to match the coarse model with the fine model. The calibrated coarse model (the surrogate) is then (re)optimized to predict a better fine model solution. This is an easy SM technique to implement since the mapping itself is embedded in the calibrated coarse model and updated automatically in the procedure of parameter extraction. We illustrate our approach through optimization of an HTS filter using Agilent ADS with Momentum and Agilent ADS with Sonnet’s *em*.

In Bandler, Biernacki, Chen, Grobelny and Hemmers (1994), Bandler, Biernacki, Chen, Hemmers and Madsen (1995), Bandler, Ismail, Rayas-Sánchez

and Zhang (1999), Bakr, Bandler, Madsen, Rayas-Sánchez and Søndergaard (2000), a calibration is performed through a mapping between optimizable design parameters of the fine model and precisely corresponding parameters of the coarse model such that their responses match. This mapping is iteratively updated. In Ye and Mansour (1997), the coarse model is calibrated against the fine model by adding circuit components to nonadjacent individual coarse model elements. The component values are updated iteratively. The ES MDF algorithm (Bandler, Ismail and Rayas-Sánchez, 2002) calibrates the coarse model by extracting certain preassigned parameters such that corresponding responses match. It establishes an explicit mapping from the optimizable design parameters to preassigned (non-optimized) parameters.

The ISM approach does not establish an explicit mapping. We suggest an indirect approach. In each iteration we extract selected preassigned parameters to match the coarse model with the fine model. With these preassigned parameters now fixed, we reoptimize the calibrated coarse model. Then we assign its optimized design parameters to the fine model. We repeat this process until the fine model response is sufficiently close to the target response. The preassigned parameters, which are updated, calibrate the “mapping”.

Examples of preassigned parameters are physical parameters such as dielectric constant in microstrip structures, geometrical parameters such as substrate height or mathematical concepts such as frequency transformation parameters. Typically, they are not optimized but clearly they influence the

responses. As in Bandler, Ismail and Rayas-Sánchez (2002) we allow the preassigned parameters (of the coarse model) to change in some components and keep them intact in others. We implement our technique in Agilent ADS (2000).

3.2 SPACE MAPPING TECHNOLOGY

We categorize space mapping into (1) the original or explicit SM and (2) implicit space mapping. Both share the concept of “coarse” and “fine” models. Both use an iterative approach to update the mapping and predict the new design.

3.2.1 Explicit Space Mapping

In explicit SM, we should be able to draw a clear distinction between a physical coarse model and the mathematical mapping that links it to the fine

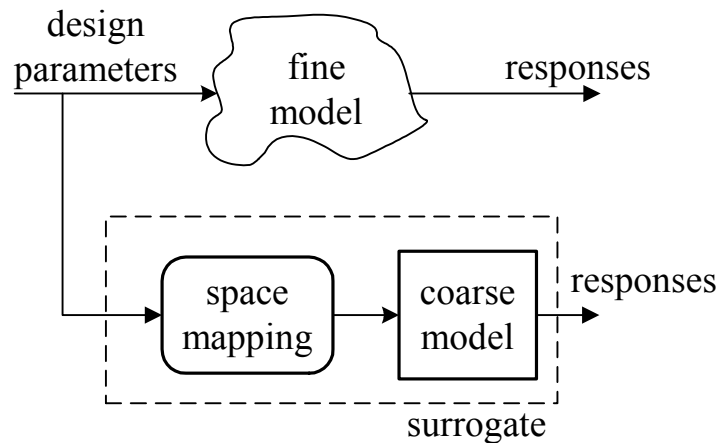


Fig. 3.1 Illustration of explicit SM.

model. See Fig. 3.1. Here, the mapping together with the coarse model constitute a “surrogate”. In each iteration, only the mapping is updated, while the physical coarse model is kept fixed. If the inverse mapping is available at each iteration, then the solution (best current prediction of the fine model) can be evaluated directly. Otherwise an optimization is performed on the mapping itself (not the mapped coarse model) to obtain the prediction. Examples of explicit SM are the original SM (Bandler, Biernacki, Chen, Grobelny and Hemmers, 1994), aggressive SM (Bandler, Biernacki, Chen, Hemmers and Madsen, 1995), neural SM (Bandler, Ismail, Rayas-Sánchez and Zhang, 1999), etc.

3.2.2 Implicit Space Mapping

Sometimes identifying the mapping is not obvious: it may be buried within the coarse model. If the “mapping” is integrated with the coarse model, the (mapped) coarse model becomes a calibrated coarse model or enhanced coarse model, which we also call a “surrogate”. See Fig. 3.2(a) (the rectangular box). In the next step, the calibrated or enhanced coarse model is optimized to obtain an “inverse” mapped solution. If the implicitly mapped model is not sufficiently good after calibration, we may add an explicit mapping or output mapping (Bandler, Cheng, Dakrouy, Mohamed, Bakr, Madsen and Søndergaard, 2004, Bandler, Cheng, Gebre-Mariam, Madsen, Pedersen and Søndergaard, 2003). See Fig. 3.2(b).

Both explicit and implicit SM iteratively calibrate the mapped model when approaching the fine model solution. Interestingly, the explicit mapping could be

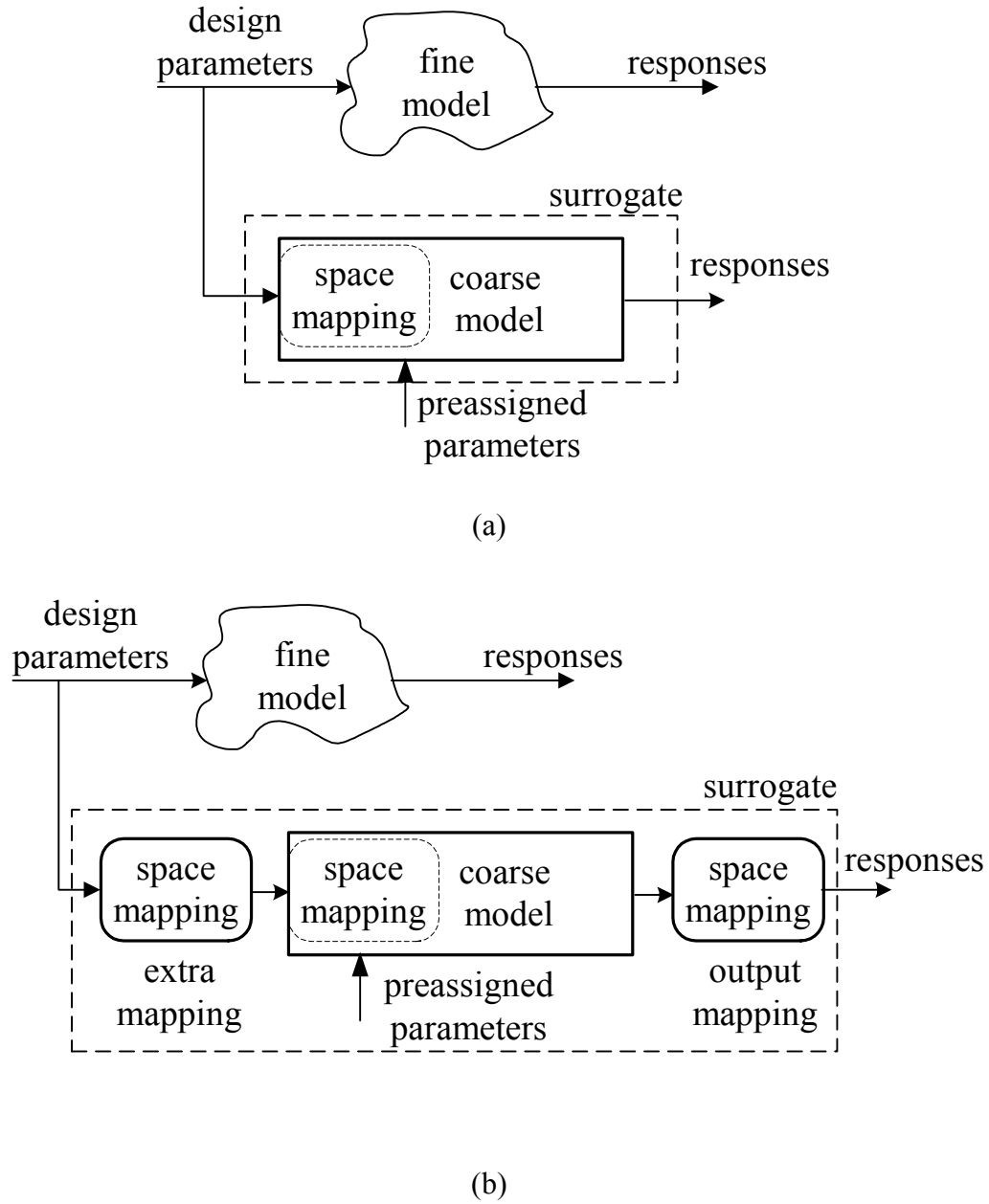


Fig. 3.2 Illustration of ISM, (a) implicit mapping within the surrogate, (b) with extra mapping and output mapping.

expressed in the form of ISM by using a simple mathematical substitution. We discuss this in Section 3.3.

3.3 IMPLICIT SPACE MAPPING (ISM): THE CONCEPT

3.3.1 Implicit Space Mapping

At the j th iteration, we denote by $\mathbf{x}_c^{*(j)}$ a coarse model optimum point (usually designable parameters) for given $\mathbf{x}^{(j)}$, a set of other (auxiliary) parameters, for example, preassigned parameters. The corresponding coarse model (the surrogate) response vector is $\mathbf{R}_c(\mathbf{x}_c^{*(j)}, \mathbf{x}^{(j)})$.

As indicated in Fig. 3.3, at the j th iteration, ISM aims at establishing an implicit mapping \mathbf{Q} between the spaces \mathbf{x}_f , \mathbf{x}_c and \mathbf{x} . We solve

$$\mathbf{Q}(\mathbf{x}_f, \mathbf{x}_c, \mathbf{x}) = \mathbf{0} \quad (3-1)$$

w.r.t. \mathbf{x} to obtain $\mathbf{x}^{(j)}$ indirectly by an optimization algorithm, during which we set

$$\mathbf{x}_f = \mathbf{x}_c = \mathbf{x}_c^{*(j-1)} \quad (3-2)$$

such that

$$\mathbf{R}_f(\mathbf{x}_c^{*(j-1)}) \approx \mathbf{R}_c(\mathbf{x}_c^{*(j-1)}, \mathbf{x}^{(j)}) \quad (3-3)$$

over a region in the parameter space. We think of this as a *modeling* procedure, also referred to as parameter extraction in this case.

As in Fig. 3.4, ISM then utilizes the mapping to obtain a *prediction* of \mathbf{x}_f .

Here, we set

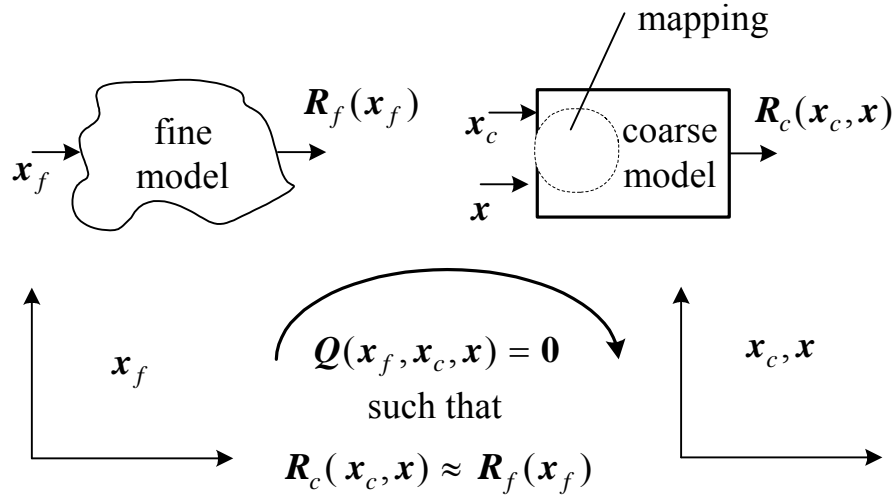


Fig. 3.3 Illustration of ISM modeling. Here, $Q = 0$ is solved for x .

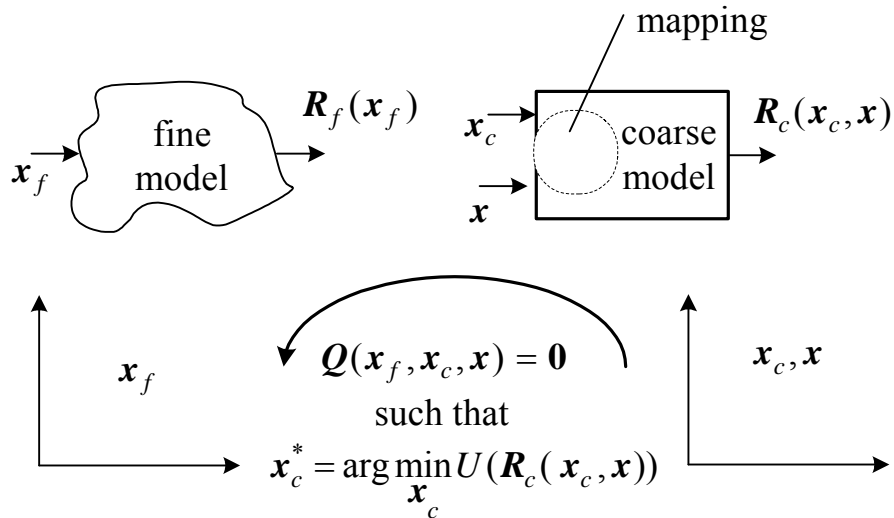


Fig. 3.4 Illustration of ISM prediction. Here, $Q = 0$ is solved for x_c^* .

$$\mathbf{x} = \mathbf{x}^{(j)} \quad (3-4)$$

where $\mathbf{x}^{(j)}$ is obtained from the foregoing modeling procedure. Since the mapping is usually nonlinear and implicit, the prediction is obtainable by optimizing a mapped coarse model or surrogate, i.e., we find

$$\mathbf{x}_c^{*(j)} \triangleq \arg \min_{\mathbf{x}_c} U(\mathbf{R}_c(\mathbf{x}_c, \mathbf{x}^{(j)})) \quad (3-5)$$

Then the fine model parameters are assigned (predicted) as

$$\mathbf{x}_f = \mathbf{x}_c^{*(j)} \quad (3-6)$$

In general, ISM optimization obtains a space-mapped design $\bar{\mathbf{x}}_f$ whose response approximates an optimized \mathbf{R}_c target. $\bar{\mathbf{x}}_f$ is a solution, found iteratively, of the nonlinear system (3-1) which is enforced through a parameter extraction (modeling) w.r.t. \mathbf{x} , and subsequent prediction of the fine model solution (through optimization of the calibrated coarse model).

3.3.2 Interpretation and Insight

As mentioned before, the mapping is buried in the coarse model. However, we can synthesize examples to develop insight into ISM, i.e., we can construct and connect a known mapping to a physical coarse model to study the behavior of the mapping. See Fig. 3.5. A set of intermediate parameters \mathbf{x}_i is introduced for this purpose.

In a physically based simulation, design parameters such as physical length and width of a microstrip line can be mapped to intermediate parameters

such as electrical length and characteristic impedance through well-known empirical formulas (Pozar, 1998). The mapping may, in that case, be extractable (detachable), and it can be (re)optimized to obtain an “inverse” mapped solution (the prediction). For a library of microstrip components, the transformation from circuit parameters to physical parameters may be implicit, and the intermediate parameters may not be directly accessible. The prediction is then obtained through optimizing suitably (the preassigned parameters of) calibrated microstrip components.

Assuming the intermediate parameters x_i are accessible, a corresponding hidden mapping in the modeling procedure can be thought of as finding

$$x_i^{(j)} = \mathbf{P}(x_c^{*(j-1)}, \mathbf{x}) \tag{3-7}$$

to match the coarse and fine model responses.

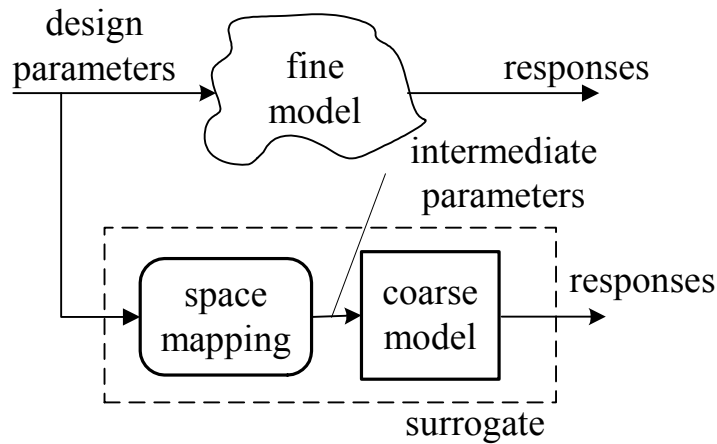


Fig. 3.5 Synthetic illustration of ISM optimization with intermediate parameters.

Let \mathbf{x}_i^* be the intermediate solution producing coarse model optimum \mathbf{R}_c^* .

Correspondingly, the prediction procedure can then be expressed as

$$\mathbf{x}_c^{*(j)} = \mathbf{P}^{-1}(\mathbf{x}_i^*, \mathbf{x}^{(j)}) \quad (3-8)$$

3.3.3 Relationship with Explicit Space Mapping

The first step in all SM-based algorithms results in an optimal coarse model design \mathbf{x}_c^* for given nominal preassigned parameters \mathbf{x} . The corresponding response is denoted by \mathbf{R}_c^* . Once obtained, \mathbf{x}_c^* is fixed, as seen in Fig. 3.6(a). In ISM, on the other hand, $\mathbf{x}_c^{*(j)}$ starts with \mathbf{x}_c^* and depends on the current value of \mathbf{x} and will change from iteration to iteration through reoptimization, as in Fig. 3.6(b).

An interesting point that relates the ISM to the explicit mapping is when we set the preassigned parameters at j th iteration

$$\mathbf{x}^{(j)} = \Delta \mathbf{x}_c^{(j)} \triangleq \mathbf{x}_c^{(j)} - \mathbf{x}_c^{*(j-1)} \quad (3-9)$$

where $\mathbf{x}_c^{(j)}$ is obtained through parameter extraction. We can show that after the modeling procedure, the prediction is

$$\mathbf{x}_f^{(j)} = \mathbf{x}_f^{(j-1)} + \mathbf{x}_c^* - \mathbf{x}_c^{(j)} \quad (3-10)$$

This agrees with the steps of aggressive space mapping (Bandler, Biernacki, Chen, Hemmers and Madsen, 1995) using a unit mapping. The ISM in this case, is consistent with the original SM with the difference, highlighted in Fig. 3.6, that ISM extracts $\Delta \mathbf{x}_c$ rather than \mathbf{x}_c during parameter extraction.

In the case of neuro SM (Bandler, Ismail, Rayas-Sánchez and Zhang, 1999), if we set

$$\mathbf{x} = \mathbf{w} \tag{3-11}$$

where \mathbf{w} represents the weights of the neurons, then by associating the artificial neural networks (ANN) with the coarse model, neuro space mapping is representable by ISM. Preassigned parameters \mathbf{x} could also represent other variables such as the space mapping parameters \mathbf{B} , \mathbf{c} , σ , and δ , in the SM-based surrogate approach (Bakr, Bandler, Madsen, Rayas-Sánchez and Søndergaard, 2000), in frequency SM (Bandler, Biernacki, Chen, Hemmers and Madsen, 1995),

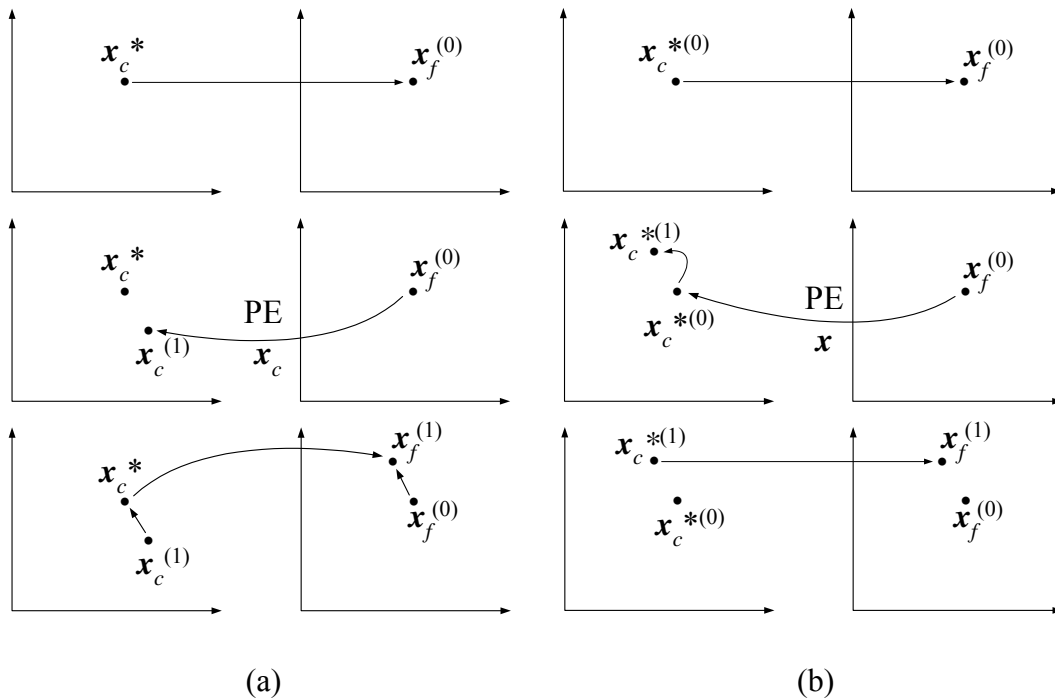


Fig. 3.6 When we set the preassigned parameters $\mathbf{x} = \Delta\mathbf{x}_c$, ISM is consistent with the explicit SM process. (a) The original SM. (b) The ISM process interpreted in the same spaces.

etc.

3.3.4 Cheese-Cutting Illustration

The ISM process can be demonstrated by a simple example, the cheese-cutting problem, depicted in Fig. 3.7. The goal is to deliver a segment of cheese of *weight* 30 units (target “response”). The “coarse” model is a cuboidal block (top block in Fig. 3.7). A unity density and a cross-section of 3 by 1 units are assumed. The “fine” model has a corresponding cuboidal shape with a defect of 6 missing units of *weight* (the second block from top).

A *length* of 10 units will give 30 units of *weight* for the coarse model (top block in Fig. 3.7). An unbiased cut of the same length in the fine model weighs 24 units (fine model evaluation). The *width* (preassigned parameter) of the (coarse) model is shrunk to 2.4 units to match the fine model weight (parameter extraction). A reoptimization of the *length* of the calibrated coarse model (the surrogate) is performed to achieve the goal. Then the new *length* of 12.5 units is assigned to the irregular block (fine model). The procedure continues in this manner until the irregular block is sufficiently close to the desired *weight* of 30 units. From the illustration, we see that the error reaches 1% after 3 iterations.

ISM, in this case, is an *indirect* approach. A *direct* approach would extract the *length* in the parameter extraction process.

The weight of the coarse cheese model can be written as

$$R_c(l, w) = l \times w \times h$$

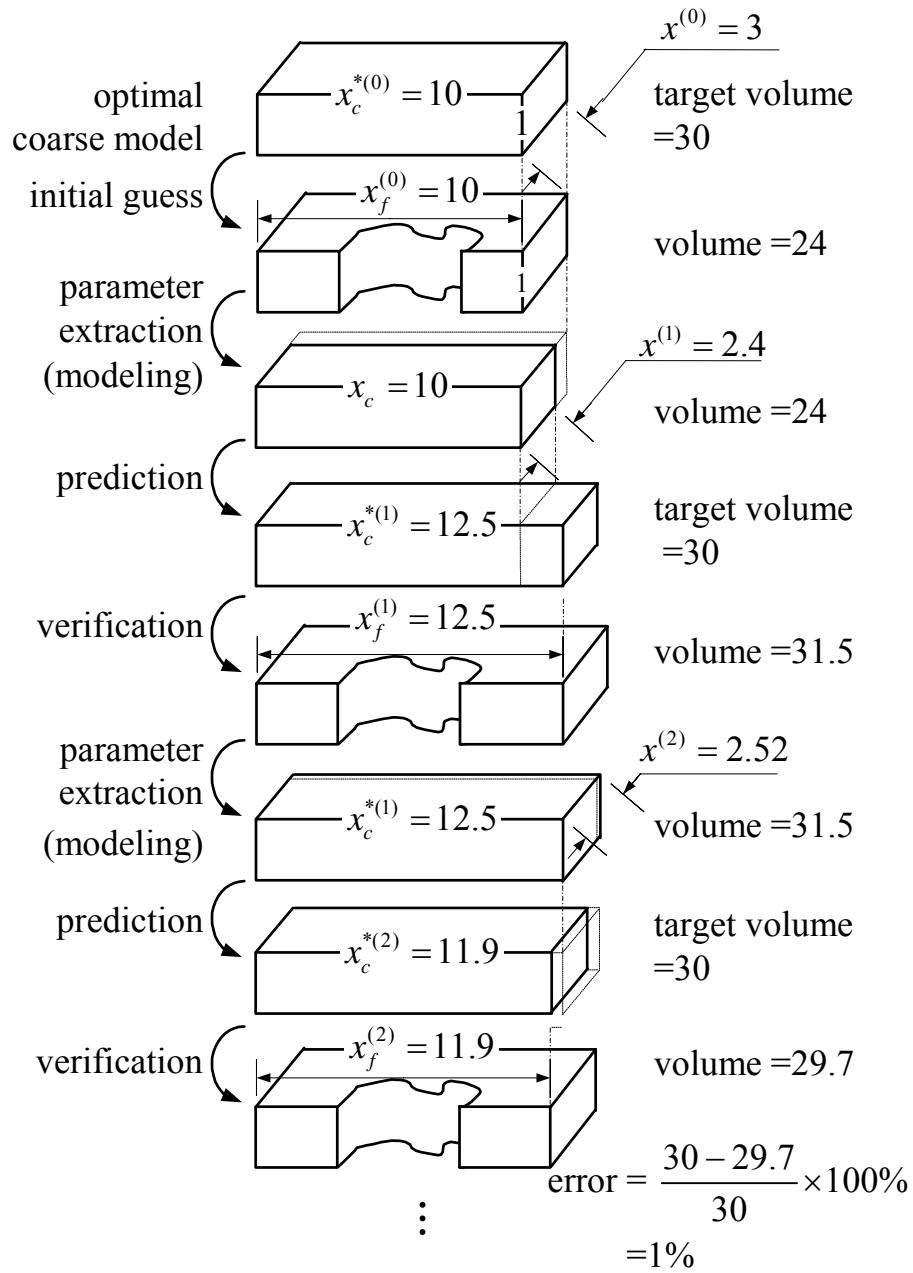


Fig. 3.7 Cheese-cutting problem—a demonstration of the ISM algorithm.

where l , w and h are the length, width and height, respectively, as in Fig. 3.8. An intermediate variable x_i is the area

$$x_i = w \times l$$

We can see that each prediction procedure returns x_i to a fixed $x_i^* = 30$, which produces the optimal coarse model design. We can feed the parameters and variables of the cheese-cutting problem in implicit SM diagram as shown in Fig. 3.9.

3.3.5 Three-section 3:1 Microstrip Transformer Illustration

We use an example of the three-section microstrip impedance transformer (Bakr, Bandler, Biernacki and Chen, 1997). The filter structure is shown in Fig. 3.10(a). The fine model utilizes a full-wave electromagnetic simulator (Agilent Momentum (2000)). The coarse model utilizes the empirical transmission line circuit models available in the circuit simulator Agilent ADS Schematic (2000) and the circuit parameters are converted (implicitly mapped) into physical dimensions of the microstrip lines using well-known empirical formulas (Pozar, 1998). The coarse model is shown in Fig. 3.10(b). The designable parameters are the width and physical length of each microstrip line. The intermediate variables x_i are the circuit parameters.

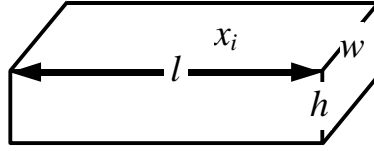


Fig. 3.8 Cheese-cutting problem—illustration of an intermediate parameter, $x_i = w \times l$.

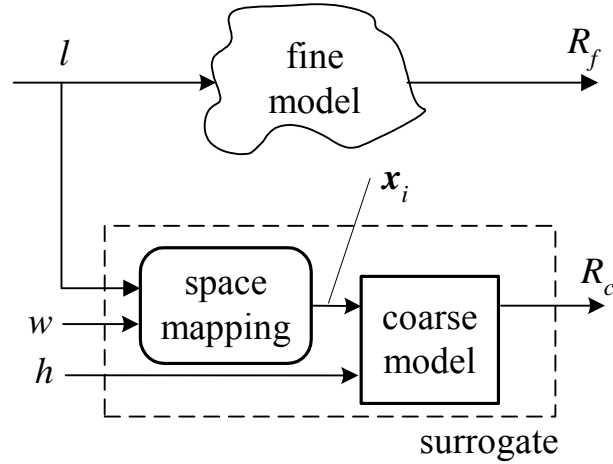


Fig. 3.9 Implicit space mapping diagram for cheese problem.

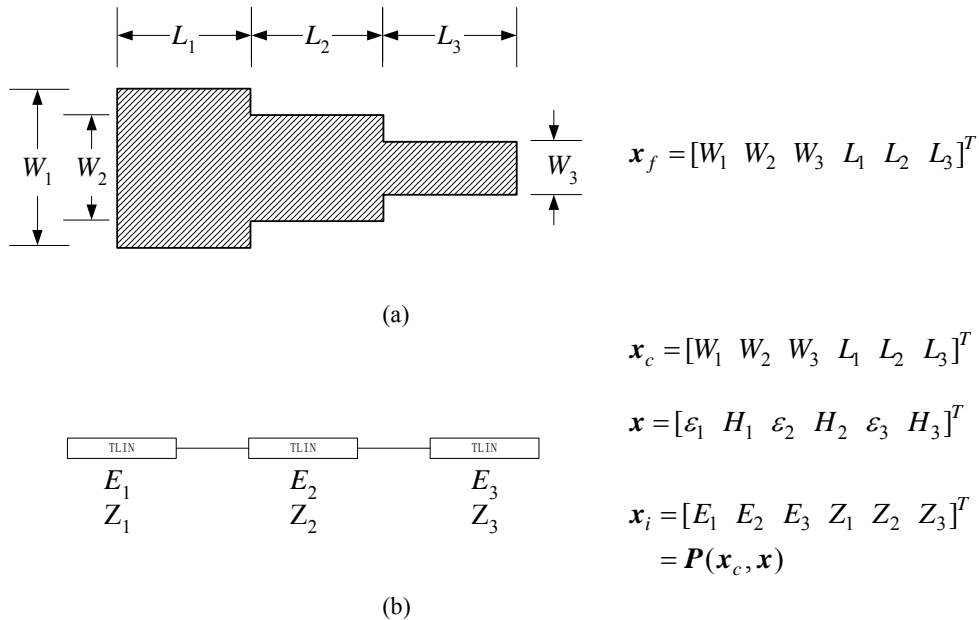


Fig. 3.10 Three-section 3:1 microstrip transformer illustration.

3.4 IMPLICIT SPACE MAPPING (ISM): AN ALGORITHM

In Fig. 3.11 we represent a microwave circuit whose coarse model is decomposed. We catalog the preassigned parameters into two sets as in (Bandler, Ismail and Rayas-Sánchez, 2002). In Set A, we vary certain preassigned parameters \mathbf{x} . In Set B, we keep preassigned parameters \mathbf{x}_0 fixed. We can follow the sensitivity approach of Bandler, Ismail and Rayas-Sánchez (2002) to formally select components for Sets A and B.

As implied in Fig. 3.11(b), in each iteration of the parameter extraction process we set

$$\mathbf{x}_c = \mathbf{x}_f^{(j)} \quad (3-12)$$

Notice also that we do not explicitly establish a mapping between the optimizable parameters and the preassigned parameters. This contrasts with Bandler, Ismail and Rayas-Sánchez (2002), where the mapping is explicit (see Fig. 3.11(c)). Therefore, our proposed approach is easier to implement in commercial microwave simulators.

The algorithm is summarized as follows

Step 1 Select candidate preassigned parameters \mathbf{x} as in Bandler, Ismail and Rayas-Sánchez (2002) or through experience.

Step 2 Set $j = 0$ and initialize $\mathbf{x}^{(0)}$.

Step 3 Obtain the optimal (calibrated) *coarse model* parameters by solving (3-5).

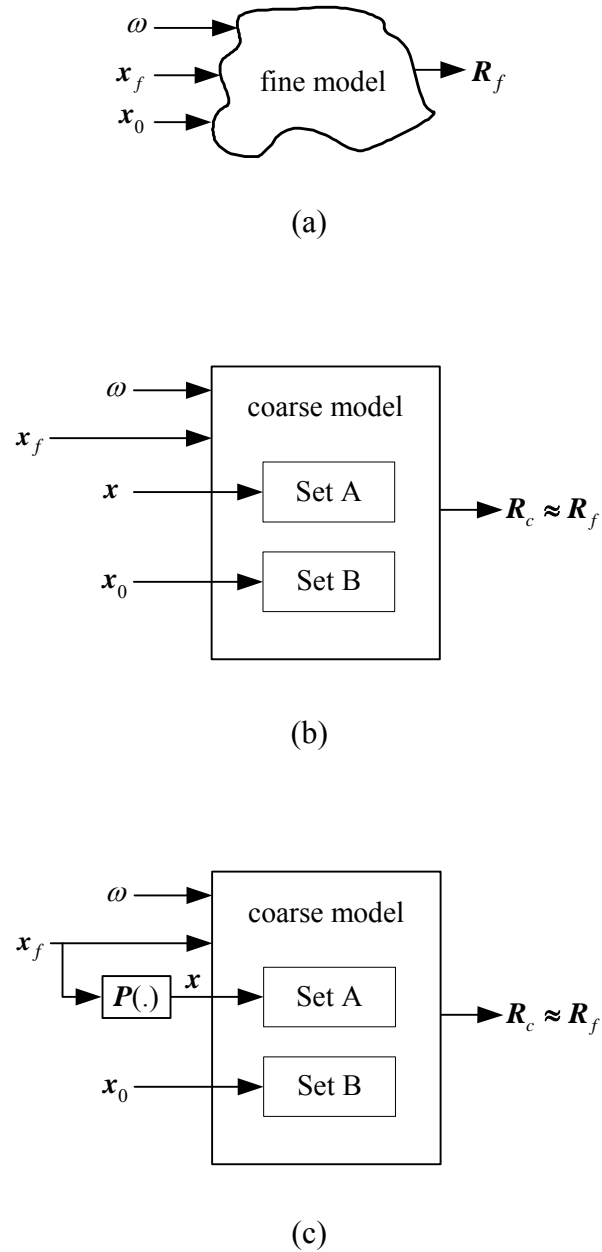


Fig. 3.11 Calibrating (optimizing) the preassigned parameters x in Set A results in aligning the coarse model (b) or (c) with the fine model (a). In (c) we illustrate the ESMDF approach (Bandler, Ismail and Rayas-Sánchez, 2002), where $P(\cdot)$ is a mapping from optimizable design parameters to preassigned parameters.

Step 4 Predict $\mathbf{x}_f^{(j)}$ from (3-6).

Step 5 Simulate the fine model at $\mathbf{x}_f^{(j)}$.

Step 6 Terminate if a stopping criterion (e.g., response meets specifications) is satisfied.

Step 7 Calibrate the coarse model by extracting (parameter extraction step) the preassigned parameters \mathbf{x} (noting (3-12))

$$\mathbf{x}^{(j+1)} = \arg \min_{\mathbf{x}} \left\| \mathbf{R}_f(\mathbf{x}_f^{(j)}) - \mathbf{R}_c(\mathbf{x}_f^{(j)}, \mathbf{x}) \right\| \quad (3-13)$$

Step 8 Increment j and go to Step 3.

3.5 FREQUENCY IMPLICIT SPACE MAPPING

Frequency implicit SM is a special kind of implicit SM. In each iteration, we extract selected frequency transforming preassigned parameters to match the updated surrogate model with the fine model. Then we assign its optimized design parameters to the fine model. We repeat this process until the fine model response is sufficiently close to the target (optimal original coarse model) response.

Algorithm

Step 1 Select a coarse model and a fine model.

Step 2 Select the frequency transformation and initialize associated preassigned parameters. For example, we can use a linear transformation of frequency $\omega_c = \sigma\omega + \delta$ (Bandler, Biernacki,

Chen, Hemmers and Madsen, 1995). The preassigned parameters are then $[\sigma \delta]^T$, initialized as $[1 \ 0]^T$.

Step 3 Optimize the coarse model (initial surrogate) w.r.t. design parameters.

Step 4 Simulate the fine model at this solution.

Step 5 Terminate if a stopping criterion is satisfied, e.g., response meets specifications.

Step 6 Apply parameter extraction (PE) to extract frequency transforming preassigned parameters.

Step 7 Reoptimize the “frequency mapped coarse model” (surrogate) w.r.t. design parameters (or evaluate the inverse mapping if it is available).

Step 8 Go to Step 4.

Examples involving frequency implicit SM have been investigated.

3.6 HTS FILTER EXAMPLE

We consider the HTS bandpass filter of Bandler, Biernacki, Chen, Getsinger, Grobelny, Moskowitz and Talisa (1995). The physical structure is shown in Fig. 3.12(a). Design variables are the lengths of the coupled lines and the separation between them, namely,

$$\mathbf{x}_f = [S_1 \ S_2 \ S_3 \ L_1 \ L_2 \ L_3]^T$$

The substrate used is lanthanum aluminate with $\varepsilon_r = 23.425$, $H = 20$ mil and

substrate dielectric loss tangent of 0.00003. The length of the input and output lines is $L_0=50$ mil and the lines are of width $W=7$ mil. We choose ε_r and H as the preassigned parameters of interest, thus $\mathbf{x}_0=[20 \text{ mil } 23.425]^T$. The design specifications are

$$|S_{21}| \leq 0.05 \quad \text{for } \omega \geq 4.099 \text{ GHz and for } \omega \leq 3.967 \text{ GHz}$$

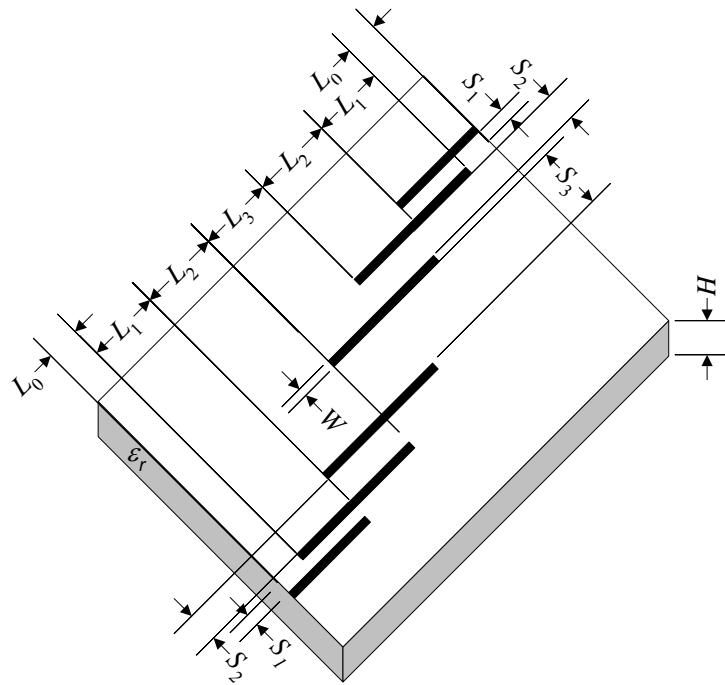
$$|S_{21}| \geq 0.95 \quad \text{for } 4.008 \text{ GHz} \leq \omega \leq 4.058 \text{ GHz}$$

This corresponds to 1.25% bandwidth.

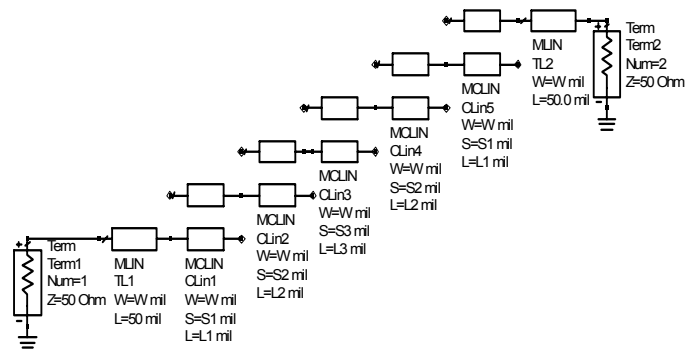
Our Agilent ADS (2000) coarse model consists of empirical models for single and coupled microstrip transmission lines, with ideal open stubs. See Fig. 3.12(b). Set A (Fig. 3.11(b)) consists of the three coupled microstrip lines. Notice the symmetry in the HTS structure, i.e., coupled lines “CLin5” are identical to “CLin1” and “CLin4” to “CLin2”. Here, Set B (Fig. 3.11(b)) is empty. The preassigned parameter vector is

$$\mathbf{x} = [\varepsilon_{r1} \ H_1 \ \varepsilon_{r2} \ H_2 \ \varepsilon_{r3} \ H_3]^T$$

The fine model is simulated first by Agilent Momentum (2000). The relevant responses at the initial solution are shown in Fig. 3.13(a), where we notice severe misalignment. The algorithm requires 2 iterations (3 fine model simulations). The total time taken is 26 min (one fine model simulation takes approximately 9 min on an Athlon 1100 MHz). Responses at the final iteration are shown in Fig. 3.13(b). Sonnet *em* (2001) has also been used as a fine model.



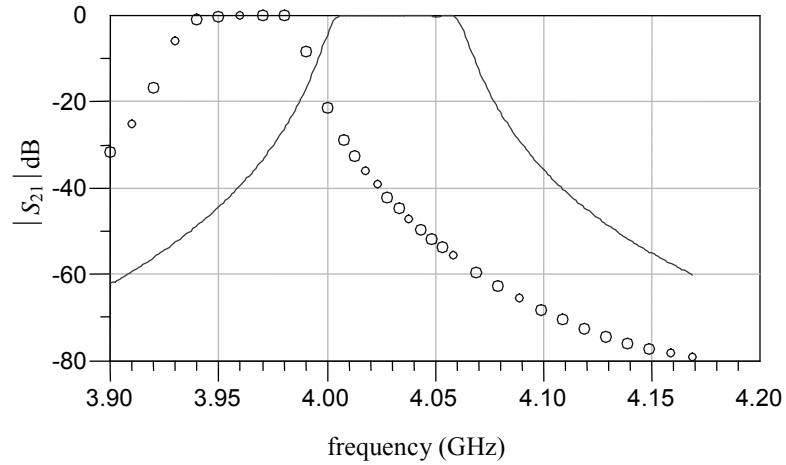
(a)



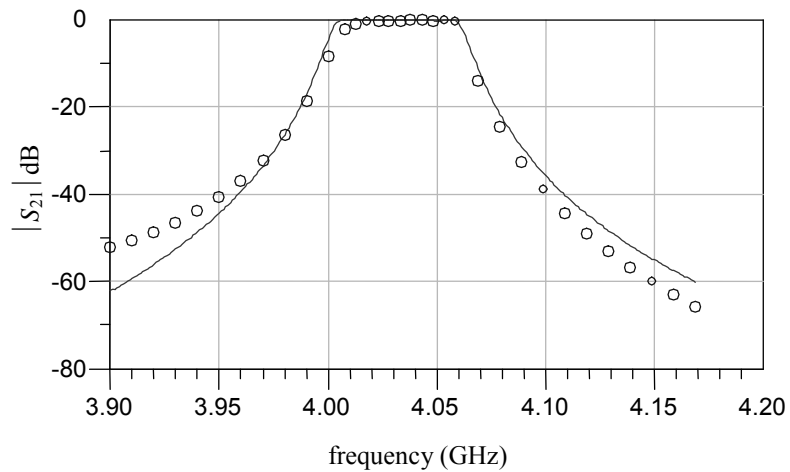
(b)

Fig. 3.12 The HTS filter (Bandler, Biernacki, Chen, Getsinger, Grobelny, Moskowitz and Talisa, 1995), (a) the physical structure, (b) the coarse model as implemented in Agilent ADS (2000).

It takes 74 minutes to complete a sweep on an Intel P4 2200 MHz machine. The initial solution and the final result in 1 iteration (2 fine model simulations) are shown in Fig. 3.14(a) and (b), respectively. TABLE 3.1 shows initial and final



(a)



(b)

Fig. 3.13 The Momentum fine (○) and optimal coarse ADS model (—) responses of the HTS filter at the initial solution (a) and at the final iteration (b) after 2 iterations (3 fine model evaluations).

designs. TABLE 3.2 shows the variation in the preassigned (coarse model) parameters.

The parameter extraction process uses real and imaginary S parameters and the ADS quasi-Newton optimization algorithm, while coarse model optima are obtained by the ADS minimax optimization algorithm.

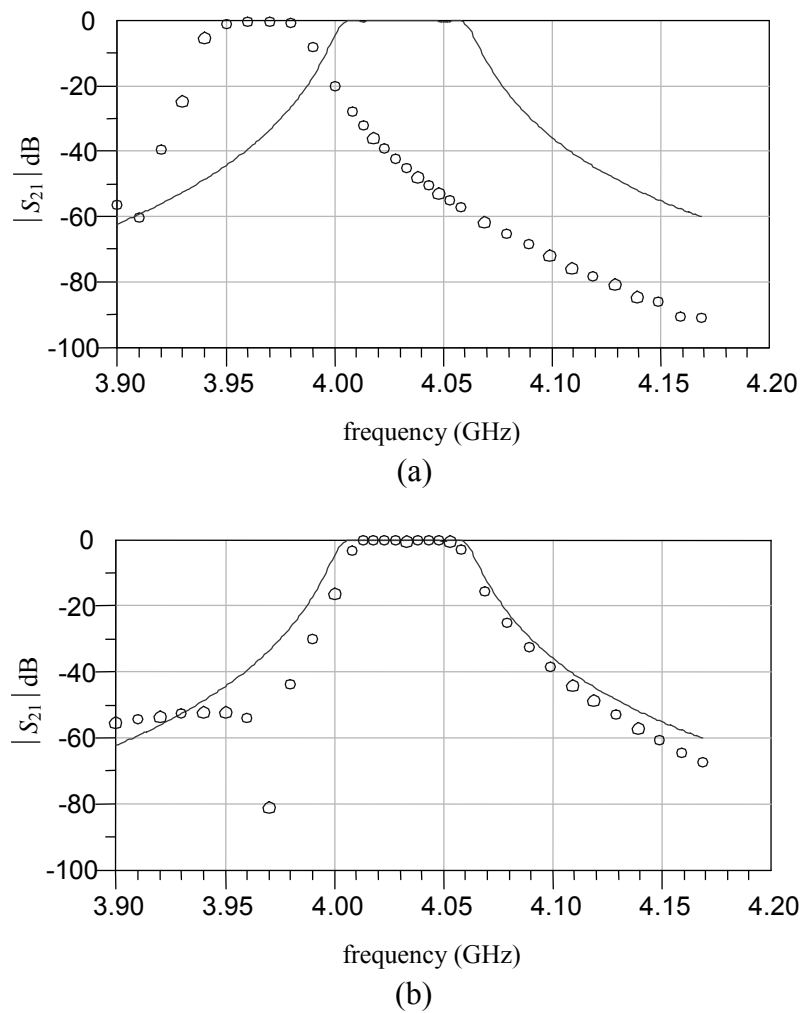


Fig. 3.14 The Sonnet *em* fine (\circ) and optimal coarse ADS model (—) responses of the HTS filter at the initial solution (a) and at the final iteration (b) after one iteration (2 fine model evaluations).

3.7 CONCLUSIONS

Based on a general concept, we present an effective technique for microwave circuit modeling and design w.r.t. full-wave EM simulations. We vary preassigned parameters in a coarse model to align it with the EM (fine) model. We believe this is the easiest to implement “Space Mapping” technique offered to date. The HTS filter design is entirely carried out by Agilent ADS and Momentum (3 frequency sweeps) or Sonnet *em*, (only 2 frequency sweeps) with no matrices to keep track of. A general SM concept is presented which enables us to verify that our implementation is correct and that no redundant steps are used.

TABLE 3.1
 AGILENT MOMENTUM/SONNET *em*
 OPTIMIZABLE PARAMETER VALUES OF THE HTS FILTER

Parameter	Initial solution (mil)	Solution (mil) Agilent Momentum	Solution (mil) Sonnet <i>em</i>
L_1	189.65	187.10	186.80
L_2	196.03	191.30	192.68
L_3	189.50	186.97	185.86
S_1	23.02	22.79	22.19
S_2	95.53	93.56	88.12
S_3	104.95	104.86	103.42

TABLE 3.2
 THE INITIAL AND FINAL PREASSIGNED PARAMETERS OF THE
 CALIBRATED COARSE MODEL OF THE HTS FILTER

Preassigned parameters	Original values	Final iteration Momentum	Final iteration <i>em</i>
H_1	20 mil	19.80 mil	18.79 mil
H_2	20 mil	19.05 mil	17.42 mil
H_3	20 mil	19.00 mil	17.67 mil
ϵ_{r1}	23.425	24.404	23.81
ϵ_{r2}	23.425	24.245	24.45
ϵ_{r3}	23.425	24.334	23.94

Chapter 4

RESPONSE RESIDUAL SPACE MAPPING TECHNIQUES

4.1 INTRODUCTION

As presented in Chapter 2, the space mapping (SM) concept exploits coarse models (usually computationally fast circuit-based models) to align with fine models (typically CPU intensive full-wave EM simulations) (Bandler, Cheng, Dakrouy, Mohamed, Bakr, Madsen and Søndergaard, 2004). The novel implicit space mapping (ISM) concept, presented in Chapter 3, exploits preassigned parameters such as the dielectric constant and substrate height (Bandler, Cheng, Nikolova and Ismail, 2004). In the parameter extraction process these parameters were exploited to match the fine model.

In this chapter, we present a significant improvement to ISM. Based on an explanation of residual misalignment close to the optimal fine model solution, where a classical Taylor model is seen to be better than SM, our new approach further fine-tunes the surrogate by exploiting an “response residual space” mapping (RRSM).

The RRSM we suggest is very simple to apply. It is consistent with the idea of pre-distorting design specifications to permit the fine model greater

latitude—anticipating violations and making the specifications correspondingly stricter. Our RRSM exploits this to fine tune the surrogate model. An accurate design of an HTS filter, easily implemented in Agilent ADS (2000), emerges after only four EM simulations using ISM and RRSM with sparse frequency sweeps (two iterations of ISM, followed by one application of the RRSM).

In this chapter we also broaden the concept of auxiliary (preassigned) parameters to frequency transformation parameters. See, e.g. (Bandler, Biernacki, Chen, Hemmers and Madsen, 1995). We embed a linear mapping to relate the actual (fine model) frequency and the transformed (coarse model) frequency into the surrogate.

At the end of this chapter, we present a microwave design framework for implementing an implicit and RRSM approach. The RRSM surrogate is matched to the fine model through parameter extraction. An intuitive “multiple cheese-cutting” example demonstrates the concept. For the first time, an ADS framework implements the SM steps interactively. A six-section H-plane waveguide filter design emerges after four iterations, using the implicit SM and RRSM optimization entirely within the design framework. We use sparse frequency sweeps and do not use the Jacobian of the fine model.

4.2 RESPONSE RESIDUAL SPACE MAPPING

The RRSM addresses residual misalignment between the optimal coarse model response and the true fine model optimum response $\mathbf{R}_f(\mathbf{x}_f^*)$. (In SM, an

exact match between the fine model and the mapped coarse model is unlikely.) For example, a coarse model such as $R_c = x^2$ will never match the fine model $R_f = x^2 - 2$ around its minimum with any mapping $x_c = P(x_f)$, $x_c, x_f \in \mathfrak{R}$. An “output” or response mapping can overcome this deficiency by introducing a transformation of the coarse model response based on a Taylor approximation (Dennis, 2001, 2002).

Fig. 4.1 depicts model effectiveness plots (Søndergaard, 2003) for a two-section capacitively loaded impedance transformer (Søndergaard, 2003) at the final iterate $\mathbf{x}_f^{(i)}$, approximately $[74.23 \ 79.27]^T$. Centered at $\mathbf{h} = \mathbf{0}$, the light grid shows $\| \mathbf{R}_f(\mathbf{x}_f^{(i)} + \mathbf{h}) - \mathbf{R}_c(\mathbf{L}_p(\mathbf{x}_f^{(i)} + \mathbf{h})) \|$. This represents the deviation of the mapped coarse model (using the Taylor approximation to the mapping, i.e., a linearized mapping) from the fine model. The dark grid shows $\| \mathbf{R}_f(\mathbf{x}_f^{(i)} + \mathbf{h}) - \mathbf{L}_f(\mathbf{x}_f^{(i)} + \mathbf{h}) \|$. This is the deviation of the fine model from its classical Taylor approximation. It is seen that the Taylor approximation is most accurate close to $\mathbf{x}_f^{(i)}$ whereas the mapped coarse model is best over a large region.

Response residual SM aims at establishing a mapping \mathbf{O} between \mathbf{R}_s (output mapped surrogate response) and \mathbf{R}_c (mapped coarse model response)

$$R_s = \mathcal{O}(R_c) \quad (4-1)$$

such that

$$R_s \approx R_f \quad (4-2)$$

We can predict the fine model solution using this surrogate.

4.3 IMPLICIT AND RESPONSE RESIDUAL SPACE MAPPING SURROGATE

Our proposed algorithm starts with ISM (Bandler, Cheng, Nikolova and

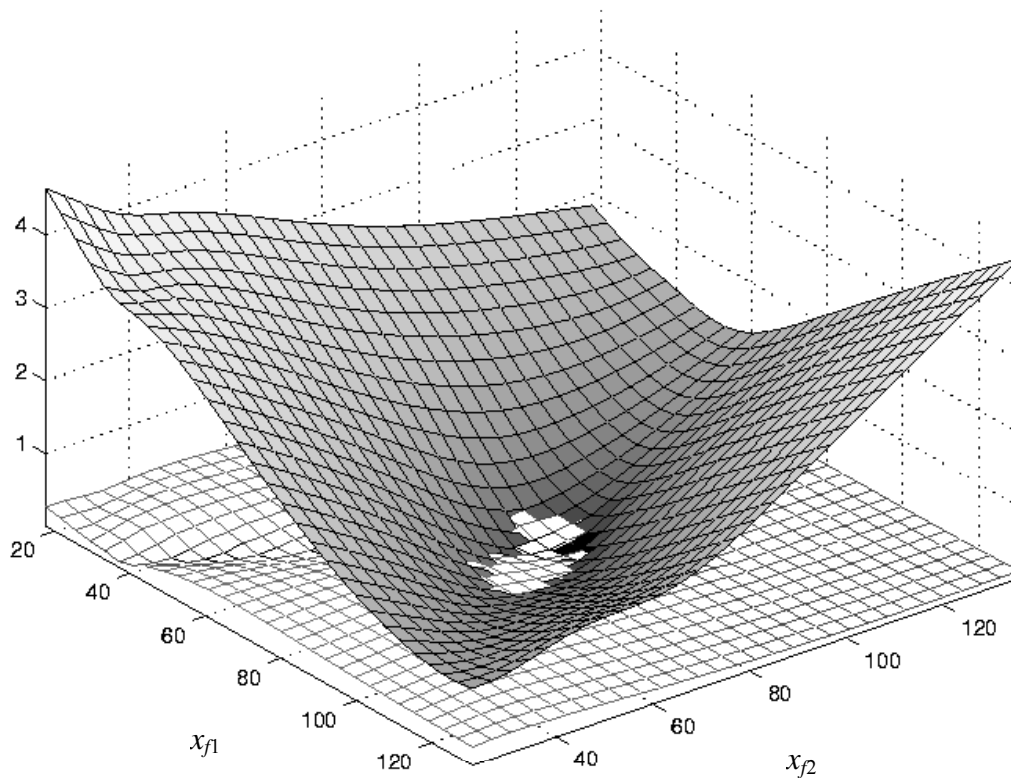


Fig. 4.1 Error plots for a two-section capacitively loaded impedance transformer (Søndergaard, 2003) exhibiting the quasi-global effectiveness of space mapping (light grid) versus a classical Taylor approximation (dark grid). See text.

Ismail, 2004). If the calibration (PE) step in (Bandler, Cheng, Nikolova and Ismail, 2004) does not improve the match, which will eventually happen close to \mathbf{x}_f^* , then we create a surrogate with response \mathbf{R}_s . In this chapter we consider a mapping of the form

$$\mathbf{R}_s = \mathbf{O}(\mathbf{R}_c) \triangleq \mathbf{R}_c(\mathbf{x}_c, \mathbf{x}) + \mathit{diag}\{\lambda_1, \lambda_2, \dots, \lambda_m\} \Delta \mathbf{R} \quad (4-3)$$

where

$$\Delta \mathbf{R} = \mathbf{R}_f(\mathbf{x}_f) - \mathbf{R}_c(\mathbf{x}_c^{*(i)}, \mathbf{x}) \quad (4-4)$$

is the residual between the mapped coarse model response after PE and the fine model response, and where the λ_j are user-defined weighting parameters, normally unity.

The coarse model parameters \mathbf{x}_c are obtained by (re)optimizing the surrogate (4-3) to give

$$\mathbf{x}_c^{*(i+1)} \triangleq \arg \min_{\mathbf{x}_c} U(\mathbf{O}(\mathbf{R}_c(\mathbf{x}_c, \mathbf{x}))) \quad (4-5)$$

Then we predict an update to the fine model solution as

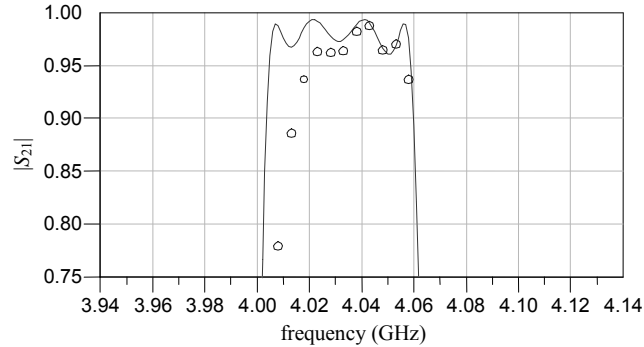
$$\mathbf{x}_f = \mathbf{x}_c^{*(i+1)} \quad (4-6)$$

4.4 HTS FILTER EXAMPLE

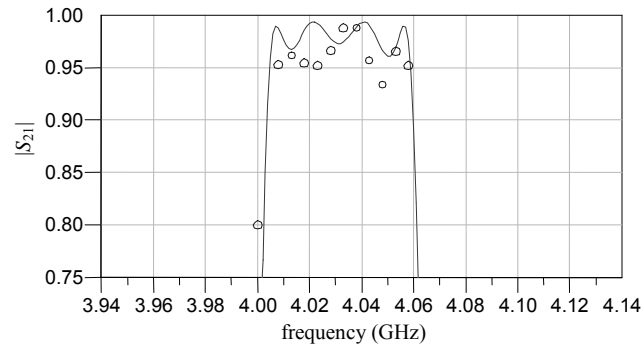
Again, we consider the HTS bandpass filter of (Bandler, Biernacki, Chen, Getsinger, Grobelny, Moskowitz and Talisa, 1995) as in Chapter 3. The physical structure is shown in Section 3.5. Design variables are the lengths of the coupled

lines and the separations between them. The design specifications are the same as described in Section 3.5. The fine model is simulated by Agilent Momentum (2000).

The relevant responses at the initial solution are shown in Fig. 4.2 (a), where we notice severe misalignment. Fig. 4.2(a) and Fig. 4.3(b) show the response after running the ISM algorithm. After two iterations (3 fine model



(a)



(b)

Fig. 4.2 The fine (\circ) and optimal coarse model (—) magnitude responses of the HTS filter, at the final iteration using ISM (a), followed by one iteration of RRS (b).

simulations), the calibration step does not improve further, as seen in Fig. 4.3(b). Since we believe we are close to the true optimal solution, we introduce the output space mapping and use the output space mapped response in (4-3) with $\lambda_j = 0.5, j = 1, 2, \dots, m$ as initial values. After one iteration of RRSM, we obtain the improved response shown in Fig. 4.2(b) and Fig. 4.3(c). This is achieved in only 4 fine model evaluations. The total time taken is 35 min (one fine model simulation takes approximately 9 min on an Athlon 1100 MHz). TABLE 4.1 shows initial and final designs. The initial and final preassigned parameters of the calibrated coarse model of the HTS filter have the same values as in (Bandler, Cheng, Nikolova and Ismail, 2004), i.e., $\mathbf{x}^{(3)} = [24.404 \ 19.80 \text{ mil} \ 24.245 \ 19.05 \text{ mil} \ 24.334 \ 19.00 \text{ mil}]^T$.

The PE uses real and imaginary S parameters and the ADS quasi-Newton optimization algorithm, while coarse model and RRSM surrogate optima are

TABLE 4.1
OPTIMIZABLE PARAMETER VALUES OF THE HTS FILTER

Parameter	Initial solution	Solution reached by the ISM algorithm	Solution by the ISM and RRSM
L_1	189.65	187.10	178.28
L_2	196.03	191.30	200.86
L_3	189.50	186.97	177.99
S_1	23.02	22.79	20.18
S_2	95.53	93.56	86.15
S_3	104.95	104.86	85.17
All values are in mils			

obtained by the ADS minimax optimization algorithm.

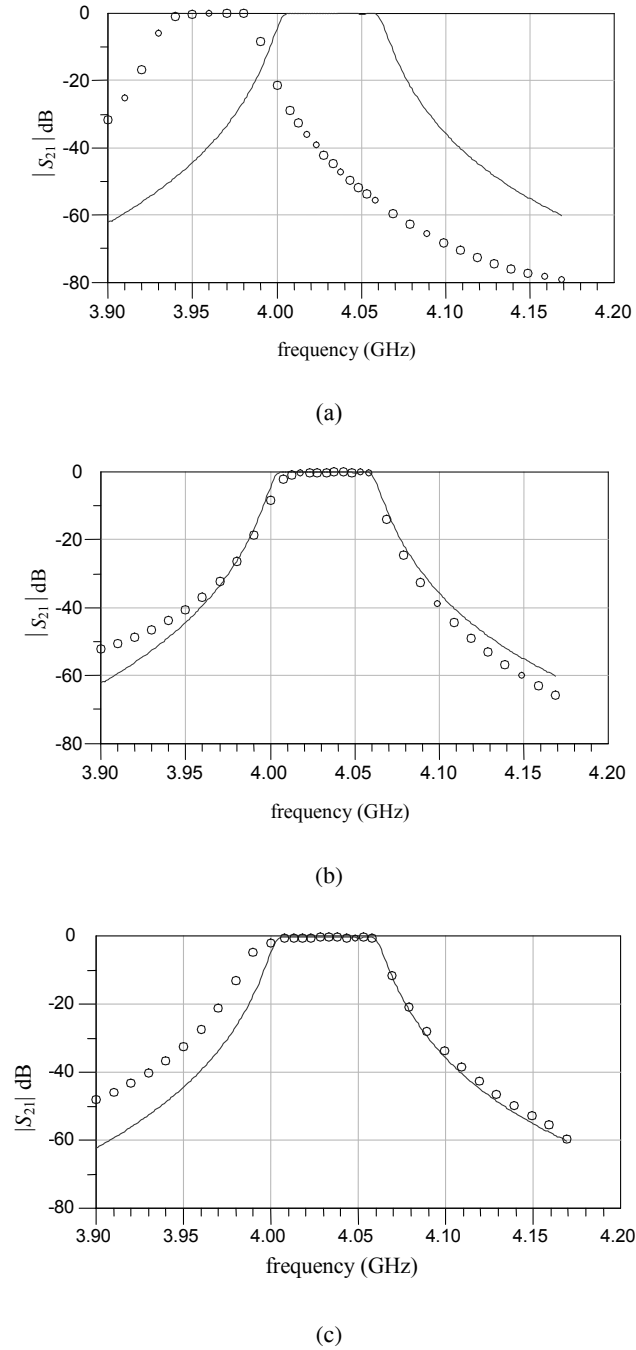


Fig. 4.3 The fine (\circ) and optimal coarse model (—) responses of the HTS filter in dB at the initial solution (a), at the final iteration using ISM (b), and at the final iteration using ISM and RRSM (c).

4.5 RESPONSE RESIDUAL SPACE MAPPING APPROACH

In this section we introduce the response residual space mapping (RRSM) approach. It differs from the approach described in (Bandler, Cheng, Gebremariam, Madsen, Pedersen and Søndergaard, 2003). Here, we match the response residual SM surrogate with the fine model in a parameter extraction (PE) process. A novel and simple “multiple cheese-cutting” problem is used as an illustration. An implementation in an ADS (2003) design framework is presented in the next chapter. Entirely in ADS, a good six-section H-plane waveguide filter (Young and Schiffman, 1963, Matthaei, Young and Jones, 1964) design is achieved after only five EM simulations (Agilent HFSS (2000)) or four iterations.

4.5.1 Surrogate

The response residual surrogate is a calibrated (implicitly or explicitly space mapped) coarse model plus an output or response residual as defined in the previous section. The residual is a vector whose elements are the differences between the calibrated coarse model response and the fine model response at each sample point after parameter extraction. The surrogate is shown in Fig. 4.4. Each residual element (sample point) may be weighted using a weighting parameter λ_j , $j = 1 \dots m$, where m is the number of sample points.

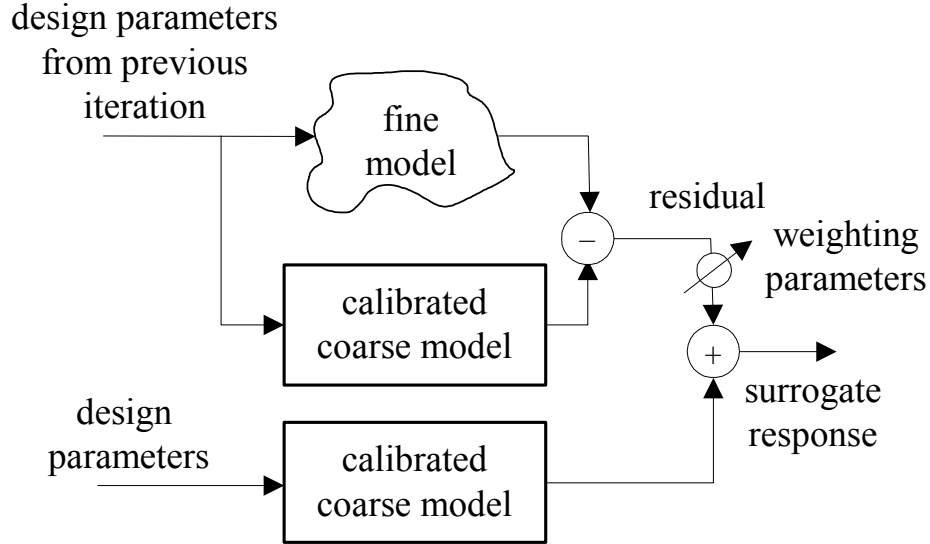


Fig. 4.4 Illustration of the RRSM surrogate.

In the parameter extraction, we match the previous output residual SM surrogate (instead of the calibrated coarse model of (Bandler, Cheng, Gebremariam, Madsen, Pedersen and Søndergaard, 2003)) to the fine model at each sample point.

4.5.2 Multiple Cheese-cutting Problem

We develop a physical example suitable for illustrating the optimization process. Our “responses” are the *weights* of individual cheese slices. The designable parameter is the *length* of the top slice [see Fig. 4.5(a)]. A density of one is assumed. The goal is to cut through the slices to obtain a *weight* for each one as close to a desired *weight* s as possible. Note that we measure the *length*

from the right-hand end. We cut on the left-hand side (the broken line).

The coarse model involves 3 slices of the same *height* x , namely, the preassigned parameter shown in Fig. 4.5(a). The lengths of the two lower slices are c units shorter than the top one. The optimal *length* x_c^* can be calculated to minimize the differences between the weights of the slices and the desired *weight* s . We use minimax optimization. The responses of the coarse model are given by

$$R_{c1} = x \cdot x_c \cdot 1$$

$$R_{c2} = x \cdot (x_c - c) \cdot 1$$

$$R_{c3} = x \cdot (x_c - c) \cdot 1$$

The fine model is similar but the lower two slices are f_1 and f_2 units shorter, respectively, than the top slice [Fig. 4.5(b)]. The *heights* of the slices are x_1 , x_2 and x_3 , respectively. The corresponding responses of the fine model are

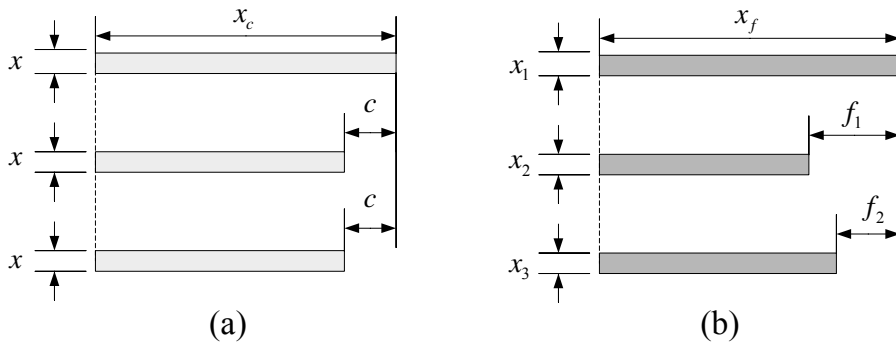


Fig. 4.5 Multiple cheese-cutting problem: (a) the coarse model (b) and fine model.

$$R_{f1} = x_1 \cdot x_f \cdot 1$$

$$R_{f2} = x_2 \cdot (x_f - f_1) \cdot 1$$

$$R_{f3} = x_3 \cdot (x_f - f_2) \cdot 1$$

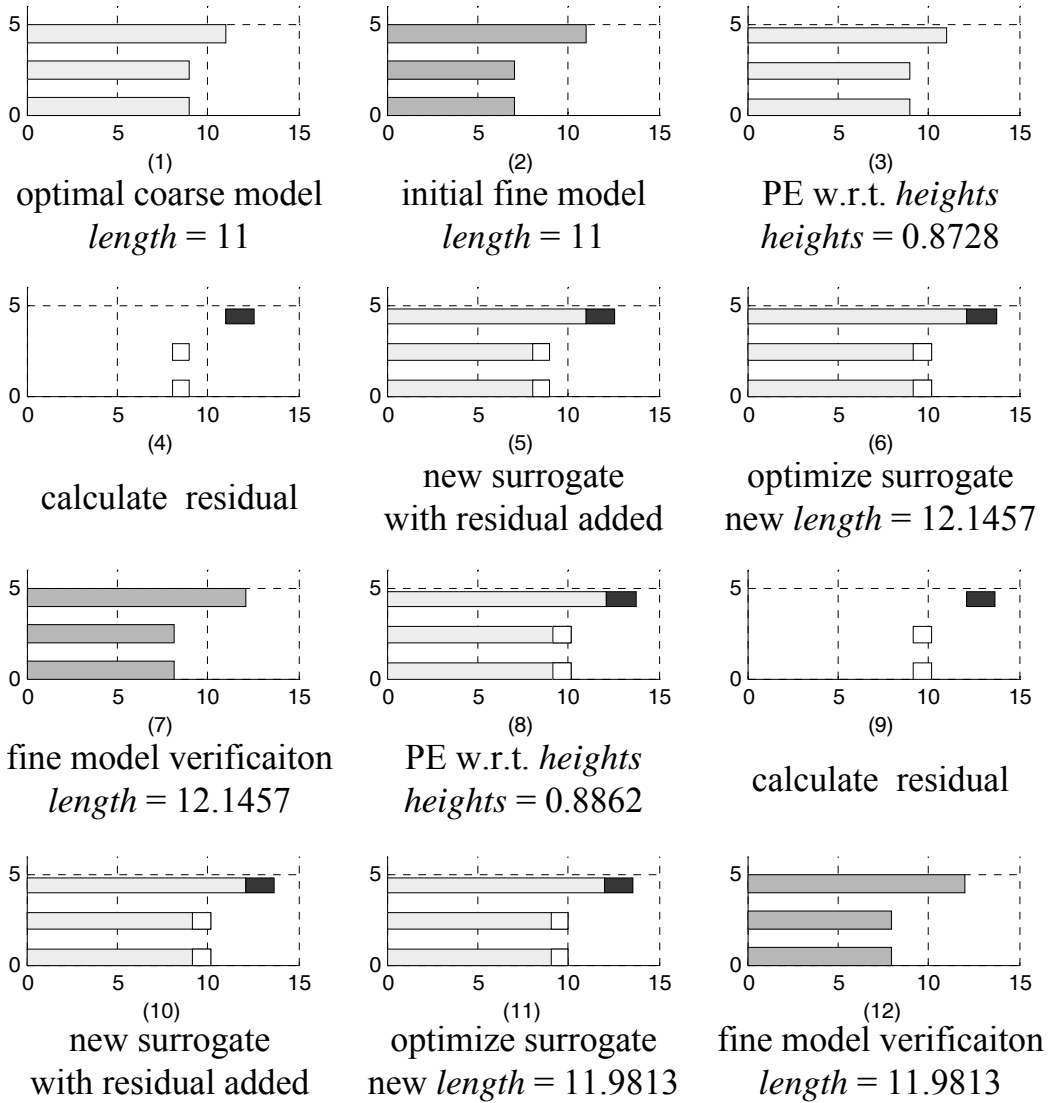


Fig. 4.6 “Multiple cheese-cutting” problem: implicit SM and RRSM optimization: step by step.

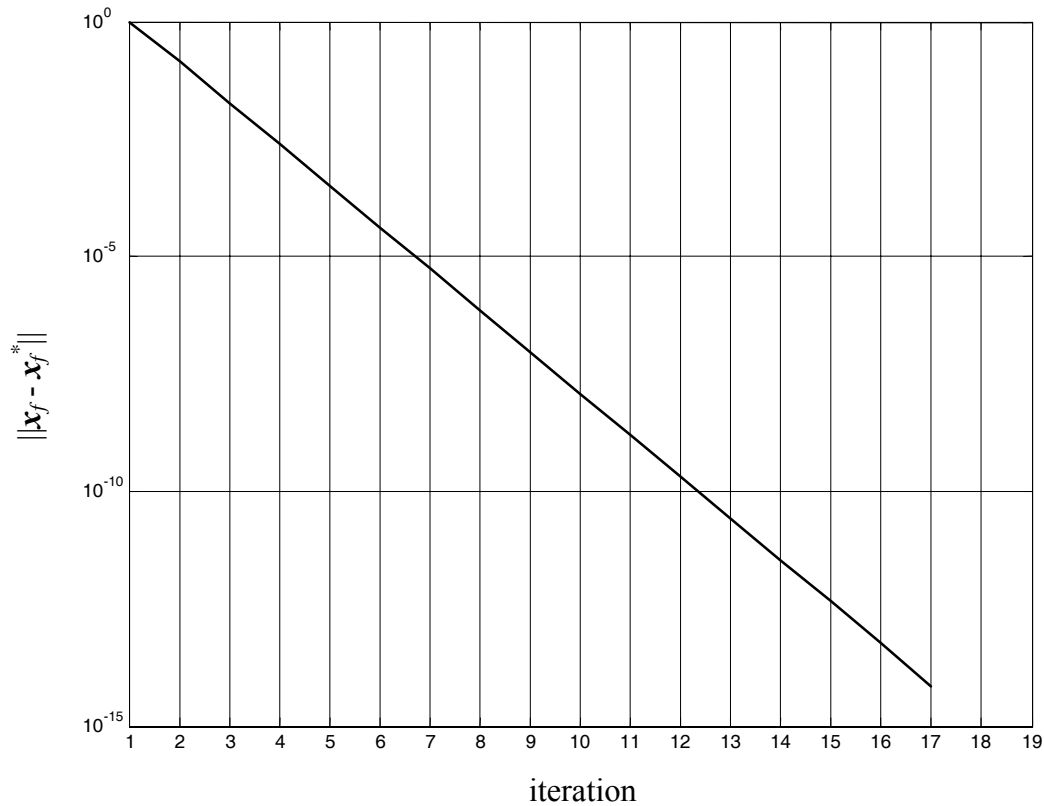


Fig. 4.7 Parameter difference between the RRSM design and minimax direct optimization. Finally, $x_f = x_f^* = 12$.

We demonstrate the implicit and RRSM optimization process. We set $c = 2$ and $f_1 = f_2 = 4$. The specification s is set to 10. The *heights* of the slices are fixed at unity for the fine model, i.e., $x_1 = x_2 = x_3 = 1$. The coarse model preassigned parameter x is initially unity. Fig. 4.6 shows the first two iterations of the algorithm, step by step. The RRSM algorithm converges to the optimal fine model solution as shown in Fig. 4.7.

4.6 H-PLANE WAVEGUIDE FILTER DESIGN

4.6.1 Optimization Steps

We use the ADS framework exploiting implicit SM and RRSM to design an H-plane filter. The following iterations are employed: two iterations of implicit SM to drive the design to be close to the optimal solution; one implicit SM and RRSM iteration using weighting parameters $\lambda_j = 0.5$, $j = 1 \dots m$ ($\lambda_j \leq 1$ because the optimizer has difficulty reoptimizing the surrogate with the full residual added); a second implicit SM and RRSM iteration with the full residual added.

4.6.2 Six-Section H-plane Waveguide Filter

The six-section H-plane waveguide filter (Young and Schiffman, 1963, Matthaei, Young and Jones, 1964) is shown in Fig. 4.8(a). The setup of the problem follows Bakr, Bandler, Georgieva and Madsen (1999). The design parameters are the lengths and widths: $\{L_1, L_2, L_3, W_1, W_2, W_3, W_4\}$. Design specifications are

$$|S_{11}| \leq 0.16, \quad \text{for frequency range } 5.4 \leq \omega \leq 9.0 \text{ GHz};$$

$$|S_{11}| \geq 0.85, \quad \text{for frequency } \omega \leq 5.2 \text{ GHz};$$

$$|S_{11}| \geq 0.5, \quad \text{for frequency } \omega \geq 9.5 \text{ GHz}.$$

We use 23 sample points.

A waveguide with a cross-section of 1.372×0.622 inches (3.485×1.58

cm) is used. The six sections are separated by seven H-plane septa, which have a finite thickness of 0.02 inches (0.508 mm). The coarse model consists of lumped inductances and waveguide sections. There are various approaches to calculate the equivalent inductive susceptance corresponding to an H-plane septum. We utilize a simplified version of a formula due to Marcuvitz (1951) in evaluating the inductances. The coarse model is simulated using ADS (2003) as in Fig. 4.8(b).

We select the waveguide width of each section as the preassigned parameter to calibrate the coarse model. The frequency coefficient of each

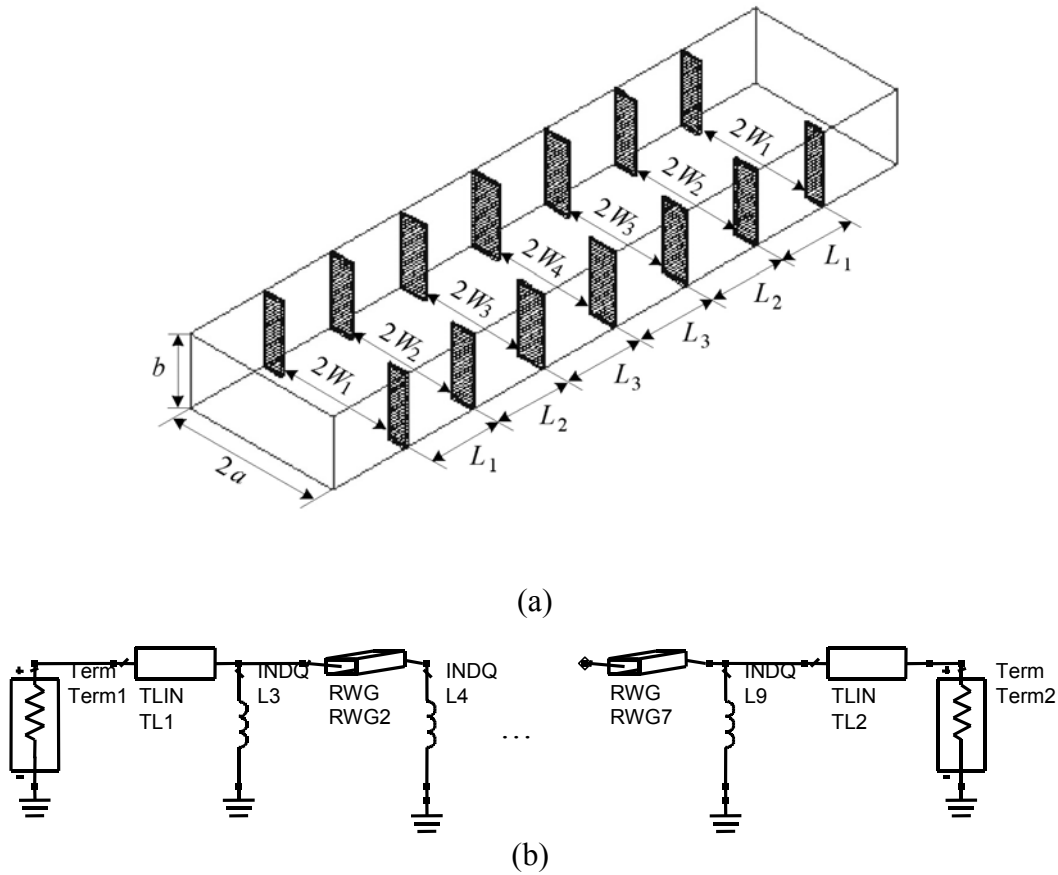
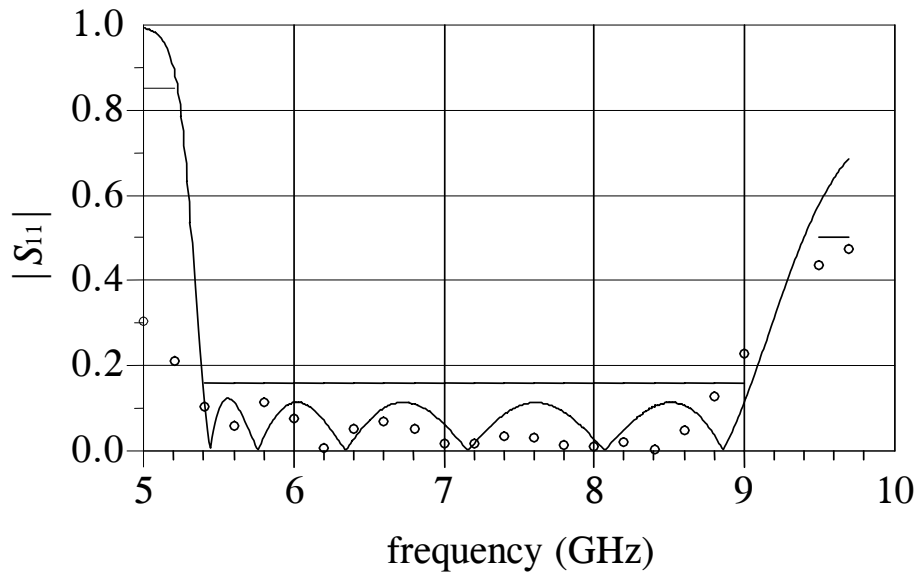


Fig. 4.8 (a) Six-section H-plane waveguide filter (b) ADS coarse model.

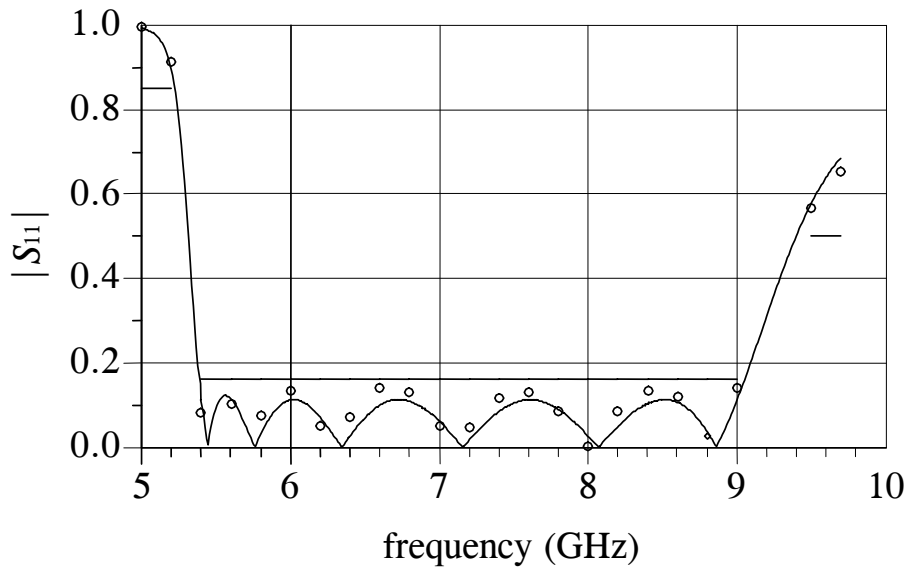
inductor, for convenience PI, is also harnessed as a preassigned parameter to compensate for the susceptance change. The fine model exploits Agilent HFSS. One frequency sweep takes 2.5 minutes on an Intel Pentium 4 (3 GHz) computer with 1 GB RAM and running in Windows XP Pro. Fig. 4.9(a) shows the fine model response at the initial solution. Fig. 4.9(b) shows the fine model response after running the algorithm using the Agilent HFSS simulator. Since no Jacobian is needed, the total time taken for five fine model simulations is 15 minutes on an Intel P4 3 GHz computer. TABLE 4.2 shows the initial and optimal design parameter values of the six-section H-plane waveguide filter.

4.7 CONCLUSIONS

We propose significant improvements to implicit space mapping for EM-based modeling and design. Based on an explanation of residual misalignment, our new approach further fine-tunes the surrogate by exploiting an “response residual space” mapping. The required HTS filter models and RRSM surrogate are easily implemented by Agilent ADS and Momentum with no matrices to keep track of. An accurate HTS microstrip filter design solution emerges after only four EM simulations with sparse frequency sweeps. We present a RRSM modeling technique that matches the RRSM surrogate with the fine model. A new “multiple cheese-cutting” design problem illustrates the concept. Our approach is implemented entirely in the ADS framework. A good H-plane filter design emerges after only five EM simulations using the implicit and RRSM with sparse



(a)



(b)

Fig. 4.9 H-plane filter optimal coarse model response (—), and the fine model response at: (a) initial solution (○); (b) solution reached via RRSM after 4 iterations (○).

frequency sweeps and no Jacobian calculations.

TABLE 4.2
OPTIMIZABLE PARAMETER VALUES OF THE SIX-SECTION
H-PLANE WAVEGUIDE FILTER

Parameter	Initial solution	Solution reached via RRSM
W_1	0.555849	0.499802
W_2	0.519416	0.463828
W_3	0.5033	0.44544
W_4	0.49926	0.44168
L_1	0.591645	0.630762
L_2	0.660396	0.644953
L_3	0.67667	0.665449

all values are in inches

Chapter 5

IMPLEMENTABLE SPACE MAPPING DESIGN FRAMEWORK

5.1 INTRODUCTION

The required interaction between coarse model, fine model and optimization tools makes SM difficult to automate within existing simulators. A set of design or preassigned parameters and frequencies have to be sent to the different simulators and corresponding responses retrieved. Software packages such as OSA90 or Matlab can provide coarse model analyses as well as optimization tools. Empipe (1997) and Momentum_Driver (Ismail, 2001) have been designed to drive and communicate with Sonnet's *em* (2001) and Agilent Momentum (2000) as fine models. Aggressive SM optimization of 3D structures (Bandler, Biernacki and Chen, 1996) has been automated using a two-level Datapipe (1997) architecture of OSA90. The Datapipe technique allows the algorithm to carry out nested optimization loops in two separate processes while maintaining a functional link between their results (e.g., the next increment to x_f is a function of the result of parameter extraction).

We present an ADS schematic framework for SM. The steps of the framework are listed. It uses Agilent ADS circuit models as coarse models. ADS

has a suite of built-in optimization tools. The ADS component S -parameter file enables S -parameters to be imported in Touchstone file format from different EM simulators (fine model) such as Sonnet’s *em* and Agilent Momentum. Imported S -parameters can be matched with the ADS circuit model (coarse model) responses. This PE procedure can be done simply by proper setup of the ADS optimization components (optimization algorithm and goals). These major steps of SM are friendly for engineers to apply. We implement these steps upfront in ADS Schematic designs. In the algorithm iteration we fill each design with proper data and optimize it.

In this chapter we provide a brief summary of applications of SM by other researchers and engineers, thereby placing our own work into context.

5.2 ADS SCHEMATIC DESIGN FRAMEWORK FOR SM

5.2.1 ADS Schematic Design Framework

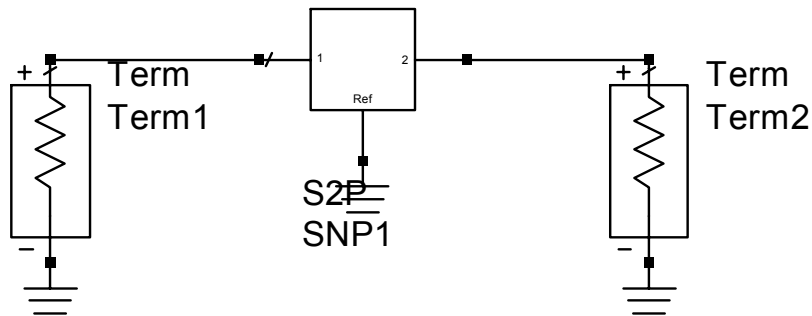


Fig. 5.1 S2P (2-Port S -Parameter File) symbol with terminals.

Agilent ADS (2003) has a huge library of circuit models that can be used as “coarse” models. ADS also has a suite of easy-to-use optimization tools, e.g., random search, gradient search, Quasi-Newton search, discrete search, genetic algorithm. An S -parameter file S_nP in ADS can import data files (S -parameters) in Dataset or Touchstone format. Here, n is the port number. Fig. 5.1 is a symbol of 2-port S -Parameter File component S2P with terminals. Many EM simulators (“fine” model) such as Sonnet’s *em* (2001), Agilent Momentum (2000), and Agilent HFSS (2000) support Touchstone file format. Using this file, we import S -parameters and match them with the ADS circuit model (coarse model) responses in the PE procedure. The residual between the calibrated coarse model and fine model can also be obtained using the S_nP file and MeasEqn (Measurement Equation) component. These major steps of SM are friendly for engineers to apply.

5.2.2 ADS Schematic Design Framework for SM

Step 1 Set up the coarse model in ADS schematic.

Step 2 Optimize the coarse model using the ADS optimizer.

Step 3 Copy and paste the parameters into the parameterized fine model (Agilent Momentum, HFSS/Empipe3D (2000), or Sonnet’s *em*).

In ADS, the Momentum fine model can also be generated using the *Generate/Update Layout* command.

Step 4 Simulate the fine model and save the responses in Touchstone

format (Agilent Momentum, HFSS, or Sonnet's *em*) or Dataset (Momentum).

Step 5 If stopping criteria are satisfied, stop.

Step 6 Parameter extraction

(a) Import the responses to the ADS schematic using *SnP* component under *Data Items*.

(b) Set up ADS (calibrated) coarse model or response residual SM (RRSM) surrogate to match the *SnP* component.

(c) Run ADS optimization to perform parameter extraction.

Comment: Here, you may extract the coarse model design parameter or the preassigned parameters to implement explicit (original or aggressive SM) or implicit space mapping, respectively.

Step 7 Predict the next fine model solution by

(a) Explicit SM: transfer extracted parameters to MATLAB (2002) (or other scientific computing tool) and calculate a prediction based on the algorithm in (Bandler, Biernacki, Chen, Grobelny and Hemmers, 1994, Bandler, Biernacki, Chen, Hemmers and Madsen, 1995), or,

(b) Implicit SM: reoptimize the calibrated coarse model w.r.t. design parameters to predict the next fine model design, and/or,

(c) RRSM: reoptimize the surrogate (calibrated coarse model plus

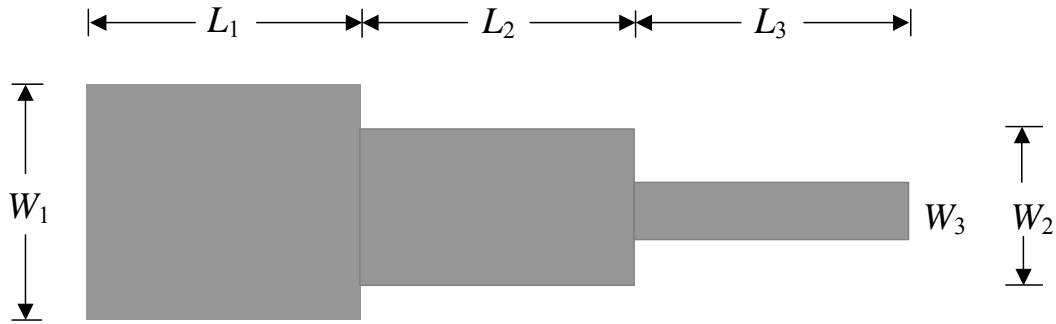


Fig. 5.2 The three-section 3:1 microstrip impedance transformer.

response residual) w.r.t. design parameters to predict the next fine model design.

Step 8 Update the fine model design and go to Step 4.

We implement implicit and response residual SM optimization in the ADS schematic framework in an interactive way. The fine model is Agilent momentum, HFSS, or Sonnet's *em*.

5.2.3 Three-Section Microstrip Transformer

An example of ADS implementation ISM optimization is the three-section microstrip impedance transformer (Bakr, Bandler, Biernacki and Chen, 1997) (Fig. 5.2) as we described in Section 3.3. The coarse model is shown in Fig. 5.3.

The design specifications are

$$|S_{11}| \leq 0.11 \text{ for } 5 \text{ GHz} \leq \omega \leq 15 \text{ GHz}$$

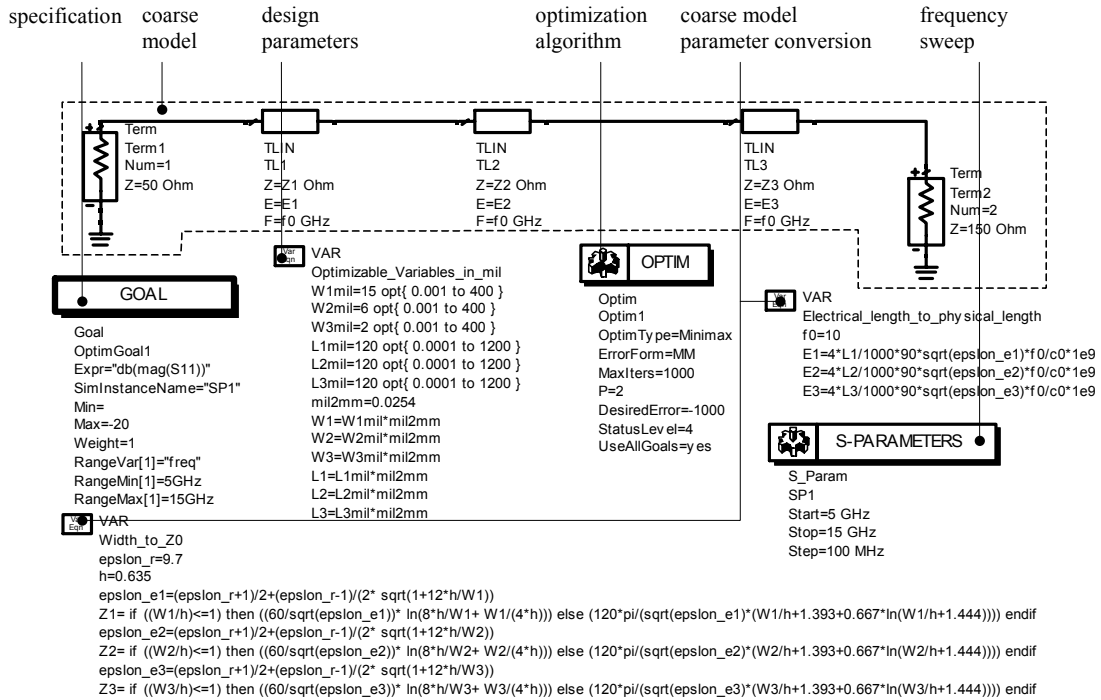


Fig. 5.3 Coarse model optimization. Coarse model optimization of the three-section impedance transformer. The coarse model is optimized using the minimax algorithm.

The designable parameters are the width and physical length of each microstrip line. Here, the reflection coefficient S_{11} is used to match the two model responses. The fine model is an Agilent Momentum model. The designable parameters for the fine model are the widths and physical lengths of the three microstrip lines. The thickness of the dielectric substrate is 0.635 mm (25 mil) and its relative permittivity is 9.7. The effect of nonideal dielectric is considered



Fig. 5.4 Fine model simulated in ADS Momentum.

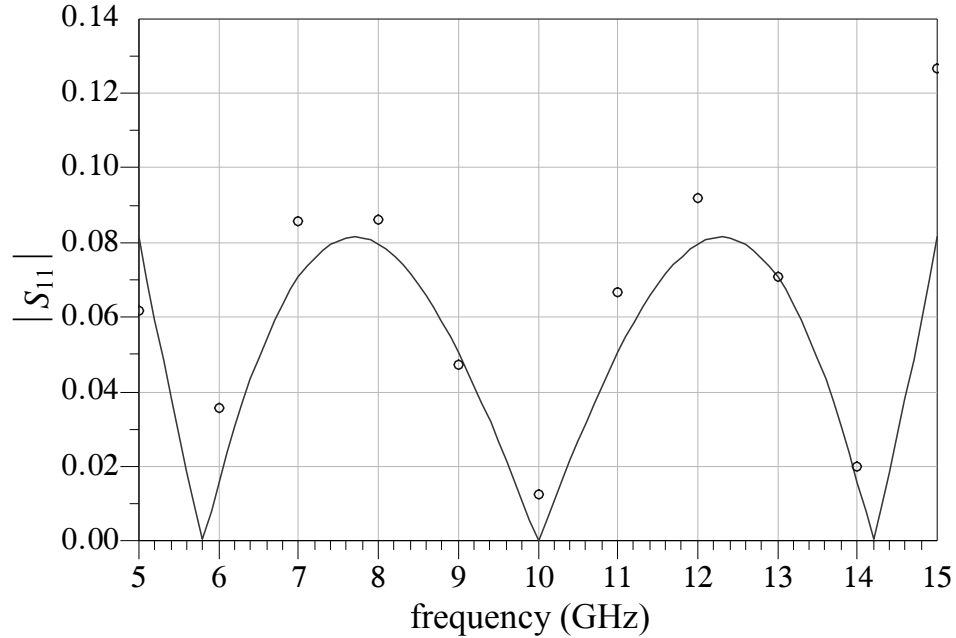


Fig. 5.5 Coarse (—) and fine (\circ) model responses $|S_{11}|$ at the initial solution of the three-section transformer.

by setting the loss tangent to 0.002. We use 11 frequency points in the sweep.

The first step is to obtain an optimal coarse model design using the ADS Schematic (minimax) optimization utilities as in Fig. 5.3. In this schematic, we show the starting point (in mils) of the coarse model design parameter values. The coarse model parameter conversion components implement well-known empirical formulas (Pozar, 1998). The schematic will sweep S -parameters in the band. When we “simulate” the schematic, ADS provides an optimal coarse model solution. We apply the obtained design parameters to the fine model (Fig. 5.4). To achieve this, we can create a Momentum layout from schematic layout

directly or copy and paste the parameters to the parameterized Momentum fine model. In the fine model preassigned parameters are (always) kept fixed at nominal values.

We obtain the fine model response as Fig. 5.5. Imported by S2P (2-Port S-Parameter File), the fine model real and imaginary responses are used in the parameter extraction (calibration) step (Fig. 5.6). In this step, the preassigned parameters of coarse model are calibrated to match the fine and coarse model responses. The goal is to match the real and imaginary parts of S_{11} at the same

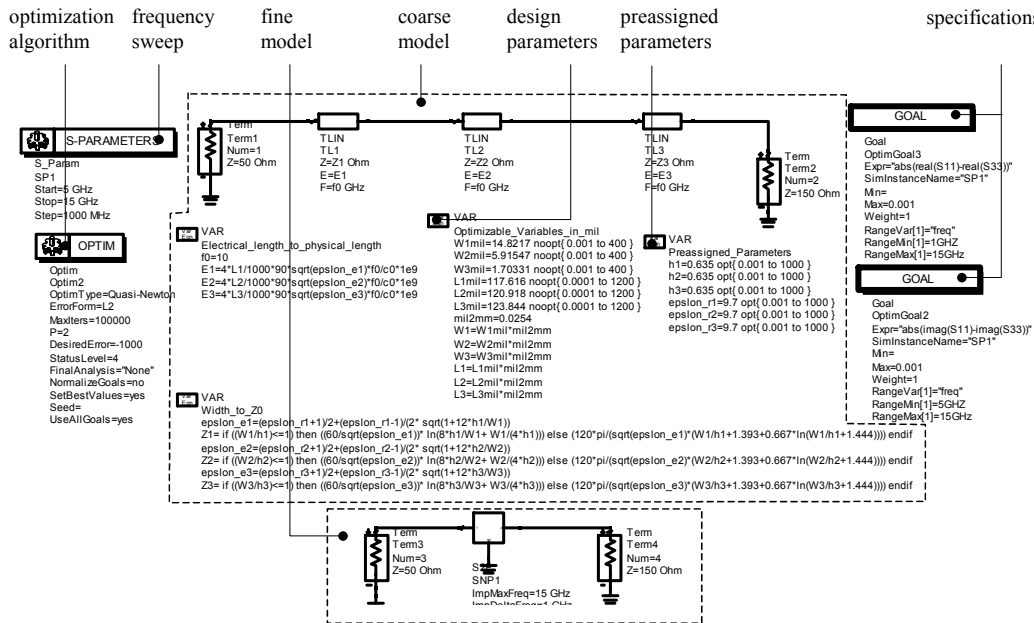


Fig. 5.6 The calibration of the coarse model of the three-section impedance transformer. This schematic extracts preassigned parameters x . The coarse and fine models are within the broken line. The goal is to match the coarse and fine model real and imaginary S_{11} from 5 to 15 GHz. The optimization algorithm uses the Quasi-Newton method.

time. A quasi-Newton algorithm is used to perform this procedure.

Supposedly we obtain a good match between the fine and coarse model, i.e., a set of preassigned parameter values providing the best match are found, we proceed to the next step. With fixed preassigned parameters the new coarse model (surrogate) is reoptimized w.r.t. the original specification. This is done as in Fig. 5.7. This schematic is similar to Fig. 5.3, but with a different set of preassigned parameter values. The ADS minimax algorithm is used again in this case.

We apply the prediction to the fine model again. The fine model simulation gives a satisfying result as in Fig. 5.8. It takes 2 fine model simulations.

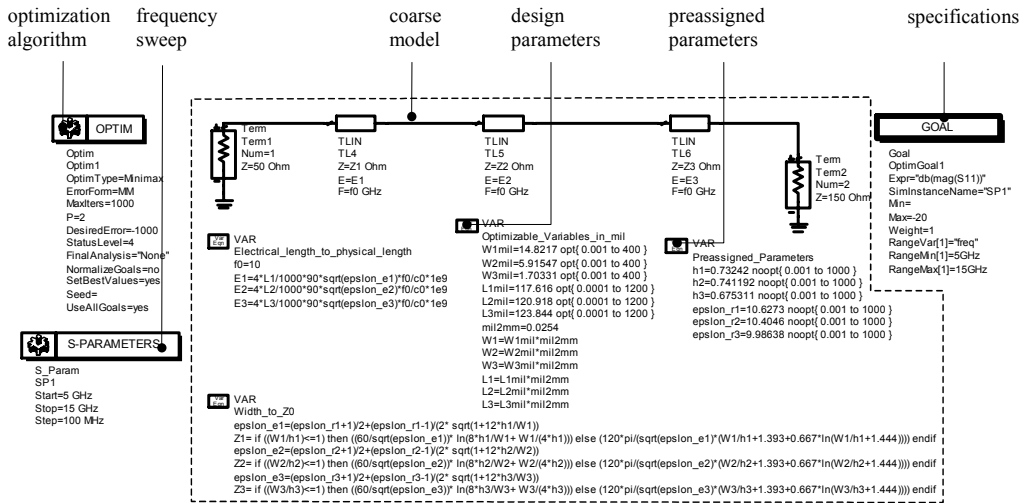


Fig. 5.7 Reoptimization of the coarse model of the three-section impedance transformer using the fixed preassigned parameter values obtained from the previous calibration (parameter extraction). This schematic uses the minimax optimization algorithm. The goal is to minimize $|S_{11}|$ of the calibrated coarse model.

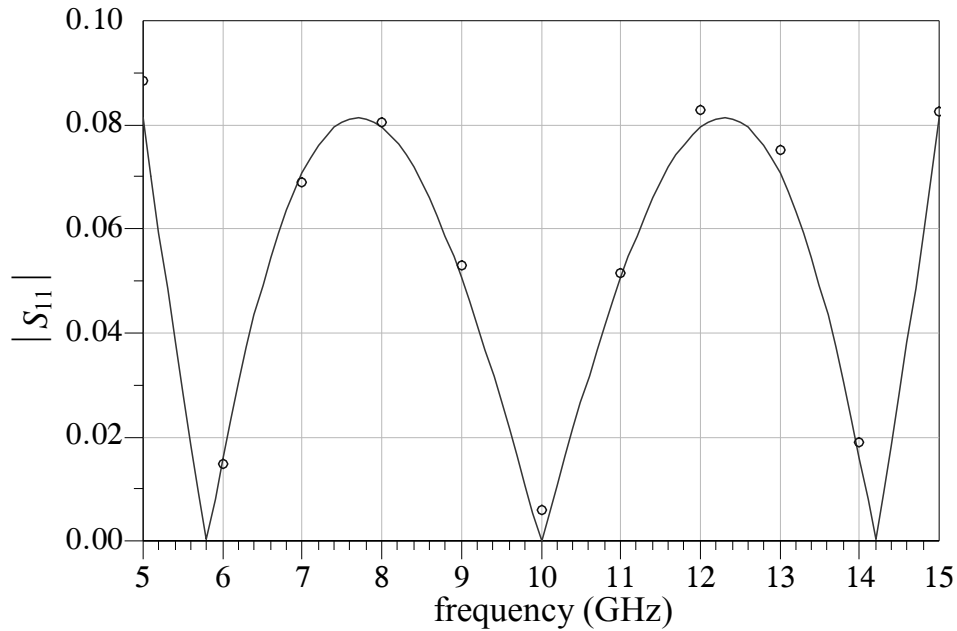


Fig. 5.8 Optimal coarse (—) and fine model (\circ) responses $|S_{11}|$ for the three-section transformer using Momentum after 1 iteration (2 fine model simulations). The process satisfies the stopping criteria.

TABLE 5.1
OPTIMIZABLE PARAMETER VALUES OF THE THREE-SECTION
IMPEDANCE TRANSFORMER

Parameter	Initial solution	Solution reached via ISM
W_1	14.8217	15.354
W_2	5.91547	6.34991
W_3	1.70331	1.70155
L_1	117.616	113.749
L_2	120.918	117.141
L_3	123.844	121.733

all values are in mils

5.2.4 Response Residual SM Implementation of HTS Filter

The Response Residual SM example of the HTS filter is described in Chapter 4. We discuss the implementation technique in this section. A coarse model is optimized as in the previous sub-section. A fine model is simulated using the coarse model design parameters. The coarse model is calibrated to match the fine model response. In Fig. 5.9, previous coarse model is the

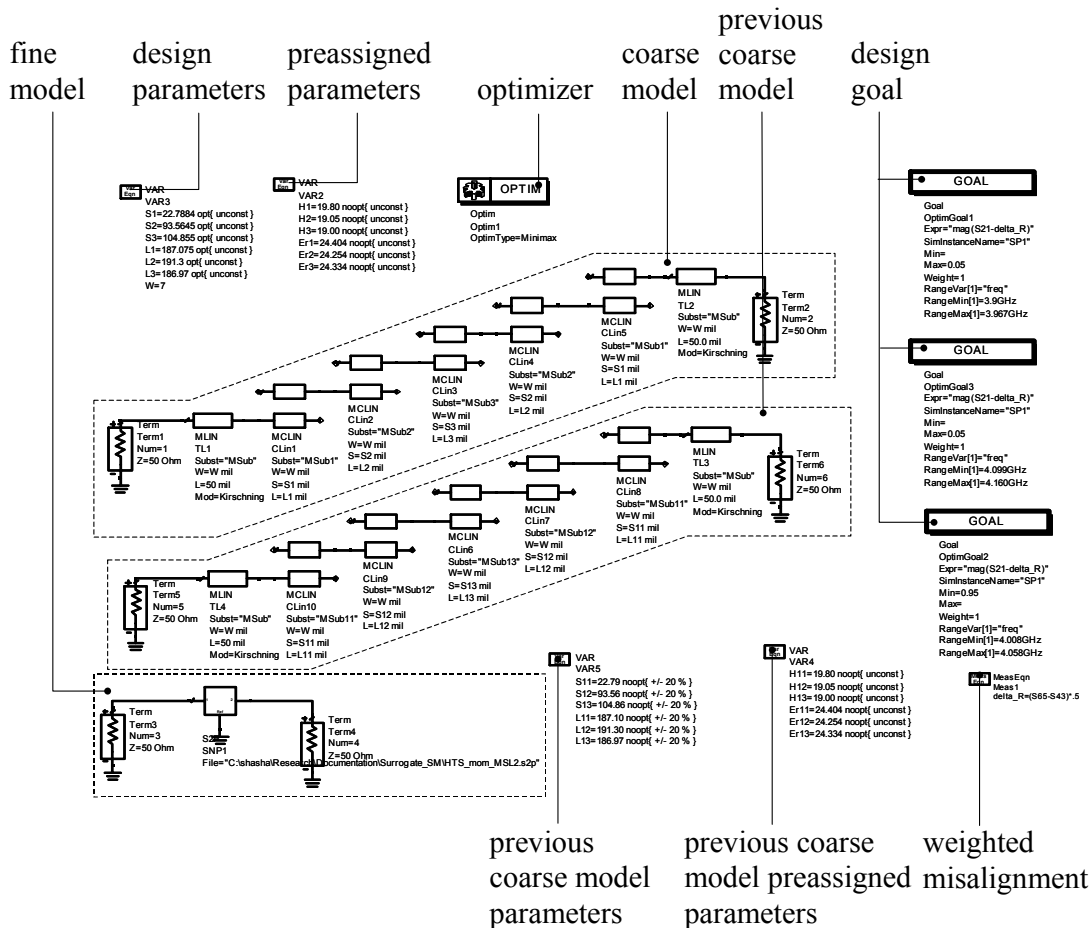


Fig. 5.9 Implementation of response residual space mapping in Agilent ADS.

calibrated coarse model in which the design parameters and preassigned parameters are fixed. The fine model response is imported from the fine model simulation. The residual is calculated using weighted misalignment between the fine model and previous coarse model. The new surrogate is generated using residual and the calibrated coarse model. We optimize the surrogate to predict next fine model design.

5.3 REVIEW OF OTHER SM IMPLEMENTATIONS AND APPLICATIONS

5.3.1 RF and Microwave Implementation

The required interaction between coarse model, fine model and optimization tools makes SM difficult to automate within existing simulators. A set of design or preassigned parameters and frequencies have to be sent to the different simulators and corresponding responses retrieved. Software packages such as OSA90 or MATLAB can provide coarse model analyses as well as optimization tools. Empipe (1997) and Momentum_Driver (Ismail, 2001) have been designed to drive and communicate with Sonnet's *em* (2001) and Agilent Momentum (2000) as fine models. Aggressive SM optimization of 3D structures (Bandler, Biernacki and Chen, 1996) has been automated using a two-level Datapipe (OSA90/hope, 1997) architecture of OSA90. The Datapipe technique allows the algorithm to carry out nested optimization loops in two separate processes while maintaining a functional link between their results (e.g., the next

increment to \mathbf{x}_f is a function of the result of parameter extraction).

SMX system

The object-oriented SMX (Bakr, Bandler, Cheng, Ismail and Rayas-Sánchez, 2001) (see Appendix A) optimization system implements the surrogate model-based SM algorithm (Bakr, Bandler, Madsen, Rayas-Sánchez and Søndergaard, 2000), which is automated for the first time. SMX has been linked with Empipe and Momentum_Driver to drive Sonnet's *em* and Agilent Momentum, as well as with user-defined simulators.

Six-Section H-Plane Waveguide Filter

Bakr (2000) consider to apply SM technique in designing a six-section H-plane waveguide filter (Young and Schiffman, 1963, Matthaei, Young and Jones, 1964). The coarse model consists of lumped inductances and dispersive transmission line sections. It is simulated using OSA90/hope. There are various approaches to calculate the equivalent inductive susceptance corresponding to an H-plane septum. We utilize a simplified version of a formula due to Marcuvitz (1951) in evaluating the inductances. The fine model exploits HP HFSS Ver. 5.2 through HP Empipe3D. A good result is obtained using HASM (Bakr, Bandler, Georgieva and Madsen, 1999).

Automatic Model Generation, Neural Networks and Space Mapping

Devabhaktuni, Chattaraj, Yagoub and Zhang (2003) propose a technique for generating microwave neural models of high accuracy using less accurate data. The proposed Knowledge-based Automatic Model Generation (KAMG) to

make extensive use of the coarse generator and minimal use of the fine generator.

Space Mapping Implementation of Harscher et al.

This technique combines EM simulations with a minimum prototype filter network (surrogate). Harscher, Ofli, Vahldieck and Amari (2002) present two examples: a direct coupled 4-resonator E-plane filter and a dual-mode filter. The EM solver is based on Mode Matching.

CAD Technique for Microstrip Filter Design

Ye and Mansour (1997) apply SM steps to reduce the simulation overhead required in microstrip filter design. They illustrated their technique through an HTS filter.

SM Models for RF Components

Snel (2001) proposed the SM technique in RF filter design for power amplifier circuits. He suggests building a library of fast, space-mapped RF filter components. These components can be incorporated in the design of ceramic multilayer filters for different center frequencies in wireless communication systems. The library is implemented in the Agilent ADS design framework.

Multilayer Microwave Circuits (LTCC)

Pavio, Estes and Zhao (2002) apply typical SM techniques in optimization of high-density multilayer RF and microwave circuits. They apply the SM approach to a three-pole bandstop filter, Low Temperature Co-firing Ceramic (LTCC) capacitor, LTCC three-section bandstop filter and an LTCC broadband tapered transformer.

Cellular Power Amplifier Output Matching Circuit

Lobeek (2002) demonstrates the design of a DCS/PCS output match of a cellular power amplifier using SM. The design uses a 6-layer LTCC substrate, a silicon passive integration die, discrete surface mount designs as well as bond wires. Lobeek also applies the SM model to monitor the statistical behavior of the design w.r.t. parameter values. Monte Carlo analysis with EM accuracy based on the space-mapped model shows good agreement with manufactured data.

A Multilevel Design Optimization Strategy

Safavi-Naeini, Chaudhuri, Damavandi and Borji (2002) consider a 3-level design methodology for complex RF/microwave structure using an SM concept. Their technique is implemented in the *WATML-MICAD* software. Applications include a parallel-coupled line filter, combline-type filters and multiple-coupled cavity filters.

LTCC RF Passive Circuits Design

Wu, Zhang, Ehlert and Fang (2003) present an explicit knowledge embedded space mapping optimization technique. They apply the proposed scheme on the design of low temperature cofired ceramic (LTCC) RF passive circuits, along with the required CAD formulas (knowledge) for typical embedded multilayer passives. Wu, Zhao, Wang and Cheng (2004) propose a concept called the dynamic coarse model and apply to the optimization design of LTCC multilayer RF circuits with the aggressive SM technique.

Waveguide Filter Design

Steyn, Lehmsiek and Meyer (2001) consider the design of irises in multi-mode coupled cavity filters. With the aggressive SM technique only 4 coupling coefficients were sufficient to obtain the same error.

Dielectric Resonator Filter and Multiplexer Design

Ismail, Smith, Panariello, Wang and Yu (2004) apply SM optimization with FEM (fine model) to design a 5-pole dielectric resonator loaded filter and a 10-channel output multiplexer. The proposed approach reduces overall tuning time compared with traditional techniques.

Comblined Filter Design

Swanson and Wenzel (2001) introduce a design approach based on the SM concept and commercial FEM solvers. From a good starting point, one iteration is needed to implement the design process.

CAD of Integrated Passive Elements on PCBs

Draxler (2002) introduces a methodology for CAD of integrated passive elements on Printed Circuit Board (PCB) incorporating Surface Mount Technology (SMT). The proposed methodology uses the SM concept to exploit the benefits of both domains.

Coupled Resonator Filter

Pelz (2002) applies SM in realization of narrowband coupled resonator filter structures. A 5-pole coupled resonator filter design is achieved with fast convergence.

Nonlinear Device Modeling

Zhang, Xu, Yagoub, Ding and Zhang (2003) introduce a new Neuro-SM approach for nonlinear device modeling and large signal circuit simulation. The Neuro-SM approach is demonstrated by modeling the SiGe HBT and GaAs FET devices.

Comb Filter Design

Gentili, Macchiarella and Politi (2003) implement an accurate design of microwave comb filters using SM technique. They use internal circuit model parameters as preassigned parameters to apply the implicit SM.

Inductively Coupled Filters

Soto, Bergner, Gomez, Boria and Esteban (2000) apply the aggressive SM procedure to build an automated design of inductively coupled rectangular waveguide filters. The complete aggressive SM design procedure required 3 iterations to converge (10 times faster than directly using a precise simulation tool).

5.3.2 Electrical Engineering Implementation*Magnetic Systems*

Choi, Kim, Park and Hahn (2001) utilize SM to design magnetic systems. They validate the approach by two numerical examples: a magnetic device with leakage flux and a machine with highly saturated part. Both examples converge after only 5 iterations (Choi, Kim, Park and Hahn, 2001).

Photonic Devices

Feng, Zhou and Huang (2003) apply the SM technique for design optimization of antireflection (AR) coatings for photonic devices such as the semiconductor optical amplifiers (SOA). Feng and Huang (2003) employ the generalized space mapping (GSM) technique for modeling and simulation of photonic devices.

5.3.3 Other Engineering Implementation

Structural Design

Leary, Bhaskar and Keane (2001) apply the SM technique in civil engineering structural design. Their aim is to establish a mapping between the constraints of a fine model and a coarse model. They illustrate their approach with a simple structural problem of minimizing the weight of a beam subject to constraints such as stress.

Vehicle Crashworthiness Design

Redhe and Nilsson (2002) apply the SM technique and surrogate models together with response surfaces to structural optimization of crashworthiness problems. Using the SM technique CPU time is reduced relative to the traditional response surface methodology.

5.4 CONCLUSIONS

In this chapter, we discussed implementations and framework techniques. We introduced an easy to use ADS schematic framework for SM. We

demonstrate its implementation. We reviewed various successful implementations by other groups and researchers. This verifies that SM technology can be applied to substantially different design and modeling areas in science and engineering. It also places our work into context.

Chapter 6

CONCLUSIONS

This thesis presents innovative methods for electromagnetics-based computer-aided modeling and design of microwave circuits exploiting implicit and output space mapping (SM) and surrogate modeling technology. These technologies are demonstrated by the so-called “cheese problem” and illustrated by designing several practical microstrip structures. We also discuss various implementations.

In Chapter 2 we review the SM technique and the SM-oriented surrogate (modeling) concept and their applications in engineering design optimization. The simple CAD methodology follows the traditional experience and intuition of engineers, yet appears to be amenable to rigorous mathematical treatment. The aim and advantages of SM are described. The general steps for building surrogates and SM are indicated. Approaches reviewed include the original SM algorithm, the Broyden-based aggressive space mapping, trust region aggressive space mapping, hybrid aggressive space mapping, neural space mapping and implicit space mapping. Parameter extraction is an essential subproblem of any SM optimization algorithm. It is used to align the surrogate with the fine model at each iteration. Different approaches to enhance the uniqueness of parameter

extraction are reviewed, including the recent gradient parameter extraction process. An expanded space mapping design framework is reviewed. This technique expands original space mapping by allowing certain preassigned parameters (which are not used in optimization) to change in some components of the coarse model. The space mapping concept and frameworks are discussed. SM techniques are categorized based on their properties.

Based on a general concept, we present an effective technique for microwave circuit modeling and design w.r.t. full-wave EM simulations in Chapter 3. We vary preassigned parameters in a coarse model to align it with the EM (fine) model. We believe this is the easiest to implement “Space Mapping” technique offered to date. The HTS filter design is entirely carried out by Agilent ADS and Momentum (3 frequency sweeps) or Sonnet *em*, (only 2 frequency sweeps) with no matrices to keep track of. A general SM concept is presented which enables us to verify that our implementation is correct and that no redundant steps are used.

In Chapter 4 we propose significant improvements to implicit space mapping for EM-based modeling and design. Based on an explanation of residual misalignment, our new approach further fine-tunes the surrogate by exploiting an “output space” mapping (OSM) or “response residual space” mapping (RRSM). The required HTS filter models and RRSM are easily implemented by Agilent ADS and Momentum with no matrices to keep track of. An accurate HTS microstrip filter design solution emerges after only four EM simulations with

sparse frequency sweeps. We present the RRSM modeling technique that matches the output residual SM surrogate with the fine model. A new “multiple cheese-cutting” design problem illustrates the concept. Our approach is implemented entirely in the ADS framework. A good H-plane filter design emerges after only five EM simulations using the implicit and RRSM with sparse frequency sweeps and no Jacobian calculations.

Chapter 5 discusses the implementation framework techniques. We introduce an easy ADS schematic design framework for SM and demonstrate in a three-section transformer. We also review other successful implementations both from our group and from other researchers or engineers. They prove that SM technology can be applied to different design and modeling areas.

Appendix A describes the object-oriented SMX optimization system. It implements the surrogate model-based SM (SMSM) algorithm, which is automated for the first time.

Appendix B explains our so-called cheese-cutting problems. We utilize the simple physics and geometry of ideal or contrived cheese blocks (slices) to study and illustrate various space mapping techniques.

From the experience and knowledge gained in the course of this work the author is convinced that the following research topics should be interesting to investigate:

- (1) Implicit SM optimization is emphasized in this thesis. ISM is also a modeling technique. We can explore further on this aspect. For

example, we can use a set of preassigned parameters to calibrate a coarse (large) grid EM simulator to match a fine (small) grid EM simulator. Taking advantage of continuous preassigned parameters we could interpolate the responses of structures that are not on the discrete grids of the coarse EM simulator meshes. This ISM interpolated coarse grid EM simulator could act as a fast but accurate EM simulator.

- (2) The ISM discussed in this thesis uses the same preassigned parameters for all the frequency (sample) points. This may not be sufficient for frequency-sensitive devices. We can introduce a frequency-based ISM. The ISM model uses different preassigned parameters for different frequency points or different frequency bands. The new ISM could make a better surrogate.
- (3) In this thesis, output SM or RRSM is only used to calibrate the implicitly mapped coarse model. We could extend OSM/RRSM to other types of space mapping. For example, we can use the output calibrated coarse model in aggressive SM to speed up or increase the probability of convergence.
- (4) Currently, the ADS schematic design framework for SM is applicable to several kinds of space mapping (aggressive or implicit/output SM) algorithms. It is possible to apply the design framework to more SM algorithms. We could also support other

EM simulators, e.g., Ansoft HFSS under this design framework.

More examples and illustrations could be done in this framework.

- (5) The ADS schematic design framework for SM described in this thesis is not automated. It needs human intervention at each iteration because of the current limitations of ADS. However, Agilent is constantly updating its ADS. In the near future, the semi-automated interactive implementation could be automated as soon as a better sequential optimization method is available from Agilent.

Appendix A

SMX OBJECT-ORIENTED OPTIMIZATION SYSTEM

The object-oriented SMX (Bakr, Bandler, Cheng, Ismail and Rayas-Sánchez, 2001) optimization system implements the surrogate model-based SM (SMSM) algorithm (Bakr, Bandler, Madsen, Rayas-Sánchez and Søndergaard, 2000), which is automated for the first time. SMX has been linked with Empipe (1997) and Momentum_Driver (Ismail, 2001) to drive Sonnet's *em* and Agilent Momentum, as well as with user-defined simulators.

In the SMSM approach, a surrogate (Booker, Dennis, Frank, Serafini, Torczon and Trosset, 1999) of the fine model is iteratively used to solve the original design problem. This surrogate model is a convex combination of a mapped coarse model and a linearized fine model. It can exploit a frequency-sensitive mapping.

The SMX engine implements the SMSM algorithm. Object-Oriented Design (OOD) abstracts the basic behavior of the models and optimizers modules. A universal parameter setting and results retrieval method is utilized for all simulators and optimizers. The SMX architecture integrates these modules.

Another advantage of OOD is reusability and extendibility. SMX is

intended to support a number of EM and circuit simulators. Here, the basic functionality of simulators and optimizers is abstracted in the two basic classes `Simulator` and `Optimizer`. Many commercial simulators and optimizers could be derived from these classes.

The SMX system is described in the Unified Modeling Language (UML). Using this language, a complicated system can be decomposed into relatively independent small objects without losing readability and intuitiveness. The structure of each object can be represented in UML.

SMX takes advantage of the multi-thread capability of the Microsoft Windows operating system (Petzold, 1990). The user-friendly interface responds smoothly while the SMX core is running in a different thread in the background. Synchronization and communication between threads are properly arranged. SMX is capable of optimizing while showing intermediate results and interacting with the user.

A.1 SMX ARCHITECTURE

SMX automates the algorithm and drives EM/circuit simulators. Object-oriented design is employed to decompose the algorithm into independent modules (objects). Here the module or object is an instance of a certain class. Each module can carry out certain functionality. It includes data structures describing the properties of the object. Using the encapsulation concept, the SMX system is decomposed into 6 modules, as shown in Fig. A.1.

The user interface and SMX engine run in two separate threads concurrently. The user chooses the simulators and setup problem specifications through a user interface. The interface initiates the starting point $\mathbf{x}_c^{(0)}$, the constraints and the control signals for the coarse and fine models. The SMX engine performs optimization and returns the progress, the current status, responses \mathbf{R}_f and \mathbf{R}_c , etc., to the user interface. The user interface feeds back the optimization status such as objective function, designable parameters and critical mapping parameters $\mathbf{B}^{(i)}$, $\mathbf{s}^{(i)}$, $\mathbf{t}^{(i)}$, $\boldsymbol{\sigma}^{(i)}$, $\mathbf{c}^{(i)}$ and $\boldsymbol{\gamma}^{(i)}$ in graphical and numerical format to the user. The engine can optimize a model using either classical optimization methods such as gradient-based minimax or the SMSM algorithm (Bakr, Bandler, Madsen, Rayas-Sánchez and Søndergaard, 2000).

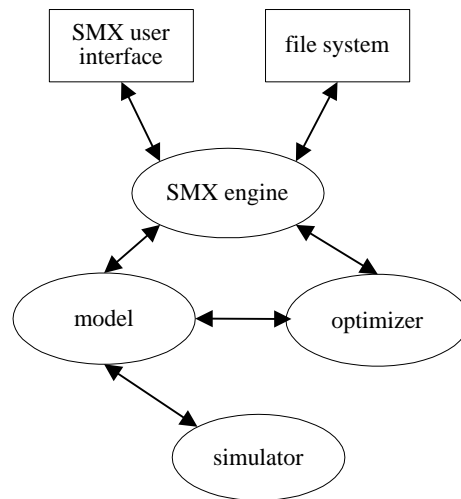


Fig. A.1 The modules of SMX.

A.2 ALGORITHM CORE: SMX ENGINE

The SMX engine is abstracted as the `SMX_Engine` class. After setup, the coarse model is optimized by the member function `OptimizeCoarseModel` from the starting point $\mathbf{x}_c^{(0)}$. This function uses `m_pCoarseModelOptimizer`, a pointer to a minimax optimizer object to obtain \mathbf{x}_c^* . Then the member function `OptimizeSurrogate` is called to optimize the surrogate model $\mathbf{R}_s^{(i)}(\mathbf{x}_f)$ starting from the optimized coarse model. The Huber optimizer is used for parameter extraction in `OptimizeSurrogate`. To carry out space mapping, three base classes, `Optimizer`, `Simulator` and `Model`, are abstracted and built.

The `Optimizer` base class is an abstract class. It provides the interface for standard optimization routines. With override of optimization routines, additional parameter setup and objective function, the `Huber`, `Minimax` or other optimization classes can be derived from `Optimizer`. Some of the important functions in `Optimizer` are `GetNorm`, `GetErrors`, `FDF` and `SetConstraintMatrix`. Different optimizers use different norms as their objective functions. The purely virtual function `GetNorm` is overridden to obtain the appropriate norm. `FDF` gets the error values and their derivatives by perturbation. It calls `GetErrors` to evaluate the error used for parameter extraction, as well as for minimax design optimization. `SetConstraintMatrix` sets constraints in matrix form. The inheritance relation of `Optimizer` is shown in Fig. A.2.

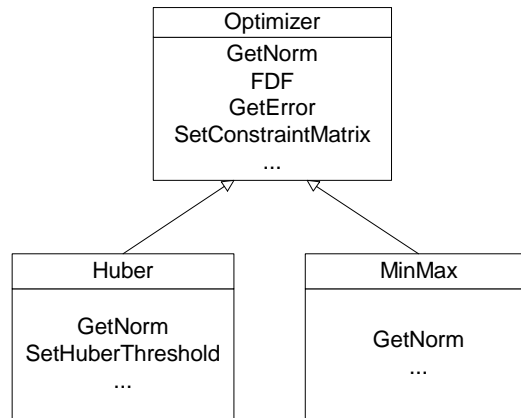


Fig. A.2 Illustration of the derivation of basic optimizer class.

Similar to `Optimizer`, the `Simulator` class is a parent class for different simulators. Commercial simulators and user defined simulators are derived classes. Interface functions are overridden for each new derived simulator class. Additional parameters may also be added. OSA90/hopeTM (1997) and Agilent MomentumTM (2000) are commercial simulators currently derived from the `Simulator` class.

The `SMX_Engine` utilizes `SurrogateModel` which is derived from a base `Model` class. The `Model` class functions as a wrapper of a simulator. The responses are obtained independent of the simulator. Obviously, `Simulator` is one of the `Model` members. The `Model` class sends data to the simulator and retrieves responses from it. Since `Optimizer` needs normalized parameters, scaling factors are added.

A.3 HTS FILTER EXAMPLE

We consider two cases of the HTS filter problem (Bandler, Biernacki,

Chen, Getsinger, Grobelny, Moskowitz and Talisa, 1995). In Case 1, the “coarse” and “fine” models are both empirical models of OSA90/hope. The “coarse” model uses the ideal open circuit for the open stubs while the “fine” model uses empirical models.

The designable parameters are the lengths L_1 , L_2 and L_3 of the coupled

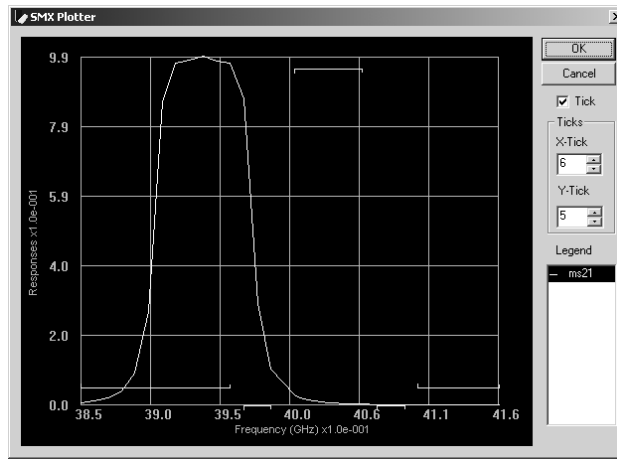


Fig. A.3 Case 1: The initial response of the HTS filter for the “fine” model (OSA90).

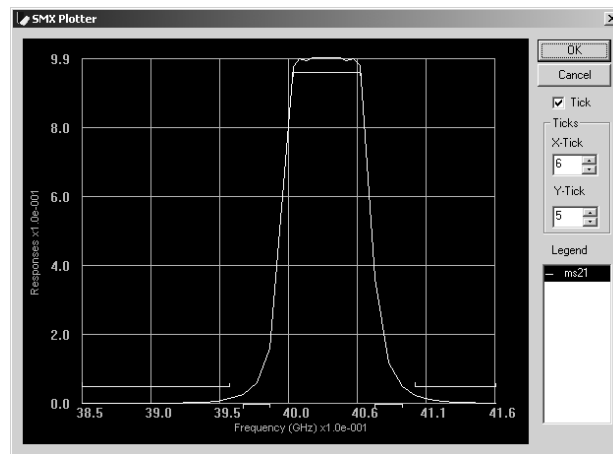


Fig. A.4 Case 1: The optimal “fine” model (OSA90) response of the HTS filter.

lines and their separation S_1 , S_2 and S_3 .

The SMX system obtained the optimal solution in 4 iterations. The “fine” model response in the first iteration is shown in Fig. A.3. The “fine” model response at the final iteration is shown in Fig. A.4. TABLE A.1 shows the initial

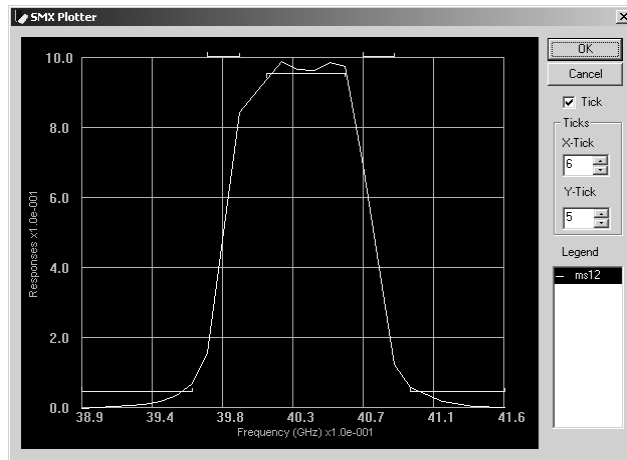


Fig. A.5 Case 2: The SMX optimized fine model (Agilent Momentum) response of the HTS filter.

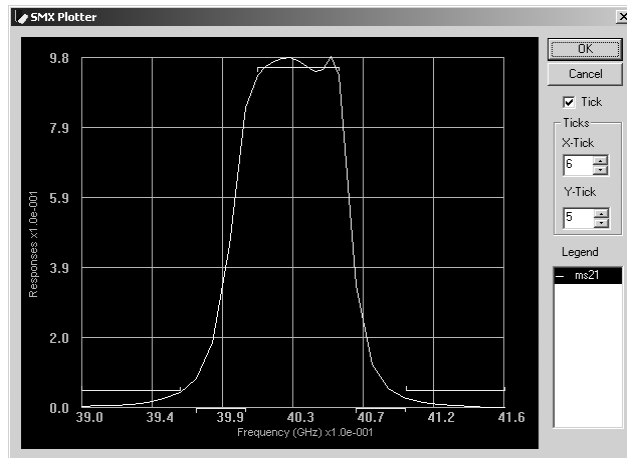


Fig. A.6 Case 2: The final Momentum optimized fine model response of the HTS filter with a fine interpolation step of 0.1mil.

and final parameters obtained by SMX optimization.

In Case 2 we use Momentum as the fine model, while the coarse model is the same as in Case 1. SMX obtains the solution in 4 iterations. Fig. A.5 shows the fine model responses at the fourth SMX iteration. Then the minimax optimizer in Momentum is used to refine this solution. It takes approximately 32 hours on an IBM Aptiva computer with AMD-K7 650MHz CPU and 384MB RAM. We use fine interpolation resolution (0.1mil for all parameters). See Fig. A.6.

TABLE A.1
THE INITIAL AND FINAL DESIGNS OF THE FINE MODEL (OSA90)
FOR THE HTS FILTER

Parameter	$x_f^{(1)}$	$x_f^{(4)}$
L_1	187.50	185.55
L_2	198.84	191.71
L_3	187.91	185.82
S_1	20.04	21.03
S_2	98.08	99.44
S_3	100.90	114.21
all values are in mils		

Appendix B

CHEESE-CUTTING PROBLEMS

Our so-called cheese-cutting problems utilize the simple physics and geometry of ideal or contrived cheese blocks (slices) to study and illustrate various space mapping techniques.

B.1 CHEESE-CUTTING PROBLEM

The cheese blocks, depicted in Fig. B.1, demonstrate how the aggressive SM approach may not converge in certain cases. Our “response” is *weight*. The designable parameter is *length*. A height and a density of one are assumed. A width of 3 units is used. The goal is a desired *weight* of 30 units.

Our idealized “coarse” model is a uniform cuboidal block (top block of Fig. B.1). The optimal *length* $x_c^* = 10$ is easily calculated. The response is evaluated by

$$R_c = x_c^* \cdot 3 \cdot 1 = 30$$

In practice, coarse models may have limitations. For example, the range of the coarse model may be smaller than the range of the fine model. The coarse model may not be capable of matching the fine model in the parameter extraction. However, in this one-dimensional linear cheese-cutting example, the coarse model

range is not limited. To mimic limitations in higher dimensions and for non-linear coarse models, we will confine the coarse model range, e.g., $[30, +\infty)$, by rewriting the coarse model as follows

$$R_c = \max \{30, 3x_c\} \cdot 1$$

Let the actual block (“fine” model) be similar but imperfect (second block of Fig. B.1). A six-unit part is missing. We take the optimal coarse model *length* as the initial guess for the fine model solution, i.e., cutting the cheese so that $x_f^{(1)} = x_c^* = 10$. The fine model response is

$$R_f = x_f^{(1)} \cdot 3 \cdot 1 - 6 = 24$$

This does not satisfy our goal. We realign (calibrate the design parameter x_c) our coarse model to match the outcome of the cut (on the fine model). This is a parameter extraction (PE) step in which we obtain a solution $x_c^{(1)} = 10$ (third block of Fig. B.1, noting the coarse model constraint). This value is equal to x_c^* . The algorithm exits. In this example, we notice that PE is not able to generate a

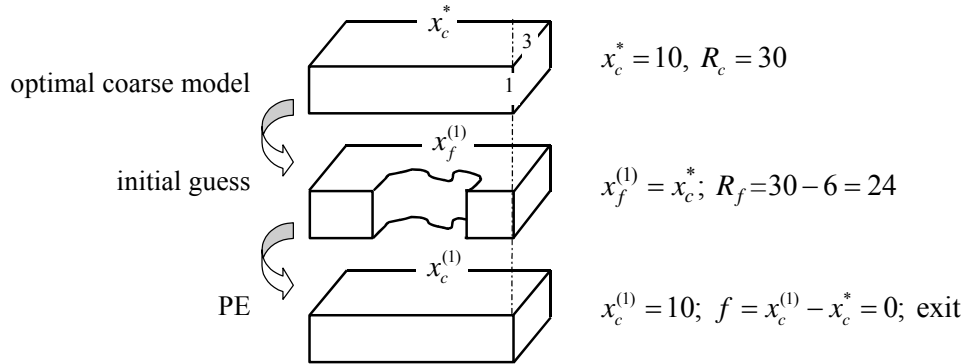


Fig. B.1 The aggressive SM may not converge to the optimal fine model solution in this case.

good match between coarse and fine model, an essential assumption in the ASM.

A response residual space mapping (RRSM) takes into account the mismatch in the parameter extraction and is able to overcome the problem. We calculate the residual ΔR after the PE (see 3rd block of Fig. B.2) and generate a surrogate R_s using the original coarse model plus the residual ΔR . This procedure can be thought of as to correct (relax or tighten) the coarse model specification by a residual. We re-optimize the surrogate w.r.t. the original specification to obtain a new (or updated) x_c^* , or in other words, re-optimize the coarse model w.r.t. the new specification. Let $x_f^{(2)} = x_c^* = 12$. We obtain the new fine model response. The optimal fine model solution is obtained in 1 iteration (2 fine model evaluations). See Fig. B.2.

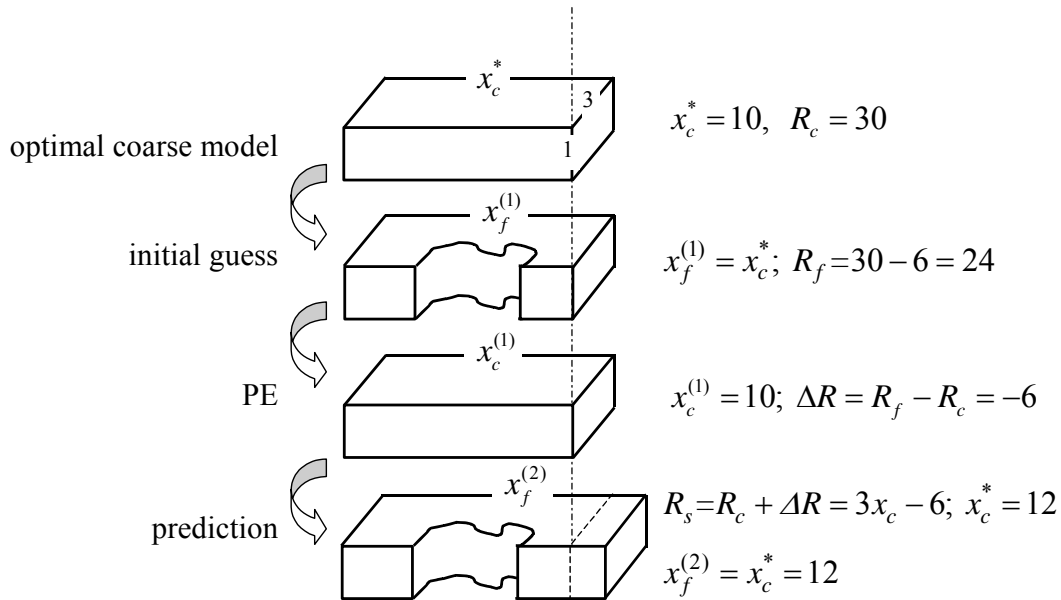


Fig. B.2 The RRSM solves the problem in one iteration (two fine model evaluations).

B.2 MULTIPLE CHEESE-CUTTING PROBLEM

We develop a physical example suitable for illustrating space mapping optimization. This example is intended to examine the mismatch problem in the parameter extraction. Our “responses” are the *weights* of individual cheese slices. The designable parameter is the *length* of the top slice [see Fig. B.3(a)]. A width and a density of one are assumed. The goal is to cut through the slices to obtain a *weight* for each one as close to a desired *weight* s as possible. Note that we measure the *length* from the right-hand end. We cut on the left-hand side.

The coarse model involves 3 slices of the same *height* x , namely, the preassigned parameter shown in Fig. B.3(a). The lengths of the two lower slices are c units shorter than the top one. The optimal *length* x_c^* can be calculated to minimize the differences between the weights of the slices and a desired *weight* s . We use minimax optimization. The responses of the coarse model are given by

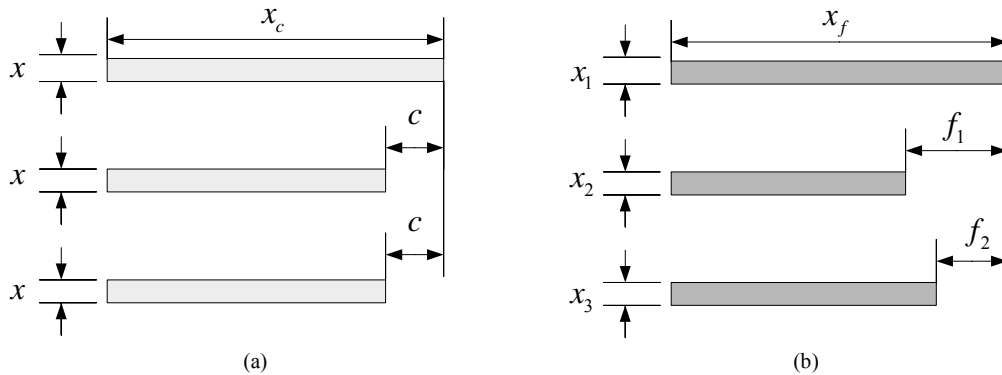


Fig. B.3 The multiple cheese-cutting problem: (a) the coarse model (b) and fine model.

$$\begin{aligned}
R_{c1} &= x \cdot x_c \cdot 1 \\
R_{c2} &= x \cdot (x_c - c) \cdot 1 \\
R_{c3} &= x \cdot (x_c - c) \cdot 1
\end{aligned} \tag{B.1}$$

The fine model is similar but the lower two slices are f_1 and f_2 units shorter, respectively, than the top slice [Fig. B.3(b)]. The *heights* of the slices are x_1 , x_2 and x_3 , respectively. The corresponding responses of the fine model are

$$\begin{aligned}
R_{f1} &= x_1 \cdot x_f \cdot 1 \\
R_{f2} &= x_2 \cdot (x_f - f_1) \cdot 1 \\
R_{f3} &= x_3 \cdot (x_f - f_2) \cdot 1
\end{aligned} \tag{B.2}$$

B.2.1 Aggressive Space Mapping

Before we apply ASM to the multiple cheese-cutting problem, we review the following ASM algorithm (Bandler, Biernacki, Chen, Hemmers and Madsen, 1995)

Step 0 Initialize $\mathbf{x}_f^{(1)} = \mathbf{x}_c^*$, $\mathbf{B}^{(1)} = \mathbf{1}$, $\mathbf{f}^{(1)} = \mathbf{P}(\mathbf{x}_f^{(1)}) - \mathbf{x}_c^*$, $j = 1$. Stop if

$$\|\mathbf{f}^{(1)}\| \leq \eta.$$

Step 1 Solve $\mathbf{B}^{(j)}\mathbf{h}^{(j)} = -\mathbf{f}^{(j)}$ for $\mathbf{h}^{(j)}$.

Step 2 Set $\mathbf{x}_f^{(j+1)} = \mathbf{x}_f^{(j)} + \mathbf{h}^{(j)}$.

Step 3 Perform parameter extraction optimization to get $\mathbf{x}_c^{(j+1)}$, i.e.,

evaluate $\mathbf{P}(\mathbf{x}_f^{(j+1)})$.

Step 4 Compute $\mathbf{f}^{(j+1)} = \mathbf{P}(\mathbf{x}_f^{(j+1)}) - \mathbf{x}_c^*$. If $\|\mathbf{f}^{(j+1)}\| \leq \eta$, stop.

Step 5 Update $\mathbf{B}^{(j)}$ to $\mathbf{B}^{(j+1)}$ using the Broyden formula.

Step 6 Set $j = j + 1$; go to Step 1.

We demonstrate the Aggressive Space Mapping algorithm using the coarse and fine model in Fig. B.3. We show the ASM algorithm may not converge to fine model optimal solution in this case (Fig. B.4). In this example we set $c = 0$ and $f_1 = f_2 = 4$. The specification s is set to 10. The *heights* of the cheese blocks are fixed at unity, i.e. $x = x_1 = x_2 = x_3 = 1$. The algorithm exits after 1 iteration since $f = 0$ as in Fig. B.4(5). We can see there is a significant residual between the coarse and fine model. A new surrogate is needed to find the real solution [Fig. B.4(6)].

We use the optimality conditions of ASM on this multiple cheese-cutting problem to show the possible non-convergence to fine model optimal solution. We assume the fine model parameters $f_1 = f_2 = f_0$, coarse mode parameter $c = c_0$ and $x_1 = x_2 = x_3 = x = 1$. We obtain the optimality conditions for ASM

$$\begin{cases} x_c^* - c_0 - 10 = 10 - x_c^* & \text{(B.3)} \end{cases}$$

$$\begin{cases} 2 \cdot (x_c - x_f) + 4 \cdot [(x_c - c_0) - (x_f - f_0)] = 0 & \text{(B.4)} \end{cases}$$

$$\begin{cases} x_c - x_c^* = 0 & \text{(B.5)} \end{cases}$$

where (B.3) is from applying the minimax optimality condition to the coarse model, (B.4) is the least-squares optimality condition (stationary point) for the parameter extraction and (B.5) is the exit condition (stopping criteria, see Step 4 of the ASM algorithm).

From (B.3) we obtain

$$x_c^* = 10 + \frac{c_0}{2} \tag{B.6}$$

From (B.4) we obtain

$$x_f = x_c - \frac{2}{3}c_0 + \frac{2}{3}f_0 \tag{B.7}$$

Incorporating (B.5) and (B.6) with (B.7) we obtain

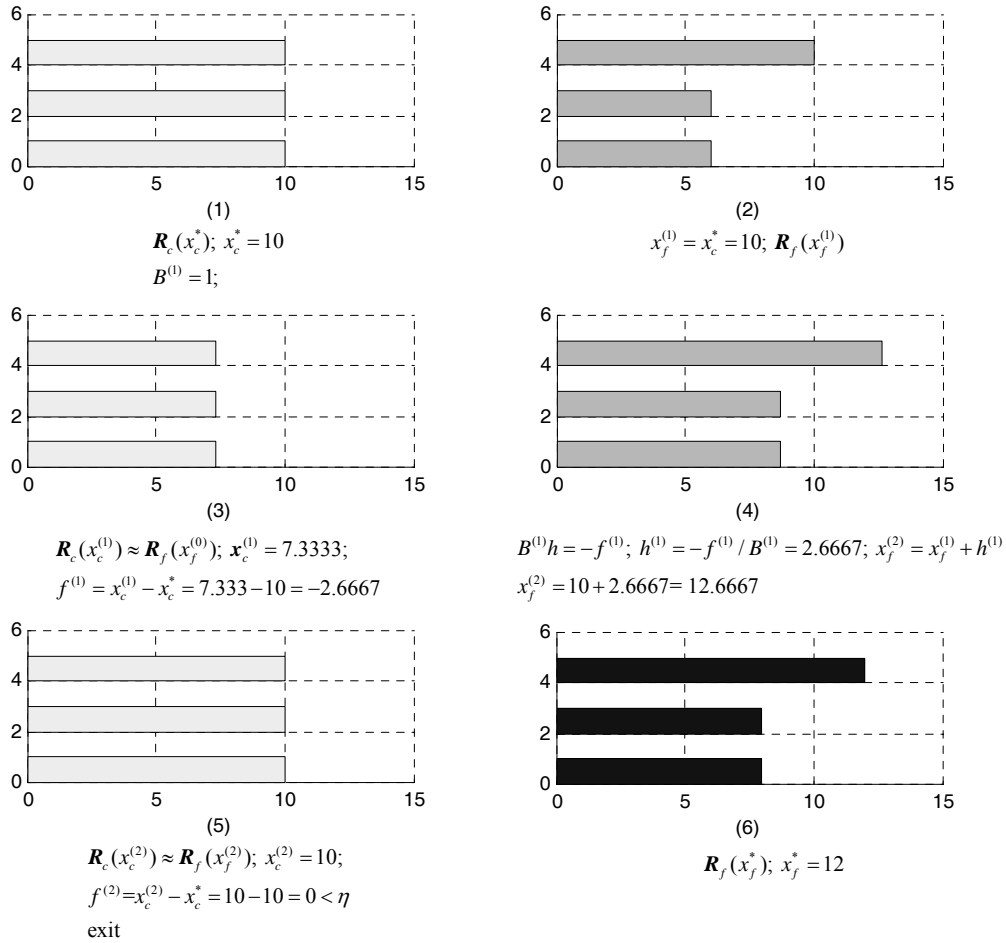


Fig. B.4 The ASM algorithm may not converge in this case.

$$x_f = 10 - \frac{c_0}{6} + \frac{2f_0}{3} \quad (\text{B.8})$$

Equation (B.8) shows the solution is a function of coarse model parameter c_0 . A misaligned coarse model may result in non-convergence of the ASM. Letting $c_0 = 0$ and $f_0 = 4$, we obtain $x_f = 12.6667$ which is consistent with the solution obtained in Fig. B.4(4). The optimal solution is not reached.

B.2.2 Response Residual ASM

Based on the observation of the non-convergence, we revise the ASM algorithm to include the response residual SM surrogate calibration. We calibrate the coarse model using the residual.

The new algorithm uses the ASM stopping criterion to switch to an RRSM surrogate calibration.

Step 0 Initialize $\mathbf{x}_f^{(1)} = \mathbf{x}_c^*$, $\mathbf{B}^{(1)} = \mathbf{1}$, $\mathbf{f}^{(1)} = \mathbf{P}(\mathbf{x}_f^{(1)}) - \mathbf{x}_c^*$, $\Delta\mathbf{R} = \mathbf{0}$ and

$j = 1$.

Step 1 Solve $\mathbf{B}^{(j)}\mathbf{h}^{(j)} = -\mathbf{f}^{(j)}$ for $\mathbf{h}^{(j)}$.

Step 2 Set $\mathbf{x}_f^{(j+1)} = \mathbf{x}_f^{(j)} + \mathbf{h}^{(j)}$. If $\|\mathbf{h}\| \leq \varepsilon$, stop.

Step 3 Perform parameter extraction optimization to get $\mathbf{x}_c^{(j+1)}$, i.e.,

evaluate $\mathbf{P}(\mathbf{x}_f^{(j+1)})$. Surrogate $\mathbf{R}_s = \mathbf{R}_c + \Delta\mathbf{R}$ is used as a coarse model to perform PE.

Step 4 Compute $\mathbf{f}^{(j+1)} = \mathbf{P}(\mathbf{x}_f^{(j+1)}) - \mathbf{x}_c^*$.

Step 5 If $\|f^{(j+1)}\| \leq \eta$ or $x_c^{(j+1)} = x_c^{(j)}$, update $\Delta R = R_f - R_c$, minimize

the surrogate $R_s = R_c + \Delta R$ to obtain a new x_c^* and $f = x_c - x_c^*$,

$B^{(j+1)} = \mathbf{1}$ else update $B^{(j)}$ to $B^{(j+1)}$ using the Broyden formula.

Step 6 Set $j = j + 1$; go to Step 1.

In this algorithm, initial condition $\Delta R = \mathbf{0}$ is added in Step 0. A new

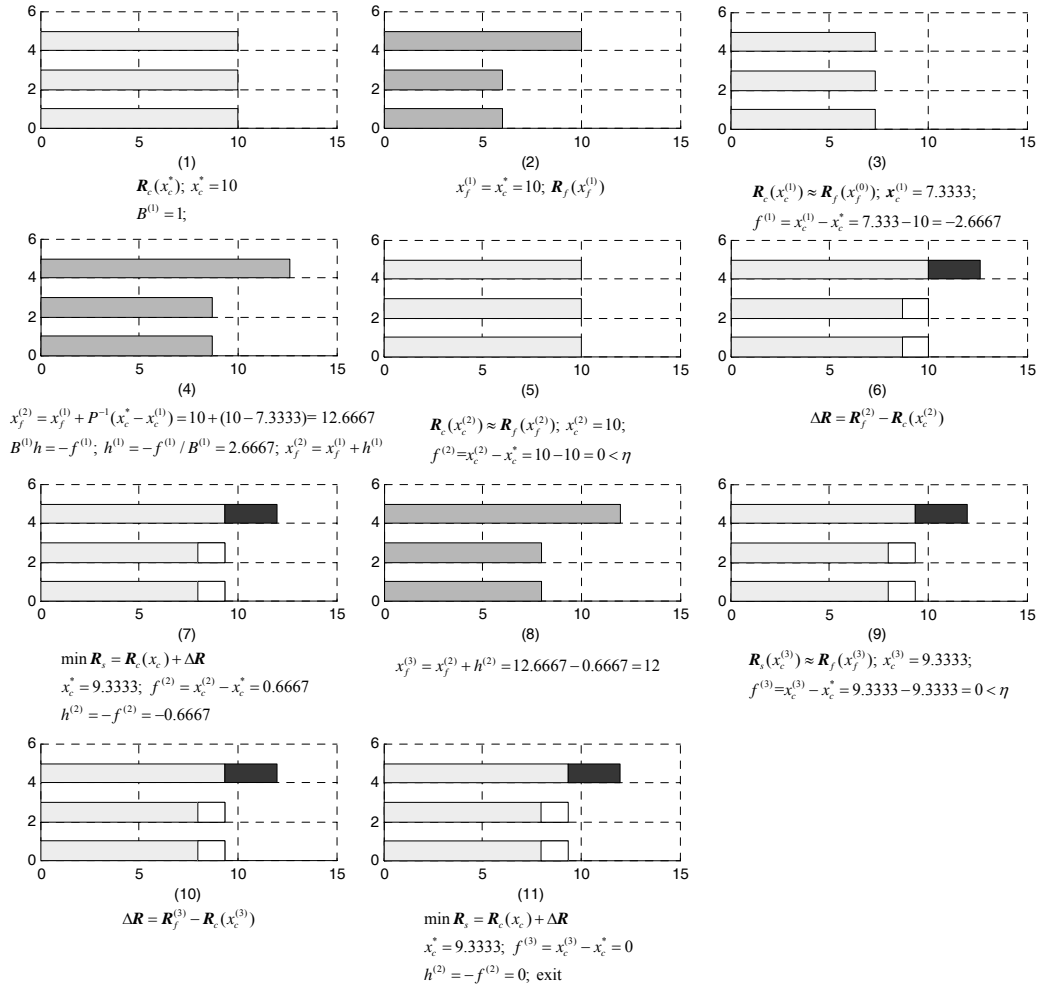


Fig. B.5 The response residual ASM algorithm converges in two iterations.

stopping criterion is added in Step 2, which stops the algorithm when a very small prediction is obtained. In Step 3, the parameter extraction uses the RRSM calibrated coarse model to match the fine model. In Step 5, we change the surrogate or update \mathbf{B} according to the original stopping criterion.

We use this new algorithm to solve the same multiple cheese-cutting problem as in Fig. B.4 again. In 2 iterations (3 fine model evaluations), we obtain the optimal solution $x_f = 12$ as shown in Fig. B.5.

B.2.3 Implicit SM

Implicit SM (ISM) may not converge for certain preassigned parameters if the mismatch of the coarse model and fine model is not compensated. We demonstrate this using the multiple cheese-cutting problem. Here we choose coarse model *height* x as a preassigned parameter, initially unity. We set the fine model parameters $f_1 = f_2 = 4$, fine model heights $x_1 = x_2 = x_3 = 1$ and coarse mode parameter $c = 2$. We obtain the convergence curve and solution $x_f = 12.2808$ as in Fig. B.6. It shows that the algorithm does not converge to the optimal solution.

We investigate the optimality condition for ISM. We assume that the least-squares solution is used for the parameter extraction and minimax for coarse (surrogate) optimization. We consider general coarse model responses $\mathbf{R}_c = [R_{c1} \dots R_{cn}]^T$ and fine model responses $\mathbf{R}_f = [R_{f1} \dots R_{fn}]^T$. Applying optimality conditions, we obtain

$$\sum_i 2 \cdot (R_{fi} - R_{ci}) \frac{\partial R_{ci}}{\partial \mathbf{x}^T} = \mathbf{0} \quad (\text{B.9})$$

$$\mathbf{x}_f = \mathbf{x}_c \quad (\text{B.10})$$

$$|R_{c1} - s_1| = |R_{c2} - s_2| \cdots = |R_{ck} - s_k| = \gamma \quad (\text{B.11})$$

$$|R_{ci} - s_{ci}| < \gamma \text{ for } i = k + 1, \dots, n \quad (\text{B.12})$$

where γ is the minimax “equal-ripple” peak deviation, R_{c1}, \dots, R_{ck} are the active calibrated coarse model function values. s_1, \dots, s_n are specifications for corresponding response functions R_{c1}, \dots, R_{cn} . Equation (B.9) is a necessary

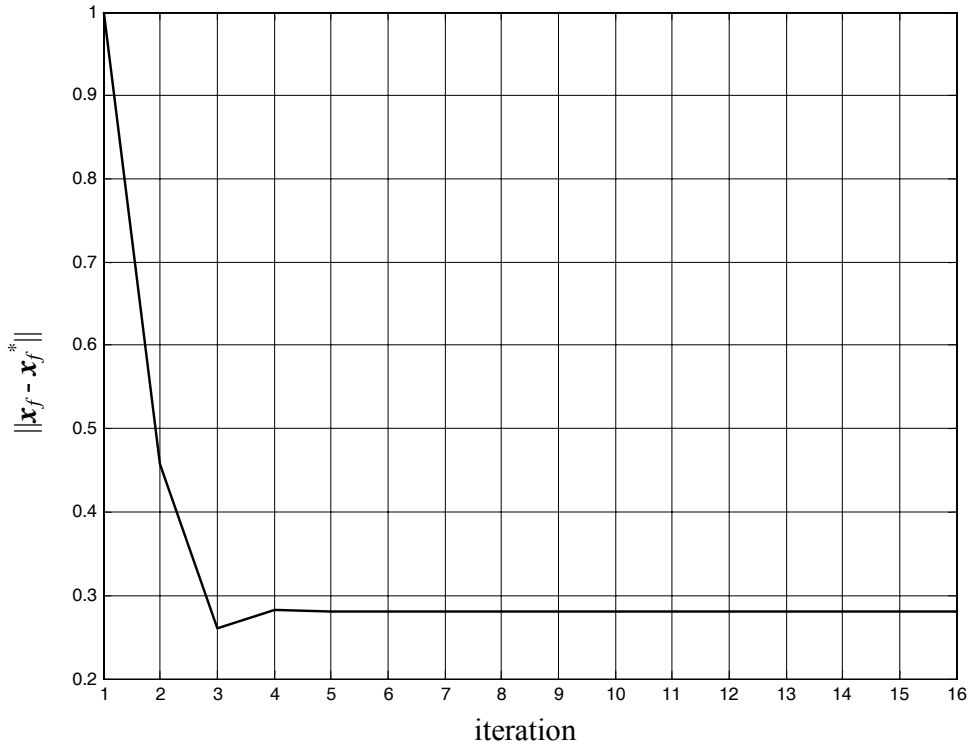


Fig. B.6 Parameter errors between the ISM algorithm and minimax direct optimization. Here $x_f = 12.2808$ and $x_f^* = 12$.

condition for minimum in the parameter extraction. Equation (B.10) is the condition enforced in each iteration. Equation (B.11) and (B.12) are the minimax (equal ripple) optimality condition.

We apply the conditions to the multiple cheese-cutting problem. Let the specification for all the responses be 10, the coarse model parameter c of (B.1) be c_0 and fine model parameters f_1 and f_2 of (B.2) be f_0 . We assume fine model preassigned parameters $x_1 = x_2 = x_3 = 1$. Using (B.9)-(B.12), we obtain

$$\begin{cases} 2 \cdot (x_c \cdot x - x_f) \cdot x_c + 4 \cdot [(x_c - c_0) \cdot x - (x_f - f_0)](x_c - c_0) = 0 & \text{(B.13)} \\ x_f = x_c & \text{(B.14)} \\ (x_c - c_0) \cdot x - 10 = 10 - x \cdot x_c & \text{(B.15)} \end{cases}$$

where (B.13) is from the derivative condition (B.9) and (B.15) is from the minimax optimality condition (B.11).

From (B.15) we obtain

$$x = \frac{20}{2x_c - c_0} \quad \text{(B.16)}$$

Substituting (B.14) and (B.16) into (B.13), we have

$$12x_c^3 - (120 + 8f_0 + 14c_0)x_c^2 + (12c_0f_0 + 4c_0^2 + 160c_0)x_c - 4c_0^2f_0 - 80c_0^2 = 0 \quad \text{(B.17)}$$

We define

$$g(x_c) \triangleq 12x_c^3 - (120 + 8f_0 + 14c_0)x_c^2 + (12c_0f_0 + 4c_0^2 + 160c_0)x_c - 4c_0^2f_0 - 80c_0^2 \quad \text{(B.18)}$$

The root of equation (B.18) is the solution that ISM converges to. If we choose $[c_0 \ f_0] = [2 \ 4]$, the root is 12.2808, as shown in Fig. B.7. It is consistent

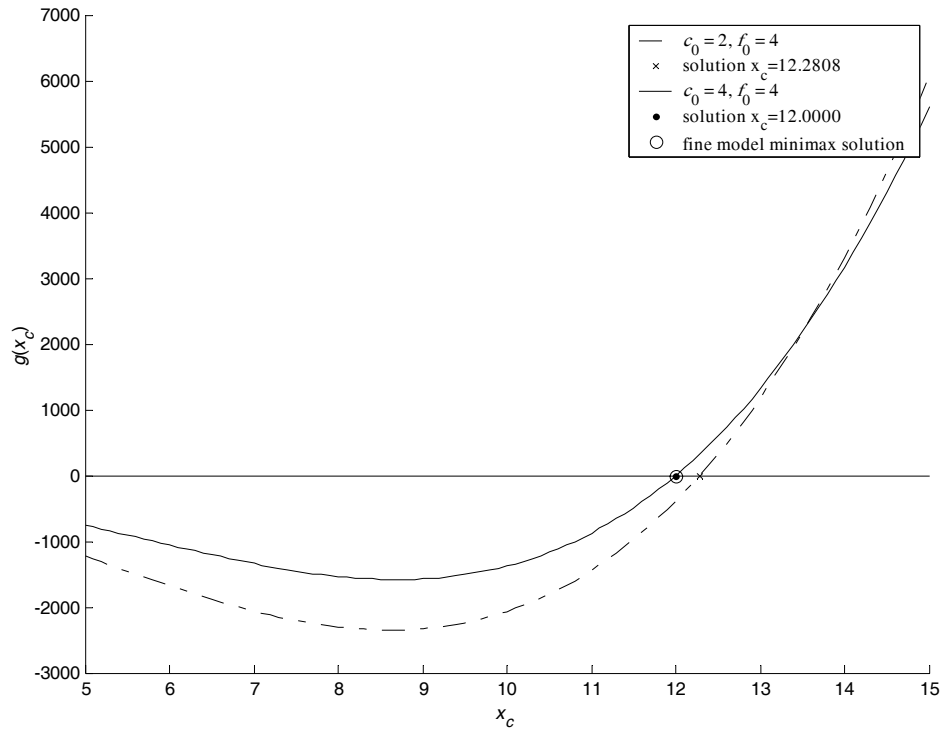


Fig. B.7 Case 1: $c_0 = 2$, $f_0 = 4$, the ISM solution is $\bar{x}_f = 12.2808$ vs. minimax solution $x_f = 12$; case 2: $c_0 = 4$, $f_0 = 4$, the ISM solution is $\bar{x}_f = 12$ vs. minimax solution $x_f = 12$.

with the experimental solution shown in Fig. B.6. When we set $[c_0 \ f_0] = [4 \ 4]$, the root of (B.18) is obtained as 12, which is the minimax solution of the fine model. This shows that ISM may not converge to the optimal solution if there is a misalignment ($c_0 \neq f_0$) between the coarse and fine model responses.

B.2.4 Response Residual SM Surrogate

If we assume that the coarse model is aligned with the fine model directionally, i.e., the first-order derivatives match, a simple RRSM calibration will push the solution to the optimum. We again use the multiple cheese-cutting

problem as an example. We assume that the coarse and fine model gradients are the same, e.g., $x = x_1 = x_2 = x_3 = x_0$, and that the parameter extraction cannot get a better match by changing the preassigned parameters. Letting the coarse model parameter c of (B.1) be c_0 and the fine model parameters f_1 and f_2 of (B.2) be f_0 , we have the residual between the coarse and the fine models (noting $x_c = x_f$) as

$$\begin{aligned}\Delta R_1 &= R_{f1} - R_{c1} = x_c \cdot x_0 - x_c \cdot x_0 = 0 \\ \Delta R_2 &= R_{f2} - R_{c2} = (x_c - f_0) \cdot x_0 - (x_c - c_0) \cdot x_0 = (c_0 - f_0) \cdot x_0 \\ \Delta R_3 &= R_{f3} - R_{c3} = (x_c - f_0) \cdot x_0 - (x_c - c_0) \cdot x_0 = (c_0 - f_0) \cdot x_0\end{aligned}\tag{B.19}$$

The new surrogate becomes

$$\mathbf{R}_s = \mathbf{R}_c + \Delta \mathbf{R} = \begin{cases} R_{c1} + \Delta R_1 = x_c \cdot x_0 \\ R_{c2} + \Delta R_2 = R_{f2} = (x_c - c_0) \cdot x_0 + (c_0 - f_0) \cdot x_0 = (x_c - f_0) \cdot x_0 \\ R_{c3} + \Delta R_3 = R_{f3} = (x_c - c_0) \cdot x_0 + (c_0 - f_0) \cdot x_0 = (x_c - f_0) \cdot x_0 \end{cases}\tag{B.20}$$

Equation (B.20) has the same form as the fine model (B.2). When we find the optimal solution of the surrogate, we obtain that of the fine model.

B.2.5 Implicit SM and RRSM

We demonstrate the response residual space mapping (RRSM) using this multiple cheese-cutting problem in Chapter 4. We now show a variation of the problem. The coarse model is the same as the previous coarse model. For the fine model, the *heights* of the cheese blocks are $x_1 = 1$, $x_2 = 0.6$ and $x_3 = 0.6$ and the lengths are the same: $f_1 = f_2 = 0$. The algorithm will not converge to the fine model optimal solution using ASM or ISM. With RRSM calibration, we are able to find the solution. We show the two RRSM stepwise iterations in Fig. B.8. And

the convergence is shown in Fig. B.9.

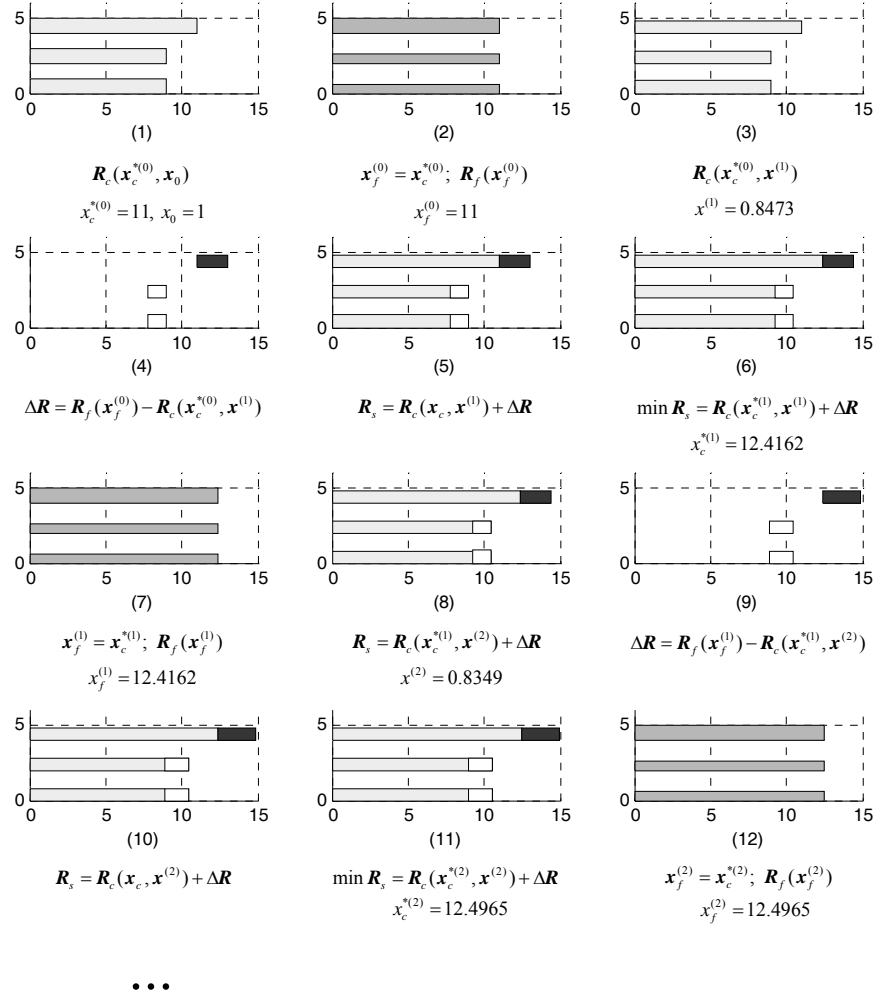


Fig. B.8 RRSM step-by-step iteration demonstration—different heights for the fine model.

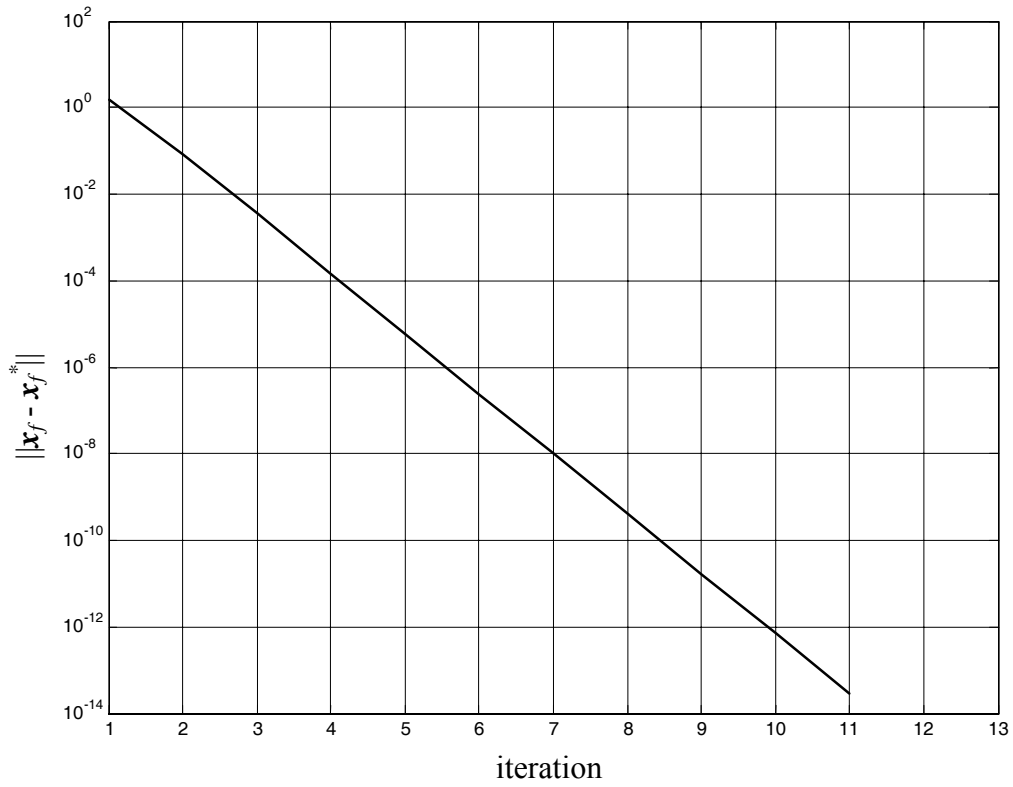


Fig. B.9 Parameter errors between the RRSM algorithm and minimax direct optimization. Here $x_f = 12.5$ and $x_f^* = 12.5$ in the final iteration (different heights for the fine model).

BIBLIOGRAPHY

First International Workshop on Surrogate Modelling and Space Mapping for Engineering Optimization, (2000), Technical University of Denmark, Lyngby, Denmark.

Agilent ADS (2000), Version 1.5, Agilent Technologies, 1400 Fountaingrove Parkway, Santa Rosa, CA 95403-1799.

Agilent ADS (2003), Version 2003A, Agilent Technologies, 1400 Fountaingrove Parkway, Santa Rosa, CA 95403-1799.

Agilent HFSS (2000), Version 5.6, Agilent EEsoft EDA, 1400 Fountaingrove Parkway, Santa Rosa, CA 95403-1799.

Agilent Momentum (2000), Version 4.0, Agilent Technologies, 1400 Fountaingrove Parkway, Santa Rosa, CA 95403-1799.

F. Alessandri, M. Mongiardo, and R. Sorrentino (1993), "New efficient full wave optimization of microwave circuits by the adjoint network method," *IEEE Microwave and Guided Wave Letters*, vol. 3, pp. 414-416.

N. Alexandrov, J.E. Dennis, Jr., R.M. Lewis, and V. Torczon (1998), "A trust region framework for managing the use of approximation models in optimization," *Structural Optimization and Engineering*, vol. 15, pp. 16-23.

M.H. Bakr (2000), *Advances in Space Mapping Optimization of Microwave Circuits*, Ph.D. Thesis, Department of Electrical and Computer Engineering, McMaster University, Hamilton, ON, Canada.

M.H. Bakr, J.W. Bandler, R.M. Biernacki, and S.H. Chen (1997), "Design of a three-section 3:1 microstrip transformer using aggressive space mapping," Report SOS-97-1-R.

M.H. Bakr, J.W. Bandler, R.M. Biernacki, S.H. Chen, and K. Madsen (1998), "A trust region aggressive space mapping algorithm for EM optimization," *IEEE Trans. Microwave Theory Tech.*, vol. 46, pp. 2412-2425.

BIBLIOGRAPHY

M.H. Bakr, J.W. Bandler, Q.S. Cheng, M.A. Ismail, and J.E. Rayas-Sánchez (2001), “SMX—A novel object-oriented optimization system,” *IEEE MTT-S IMS Digest*, Phoenix, AZ, pp. 2083-2086.

M.H. Bakr, J.W. Bandler, and N.K. Georgieva (1999), “An aggressive approach to parameter extraction,” *IEEE Trans. Microwave Theory Tech.*, vol. 47, pp. 2428-2439.

M.H. Bakr, J.W. Bandler, N.K. Georgieva, and K. Madsen (1999), “A hybrid aggressive space-mapping algorithm for EM optimization,” *IEEE Trans. Microwave Theory Tech.*, vol. 47, pp. 2440-2449.

M.H. Bakr, J.W. Bandler, M.A. Ismail, J.E. Rayas-Sánchez, and Q.J. Zhang (2000), “Neural space-mapping optimization for EM-based design,” *IEEE Trans. Microwave Theory Tech.*, vol. 48, pp. 2307-2315.

M.H. Bakr, J.W. Bandler, K. Madsen, J.E. Rayas-Sánchez, and J. Søndergaard (2000), “Space-mapping optimization of microwave circuits exploiting surrogate models,” *IEEE Trans. Microwave Theory Tech.*, vol. 48, pp. 2297-2306.

M.H. Bakr, J.W. Bandler, K. Madsen, and J. Søndergaard (2000), “Review of the space mapping approach to engineering optimization and modeling,” *Optimization and Engineering*, vol. 1, pp. 241-276.

M.H. Bakr, J.W. Bandler, K. Madsen, and J. Søndergaard (2001), “An introduction to the space mapping technique,” *Optimization and Engineering*, vol. 2, pp. 369-384.

J.W. Bandler, R.M. Biernacki, and S.H. Chen (1996), “Fully automated space mapping optimization of 3D structures,” *IEEE MTT-S IMS Digest*, San Francisco, CA, pp. 753-756.

J.W. Bandler, R.M. Biernacki, S.H. Chen, W.J. Getsinger, P.A. Grobelny, C. Moskowitz, and S.H. Talisa (1995), “Electromagnetic design of high-temperature superconducting microwave filters,” *Int. J. RF and Microwave CAE*, vol. 5, pp. 331-343.

J.W. Bandler, R.M. Biernacki, S.H. Chen, P.A. Grobelny, and R.H. Hemmers (1994), “Space mapping technique for electromagnetic optimization,” *IEEE Trans. Microwave Theory Tech.*, vol. 42, pp. 2536-2544.

J.W. Bandler, R.M. Biernacki, S.H. Chen, R.H. Hemmers, and K. Madsen (1995), “Electromagnetic optimization exploiting aggressive space mapping,” *IEEE Trans. Microwave Theory Tech.*, vol. 43, pp. 2874-2882.

BIBLIOGRAPHY

J.W. Bandler, R.M. Biernacki, S.H. Chen, and Y.F. Huang (1997), "Design optimization of interdigital filters using aggressive space mapping and decomposition," *IEEE Trans. Microwave Theory Tech.*, vol. 45, pp. 761-769.

J.W. Bandler, R.M. Biernacki, S.H. Chen, and D. Omeragic (1999), "Space mapping optimization of waveguide filters using finite element and mode-matching electromagnetic simulators," *Int. J. RF and Microwave Computer-Aided Engineering*, vol. 9, pp. 54-70.

J.W. Bandler and S.H. Chen (1988), "Circuit optimization: the state of the art," *IEEE Trans. Microwave Theory Tech.*, vol. 36, pp. 424-443.

J.W. Bandler, S.H. Chen, S. Daijavad, and K. Madsen (1988), "Efficient optimization with integrated gradient approximations," *IEEE Trans. Microwave Theory Tech.*, vol. 36, pp. 444-455.

J.W. Bandler, Q.S. Cheng, S.A. Dakroury, D.M. Hailu, K. Madsen, A.S. Mohamed, and F. Pedersen (2004), "Space mapping interpolating surrogates for highly optimized EM-based design of microwave devices," *IEEE MTT-S IMS Digest*, Fort Worth, TX, pp. 1565-1568.

J.W. Bandler, Q.S. Cheng, S.A. Dakroury, A.S. Mohamed, M.H. Bakr, K. Madsen, and J. Søndergaard (2004), "Space mapping: the state of the art," *IEEE Trans. Microwave Theory Tech.*, vol. 52, pp. 337-361.

J.W. Bandler, Q.S. Cheng, D.H. Gebre-Mariam, K. Madsen, F. Pedersen, and J. Søndergaard (2003), "EM-based surrogate modeling and design exploiting implicit, frequency and output space mappings," *IEEE MTT-S IMS Digest*, Philadelphia, PA, pp. 1003-1006.

J.W. Bandler, Q.S. Cheng, D.M. Hailu, and N.K. Nikolova (2004), "An implementable space mapping design framework," *IEEE MTT-S IMS Digest*, Fort Worth, TX, pp. 703-706.

J.W. Bandler, Q.S. Cheng, N.K. Nikolova, and M.A. Ismail (2004), "Implicit space mapping optimization exploiting preassigned parameters," *IEEE Trans. Microwave Theory Tech.*, vol. 52, pp. 378-385.

J.W. Bandler, N.K. Georgieva, M.A. Ismail, J.E. Rayas-Sánchez, and Q.J. Zhang (1999), "A generalized space mapping tableau approach to device modeling," *29th European Microwave Conf.*, Munich, Germany, pp. 231-234.

J.W. Bandler, N.K. Georgieva, M.A. Ismail, J.E. Rayas-Sánchez, and Q.J. Zhang (2001), "A generalized space mapping tableau approach to device modeling," *IEEE Trans. Microwave Theory Tech.*, vol. 49, pp. 67-79.

BIBLIOGRAPHY

- J.W. Bandler, M.A. Ismail, and J.E. Rayas-Sánchez (2002), “Expanded space mapping EM-based design framework exploiting preassigned parameters,” *IEEE Trans. Circuits and Systems—I*, vol. 49, pp. 1833-1838.
- J.W. Bandler, M.A. Ismail, J.E. Rayas-Sánchez, and Q.J. Zhang (1999), “Neuromodeling of microwave circuits exploiting space mapping technology,” *IEEE Trans. Microwave Theory Tech.*, vol. 47, pp. 2417-2427.
- J.W. Bandler, M.A. Ismail, J.E. Rayas-Sánchez, and Q.J. Zhang (2003), “Neural inverse space mapping (NISM) optimization for EM-based microwave design,” *Int. J. RF and Microwave Computer-Aided Engineering*, vol. 13, pp. 136-147.
- J.W. Bandler, W. Kellermann, and K. Madsen (1985), “A superlinearly convergent minimax algorithm for microwave circuit design,” *IEEE Trans. Microwave Theory Tech.*, vol. MTT-33, pp. 1519-1530.
- J.W. Bandler and K. Madsen (2001), “Editorial—surrogate modelling and space mapping for engineering optimization,” *Optimization and Engineering*, vol. 2, pp. 367-368.
- J.W. Bandler, A.S. Mohamed, M.H. Bakr, K. Madsen, and J. Søndergaard (2002), “EM-based optimization exploiting partial space mapping and exact sensitivities,” *IEEE Trans. Microwave Theory Tech.*, vol. 50, pp. 2741-2750.
- J.W. Bandler and Q.J. Zhang (1999), “Next generation optimization methodologies for wireless and microwave circuit design,” *IEEE MTT-S Int. Topical Symp. on Technologies for Wireless Applications*, Vancouver, BC, pp. 5-8.
- J.W. Bandler, Q.J. Zhang, and R.M. Biernacki (1988), “A unified theory for frequency-domain simulation and sensitivity analysis of linear and nonlinear circuits,” *IEEE Trans. Microwave Theory Tech.*, vol. 36, pp. 1661-1669.
- J.W. Bandler, Q.J. Zhang, J. Song, and R.M. Biernacki (1990), “FAST gradient based yield optimization of nonlinear circuits,” *IEEE Trans. Microwave Theory Tech.*, vol. 38, pp. 1701-1710.
- S. Bila, D. Baillargeat, S. Verdeyme, and P. Guillon (1998), “Automated design of microwave devices using full em optimization method,” *IEEE MTT-S IMS Digest*, Baltimore, MD, pp. 1771-1774.
- A.J. Booker, J.E. Dennis, Jr., P.D. Frank, D.B. Serafini, V. Torczon, and M.W. Trosset (1999), “A rigorous framework for optimization of expensive functions by surrogates,” *Structural Optimization and Engineering*, vol. 17, pp. 1-13.

BIBLIOGRAPHY

C.G. Broyden (1965), "A class of methods for solving nonlinear simultaneous equations," *Math. Comp.*, vol. 19, pp. 577-593.

H.-S. Choi, D.H. Kim, I.H. Park, and S.Y. Hahn (2001), "A new design technique of magnetic systems using space mapping algorithm," *IEEE Trans. Magnetics*, vol. 37, pp. 3627-3630.

A.R. Conn, N.I.M. Gould, and P.L. Toint (2000), *Trust—Region Methods*, Philadelphia, PA: SIAM and MPS, pp. 11.

J.E. Dennis, Jr. (2000), "A Summary of the Danish Technical University November 2000 Workshop," Dept. Computational and Applied Mathematics, Rice University, Houston, Texas, 77005-1892, USA.

J.E. Dennis, Jr. (2001, 2002), "private discussions," Dept. Computational and Applied Mathematics, Rice University, Houston, Texas, 77005-1892, USA.

V.K. Devabhaktuni, B. Chattaraj, M.C.E. Yagoub, and Q.J. Zhang (2003), "Advanced microwave modeling framework exploiting automatic model generation, knowledge neural networks, and space mapping," *IEEE Trans. Microwave Theory Tech.*, vol. 51, pp. 1822-1833.

P. Draxler (2002), "CAD of integrated passives on printed circuit boards through utilization of multiple material domains," *IEEE MTT-S IMS Digest*, Seattle, WA, pp. 2097-2100.

Sonnet *em* (2001), Version 7.0b, Sonnet Software, Inc., 100 Elwood Davis Road, North Syracuse, NY 13212.

Empipe3D (2000), Version 5.6, Agilent EESof EDA, Agilent Technologies, 1400 Fountaingrove Parkway, Santa Rosa, CA 95403-1799.

N.-N. Feng, G.-R. Zhou, and W.-P. Huang (2003), "Space mapping technique for design optimization of antireflection coatings in photonic devices," *Journal of Lightwave Technology*, vol. 21, pp. 281-285.

N.-N. Feng and W.-P. Huang (2003), "Modeling and simulation of photonic devices by generalized space mapping technique," *Journal of Lightwave Technology*, vol. 21, pp. 1562-1567.

G.G. Gentili, G. Macchiarella, and M. Politi (2003), "A space-mapping technique for the design of comb filters," *33rd European Microwave Conference*, Munich, Germany, pp. 171-174.

BIBLIOGRAPHY

N.K. Georgieva, S. Glavic, M.H. Bakr, and J.W. Bandler (2002a), "Adjoint variable method for design sensitivity analysis with the method of moments," *ACES'2002*, Monterey, CA, pp. 195-201.

N.K. Georgieva, S. Glavic, M.H. Bakr, and J.W. Bandler (2002b), "Feasible adjoint sensitivity technique for EM design optimization," *IEEE Trans. Microwave Theory Tech.*, vol. 50, pp. 2751-2758.

P. Harscher, E. Ofli, R. Vahldieck, and S. Amari (2002), "EM-simulator based parameter extraction and optimization technique for microwave and millimeter wave filters," *IEEE MTT-S IMS Digest*, Seattle, WA, pp. 1113-1116.

J.-S. Hong and M.J. Lancaster (2001), *Microstrip Filters For RF/Microwave Applications*, New York, NY: John Wiley and Sons, pp. 295-299.

M.A. Ismail (2001), *Space Mapping Framework for Modeling and Design of Microwave Circuits*, Ph.D. Thesis, Department of Electrical and Computer Engineering, McMaster University, Hamilton, ON, Canada.

M.A. Ismail, D. Smith, A. Panariello, Y. Wang, and M. Yu (2004), "EM-based design of large-scale dielectric-resonator filters and multiplexers by space mapping," *IEEE Trans. Microwave Theory Tech.*, vol. 52, pp. 386-392.

S.J. Leary, A. Bhaskar, and A.J. Keane (2001), "A constraint mapping approach to the structural optimization of an expensive model using surrogates," *Optimization and Engineering*, vol. 2, pp. 385-398.

J.-W. Lobeek (2002), "Space mapping in the design of cellular PA output matching circuits," *Workshop on Microwave Component Design Using Space Mapping Methodologies, IEEE MTT-S IMS*, Seattle, WA.

K. Madsen and J. Søndergaard (2004), "Convergence of hybrid space mapping algorithms," *Optimization and Engineering*, vol. 5.2, pp. 145-156.

N. Marcuvitz (1951), *Waveguide Handbook*, First ed., New York: McGraw-Hill, pp. 221.

MATLAB (2002), Version 6.5, The MathWorks, Inc., 3 Apple Hill Drive, Natick, MA 01760-2098.

G.L. Matthaei, L. Young, and E.M.T. Jones (1964), *Microwave Filters, Impedance-Matching Network and Coupling Structures*, First ed., New York: McGraw-Hill.

BIBLIOGRAPHY

J.V. Morro, H. Esteban, P. Soto, V.E. Boria, C. Bachiller, S. Cogollos, and B. Gimeno (2003), "Automated design of waveguide filters using aggressive space mapping with a segmentation strategy and hybrid optimization techniques," *IEEE MTT-S IMS Digest*, Philadelphia, PA, pp. 1215-1218.

N.K. Nikolova, J.W. Bandler, and M.H. Bakr (2004), "Adjoint techniques for sensitivity analysis in high-frequency structure CAD," *IEEE Trans. Microwave Theory Tech.*, vol. 52, pp. 403-419.

OSA90/hope (1997), formerly Optimization Systems Associates Inc., P.O. Box 8083, Dundas, Ontario, Canada L9H 5E7, now Agilent EEsof EDA, 1400 Fountaingrove Parkway, Santa Rosa, CA 95403-1799, USA.

A.M. Pavio (1999), "The electromagnetic optimization of microwave circuits using companion models," *Workshop on Novel Methodologies for Device Modeling and Circuit CAD*, *IEEE MTT-S IMS*, Anaheim, CA.

A.M. Pavio, J. Estes, and L. Zhao (2002), "The optimization of complex multi-layer microwave circuits using companion models and space mapping techniques," *Workshop on Microwave Component Design Using Space Mapping Methodologies*, *IEEE MTT-S IMS*, Seattle, WA.

F. Pedersen (2001), *Advances on the Space Mapping Optimization Method*, Masters Thesis, Informatics and Mathematical Modelling (IMM), Technical University of Denmark (DTU), Lyngby, Denmark.

D. Pelz (2002), "Coupled resonator filter realization by 3D-EM analysis and space mapping," *Workshop on Microwave Component Design Using Space Mapping Methodologies*, *IEEE MTT-S IMS*, Seattle, WA.

C. Petzold (1990), *Programming Windows*: Microsoft Press.

D.M. Pozar (1998), *Microwave Engineering*, 2nd Edition: New York: Addison-Wesley, pp. 162-163.

J.C. Rautio and R.F. Harrington (1987a), "An efficient electromagnetic analysis of arbitrary microstrip circuits," *IEEE MTT-S IMS Digest*, Las Vegas, NV, pp. 295-298.

J.C. Rautio and R.F. Harrington (1987b), "An electromagnetic time-harmonic analysis of shielded microstrip circuits," *IEEE Trans. Microwave Theory Tech.*, vol. 35, pp. 726-730.

BIBLIOGRAPHY

J.E. Rayas-Sánchez (2001), *Neural Space Mapping Methods for Modeling and Design of Microwave Circuits*, Ph.D. Thesis, Department of Electrical and Computer Engineering, McMaster University, Hamilton, ON, Canada.

M. Redhe (2001), *Simulation Based Design-Structural Optimization at the Early Design Stages*, Master Thesis, Dept. of Mechanical Engineering, Division of Solid Mechanics, Linköping University.

M. Redhe and L. Nilsson (2002), "Using space mapping and surrogate models to optimize vehicle crashworthiness design," *9th AIAA/ISSMO Symposium on Multidisciplinary Analysis and Optimization*, Atlanta, GA, AIAA-2002-5536.

S. Safavi-Naeini, S.K. Chaudhuri, N. Damavandi, and A. Borji (2002), "A multi-level design optimization strategy for complex RF/microwave structures," *Workshop on Microwave Component Design Using Space Mapping Methodologies, IEEE MTT-S IMS*, Seattle, WA.

J. Snel (2001), "Space mapping models for RF components," *Workshop on Statistical Design and Modeling Techniques For Microwave CAD, IEEE MTT-S IMS*, Phoenix, AZ.

J. Søndergaard (1999), *Non-linear Optimization Using Space Mapping*, Masters Thesis, Informatics and Mathematical Modelling (IMM), Technical University of Denmark (DTU), Lyngby, Denmark.

J. Søndergaard (2003), *Optimization Using Surrogate Models-by the Space Mapping Technique*, Ph.D. Thesis, Informatics and Mathematical Modelling (IMM), Technical University of Denmark (DTU), Lyngby, Denmark.

P. Soto, A. Bergner, J.L. Gomez, V.E. Boria, and H. Esteban (2000), "Automated design of inductivity coupled rectangular waveguide filters using space mapping optimization," *European Congress on Computational Methods in Applied Science And Engineering*, Barcelona, Spain.

M.B. Steer, J.W. Bandler, and C.M. Snowden (2002), "Computer-aided design of RF and microwave circuits and systems," *IEEE Trans. Microwave Theory Tech.*, vol. 50, pp. 996-1005.

W. Steyn, R. Lehmensiek, and P. Meyer (2001), "Integrated CAD procedure for IRIS design in a multi-mode waveguide environment," *IEEE MTT-S IMS Digest*, Phoenix, AZ, pp. 1163-1166.

D.G. Swanson, Jr. (2001) CLD - Compline Design Version 3.0, Bartley R.F. Systems, Amesbury, MA.

BIBLIOGRAPHY

D.G. Swanson, Jr. and R.J. Wenzel (2001), "Fast analysis and optimization of combline filters using FEM," *IEEE MTT-S IMS Digest*, Phoenix, AZ, pp. 1159-1162.

G.C. Temes and D.A. Calahan (1967), "Computer-aided network optimization the state-of-the-art," *Proc. IEEE*, vol. 55, pp. 1832-1863.

UML Training in Object Oriented Analysis and Design page at http://www.cragssystem.co.uk/uml_training_080.htm.

L.N. Vicente (2002), "Space mapping: models, sensitivities, and trust-regions methods," *Workshop on Optimization in Engineering Design, SIAM Conference on Optimization*, Toronto, Canada.

L.N. Vicente (2003a), "Space mapping: models, algorithms, and applications," *IMA*, University of Minnesota, Minneapolis, MN <http://www.mat.uc.pt/~lnv/talks/ima-sm2.pdf>.

L.N. Vicente (2003b), "Space mapping: models, sensitivities, and trust-regions methods," *Optimization and Engineering*, vol. 4, pp. 159-175.

K.-L. Wu, R. Zhang, M. Ehlert, and D.-G. Fang (2003), "An explicit knowledge-embedded space mapping technique and its application to optimization of LTCC RF passive circuits," *IEEE Trans. Components and Packaging Technologies*, vol. 26, pp. 399-406.

K.-L. Wu, Y.-J. Zhao, J. Wang, and M.K.K. Cheng (2004), "An effective dynamic coarse model for optimization design of LTCC RF circuits with aggressive space mapping," *IEEE Trans. Microwave Theory Tech.*, vol. 52, pp. 393-402.

S. Ye and R.R. Mansour (1997), "An innovative CAD technique for microstrip filter design," *IEEE Trans. Microwave Theory Tech.*, vol. 45, pp. 780-786.

L. Young and B.M. Schiffman (1963), "A useful high-pass filter design," *Microwave J.*, vol. 6, pp. 78-80.

L. Zhang, J.J. Xu, M.C.E. Yagoub, R.T. Ding, and Q.J. Zhang. (2003), "Neuro-space mapping technique for nonlinear device modeling and large signal simulation," *IEEE MTT-S IMS Digest*, Philadelphia, PA, pp. 173-176.

Q.J. Zhang and K.C. Gupta (2000), *Neural Networks For RF and Microwave Design*, Chapter 9, Norwood, MA: Artech House Publishers.

BIBLIOGRAPHY

AUTHOR INDEX

A

Alessandri	25
Alexandrov	27
Amari	94

B

Baillargeat	19
Bakr	2, 3, 6, 8, 10, 11, 12, 15, 16, 19, 20, 23, 24, 25, 27, 38, 40, 47, 50, 63, 76, 85, 93, 107, 109
Bandler	2, 3, 6, 7, 8, 9, 10, 11, 12, 13, 14, 15, 16, 17, 19, 20, 22, 23, 24, 25, 26, 27, 28, 29, 31, 37, 38, 39, 40, 46, 47, 50, 52, 53, 54, 55, 57, 63, 64, 66, 67, 69, 71, 72, 76, 81, 84, 85, 92, 93, 107, 109, 111, 119
Bergner	97

AUTHOR INDEX

Bhaskar	98
Biernacki	2, 3, 9, 10, 13, 16, 17, 22, 23, 24, 25, 26, 27, 37, 40, 46, 47, 50, 54, 55, 57, 64, 67, 81, 84, 85, 92, 111, 119
Bila	19
Booker	107
Boria	97
Borji	95
Broyden	4, 17, 18, 19, 20, 29, 35, 101, 120, 123
C	
Calahan	1
Chattaraj	93
Chaudhuri	95
Chen	2, 3, 7, 9, 10, 13, 16, 17, 19, 22, 23, 24, 25, 26, 27, 37, 40, 46, 47, 50, 55, 57, 64, 67, 81, 84, 85, 92, 112, 119
Cheng, Q.S.	2, 3, 8, 10, 11, 12, 28, 37, 40, 63, 66, 67, 69, 71, 72, 93, 107
Cheng, M.M.K.	95
Choi	97
Conn	12

AUTHOR INDEX

D

Daijavad	19
Dakroury	2, 3, 8, 10, 40, 63
Damavandi	95
Dennis	27, 28, 29, 65, 107
Devabhaktuni	93
Ding	97
Draxler	96

E

Ehlert	95
Esteban	97
Estes	94

F

Fang	95
Feng	98
Frank	107

G

Gebre-Mariam	(<i>see Hailu</i>)
Gentili	97

AUTHOR INDEX

Georgieva	<i>(see Nikolova)</i>
Getsinger	55, 57, 67, 112
Glavic	25
Gomez	97
Gould	12
Grobelny	2, 3, 9, 13, 16, 22, 26, 37, 40, 55, 57, 67, 84, 112
Guillon	19
Gupta	11, 12

H

Hahn	97
Hailu (formerly Gebre-Mariam)	3, 28, 40, 71, 72
Harrington	1
Harscher	94
Hemmers	2, 3, 9, 13, 16, 17, 22, 24, 26, 37, 40, 46, 47, 55, 64, 84, 119
Hong	12
Huang, W.-P.	98
Huang, Y.F.	10, 23

AUTHOR INDEX

I

Ismail 2, 3, 11, 12, 23, 25, 26, 27, 31, 37, 38,
39, 40, 47, 52, 53, 63, 67, 69, 81, 92, 93,
96, 107

J

Jones 71, 76, 93

K

Keane 98

Kellermann 7

Kim 97

L

Lancaster 12

Leary 98

Lehmensiek 96

Lewis 27

Lobeek 95

M

Macchiarella 97

Madsen 2, 3, 6, 7, 8, 9, 10, 11, 12, 15, 16, 17, 19,

AUTHOR INDEX

	20, 23, 24, 25, 27, 28, 29, 37, 38, 40, 46, 47, 55, 63, 64, 71, 72, 76, 84, 93, 107, 109, 119
Mansour	26, 38, 94
Marcuvitz	77, 93
Matthaei	71, 76, 93
Meyer	96
Mohamed	2, 3, 8, 10, 19, 20, 25, 40, 63
Mongiardo	25
Moskowitz	55, 57, 67, 112
 <i>N</i>	
Nikolova (formerly Georgieva)	2, 3, 10, 11, 15, 19, 23, 25, 26, 37, 63, 66, 67, 69, 76, 93
Nilsson	98
 <i>O</i>	
Ofli	94
Omeragic	10, 23
 <i>P</i>	
Panariello	96

AUTHOR INDEX

Park	97
Pavio	19, 94
Pedersen	3, 12, 28, 40, 71, 72
Pelz	96
Petzold	108
Politi	97
Pozar	45, 50, 87

R

Rautio	1
Rayas-Sánchez	2, 6, 11, 12, 23, 24, 25, 26, 31, 37, 38, 39, 40, 47, 52, 53, 93, 107, 109
Redhe	98

S

Søndergaard	2, 3, 6, 8, 10, 11, 12, 16, 19, 20, 24, 25, 27, 28, 38, 40, 47, 63, 65, 66, 71, 72, 93, 107, 109
Safavi-Naeini	95
Schiffman	71, 76, 93
Serafini	107
Smith	96

AUTHOR INDEX

Snel	94
Snowden	2, 7, 14
Song	25
Sorrentino	25
Soto	97
Steer	2, 7, 14
Steyn	96
Swanson	96

T

Talisa	55, 57, 67, 112
Temes	1
Toint	12
Torczon	27, 107
Trosset	107

V

Vahldieck	94
Verdeyme	19
Vicente	12, 13

AUTHOR INDEX

W

Wang, J	95
Wang, Y	96
Wenzel	96
Wu	95

X

Xu	97
----	----

Y

Yagoub	93, 97
Ye	26, 38, 94
Young	71, 76, 93
Yu	96

Z

Zhang, L	97
Zhang, Q.J.	2, 11, 12, 24, 25, 26, 31, 38, 40, 47, 93, 97
Zhang, R	95
Zhao, L	94
Zhao, Y.-J.	95

Zhou

98

SUBJECT INDEX

A

ADS	4, 5, 6, 37, 39, 50, 56, 57, 58, 59, 60, 64, 69, 70, 71, 76, 77, 78, 81, 82, 83, 84, 85, 86, 87, 89, 91, 94, 98, 102, 103, 104, 105
ADS schematic design framework	82, 83, 103, 104, 105
aggressive SM	4, 10, 12, 17, 18, 20, 30, 40, 81, 84, 92, 95, 96, 97, 104, 115, 116
aggressive space mapping	9, 17, 22, 32, 35, 46, 101, 119, 120
Agilent	2, 4, 5, 37, 39, 50, 56, 57, 60, 61, 64, 68, 71, 78, 81, 82, 83, 84, 85, 86, 91, 92, 93, 94, 102, 105, 107, 111, 113
ANN	11, 47
Ansoft	2, 105

SUBJECT INDEX

Artificial Neural Networks	11, 12, 30, 47
ASM	9, 33, 119, 120, 121, 122, 123, 128
Automatic Model Generation	93
C	
CAD	1, 2, 7, 13, 34, 94, 95, 96, 101
cheese-cutting	4, 5, 6, 20, 22, 37, 48, 49, 50, 51, 71, 72, 73, 74, 78, 103, 115, 118, 119, 120, 124, 126, 127, 128
coarse model	4, 5, 8, 9, 10, 11, 14, 15, 16, 18, 21, 22, 23, 24, 26, 27, 28, 29, 30, 31, 32, 35, 37, 38, 39, 40, 41, 42, 43, 44, 45, 46, 47, 48, 49, 50, 51, 52, 53, 54, 55, 56, 57, 59, 60, 61, 64, 65, 67, 68, 69, 70, 71, 72, 73, 74, 75, 77, 79, 81, 82, 83, 84, 85, 86, 87, 88, 89, 91, 92, 93, 95, 98, 102, 104, 107, 110, 112, 114, 115, 116, 117, 118, 120, 122, 124, 125, 126, 127, 128
comb filter	97

SUBJECT INDEX

comblin filter	96
computer-aided design	1
coupled resonator filter	96

D

dielectric resonator filter and multiplexer	96
direct optimization	7, 11, 14, 75, 125, 130

E

electromagnetic	1, 7, 50
electromagnetics	101
<i>em</i>	2, 4, 5, 37, 56, 59, 60, 61, 81, 82, 83, 84, 85, 92, 93, 102, 107
EM	1, 2, 3, 4, 5, 7, 8, 9, 11, 24, 26, 37, 60, 63, 64, 71, 78, 82, 83, 94, 95, 102, 103, 104, 105, 108
Empipe	81, 92, 93, 107
Empipe3D	83, 93
ESMDF	27, 38, 53
expanded space mapping design framework	27
explicit SM	4, 33, 37, 39, 40, 47
explicit space mapping	39, 46

SUBJECT INDEX

F

FEM	1, 2, 96
fine model	3, 4, 5, 8, 9, 10, 11, 13, 14, 15, 16, 17, 19, 21, 22, 23, 26, 27, 28, 29, 30, 31, 32, 33, 34, 35, 37, 38, 39, 40, 41, 43, 44, 45, 48, 50, 51, 53, 54, 55, 56, 58, 59, 60, 63, 64, 65, 66, 67, 68, 69, 71, 72, 73, 74, 75, 78, 79, 81, 82, 83, 84, 85, 86, 87, 88, 89, 90, 91, 92, 93, 96, 98, 101, 102, 103, 107, 112, 113, 114, 115, 116, 117, 118, 119, 120, 124, 126, 127, 128, 129, 130
finite element method	1

G

gradient	10, 19, 25, 33, 34, 35, 83, 102, 109
----------	---

H

HFSS	2, 5, 71, 78, 83, 84, 85, 93, 105
high frequency structure simulator	1

SUBJECT INDEX

H-plane 5, 64, 71, 76, 77, 78, 79, 80, 93,
103

HTS filter 4, 5, 37, 55, 56, 57, 58, 59, 60,
61, 64, 67, 68, 69, 70, 78, 91, 94,
102, 111, 112, 113, 114

I

implicit SM 3, 4, 6, 25, 33, 40, 50, 54, 55, 64,
74, 76, 84, 97, 103, 124, 128

implicit space mapping 4, 6, 11, 32, 35, 37, 39, 40, 42,
51, 52, 54, 63, 78, 84, 101, 102

inductively coupled filter 97

integrated passive elements 96

ISM 4, 5, 11, 30, 31, 33, 37, 38, 41,
42, 43, 44, 45, 46, 47, 48, 49, 52,
63, 64, 66, 68, 69, 70, 85, 90,
103, 104, 124, 125, 126, 127, 128

J

Jacobian 15, 18, 19, 34, 64, 78, 79, 103

K

key preassigned parameters 26

SUBJECT INDEX

KPP	26, 27
<i>L</i>	
Low Temperature Co-firing Ceramic (LTCC)	94, 95
<i>M</i>	
magnetic systems	97
mathematical motivation	3, 10
Matlab	81, 84, 92
method of moments	1
microstrip filter	12, 78, 94, 102
microstrip impedance transformer	50, 85
minimax	13, 15, 24, 59, 70, 73, 75, 86, 87, 89, 91, 109, 110, 114, 118, 120, 124, 125, 126, 127, 130
MoM	1, 2
Momentum	4, 5, 37, 50, 56, 58, 60, 61, 68, 78, 81, 82, 83, 84, 85, 86, 87, 88, 90, 92, 93, 102, 107, 113, 114
Momentum_Driver	81, 92, 93, 107
multiple cheese-cutting	5, 6, 71, 72, 73, 74, 78, 103, 118, 119, 120, 124, 126, 127, 128

SUBJECT INDEX

N

neural inverse SM	11
neural space mapping	4, 11, 31, 32, 101
NISM	33
nonlinear device modeling	97
NSM	11

O

object-oriented	93, 103, 107
original space mapping	16, 35, 102
OSA90	81, 92, 93, 111, 112, 114
OSM	5, 33, 102, 104
output SM	3, 32, 33, 104
output space mapping	5, 6, 28, 69, 101, 102

P

parameter extraction	4, 9, 16, 18, 21, 22, 23, 25, 31, 32, 35, 37, 42, 44, 46, 48, 49, 52, 54, 55, 59, 63, 64, 71, 72, 81, 84, 88, 89, 93, 101, 102, 110, 115, 116, 117, 118, 119, 120, 122, 124, 126, 128
----------------------	--

SUBJECT INDEX

PE	9, 10, 16, 17, 18, 19, 20, 21, 22, 23, 30, 31, 33, 34, 47, 55, 67, 69, 71, 74, 82, 83, 116, 117, 122
power amplifier circuits	94
preassigned parameters	3, 4, 5, 11, 25, 26, 31, 33, 35, 37, 38, 39, 41, 42, 45, 46, 47, 48, 52, 53, 54, 55, 56, 60, 61, 63, 64, 69, 73, 75, 77, 78, 81, 84, 88, 89, 91, 92, 97, 102, 104, 118, 124, 126, 128
Printed Circuit Board (PCB)	96
R	
response residual space mapping	5, 63, 64, 66, 71, 78, 91, 102, 117, 128
response residual SM	65, 71, 84, 85, 91, 122, 127
RRSM	5, 6, 63, 64, 68, 69, 70, 71, 72, 74, 75, 76, 78, 79, 80, 84, 102, 103, 104, 117, 122, 124, 127, 128, 129, 130
S	
SM-based optimization	4, 9, 30, 35

SUBJECT INDEX

SMX	6, 12, 93, 103, 107, 108, 109, 110, 111, 113, 114
Sonnet	2, 4, 5, 37, 56, 59, 60, 61, 81, 82, 83, 84, 85, 92, 93, 102, 107
space mapping design framework	27, 81, 102
Surface Mount Technology (SMT)	96
Surrogate Modelling	28
 <i>T</i>	
Taylor approximation	10, 28, 65, 66
Taylor model	10, 63
trust region	4, 12, 27, 35, 101
 <i>V</i>	
vehicle crashworthiness design	98
 <i>W</i>	
waveguide filter	64, 71, 76, 77, 78, 80, 93, 96, 97